



# ESA Climate Change Initiative Phase II Soil Moisture

Product Validation and Intercomparison Report  
Revision 3 (PVIR)

D4.1.2

Version 2.6

29 November 2018

Prepared by

Earth Observation Data Centre for Water Resources Monitoring (EODC) GmbH



in cooperation with

TU Wien, GeoVille, ETH Zürich, TRANSMISSIVITY, AWST, FMI, UCC and NILU



This document forms D4.1.2 Product Validation and Intercomparison Report, Revision 1 (PVIR) and was compiled for the ESA Climate Change Initiative Phase 2 Soil Moisture Project (ESA Contract No.4000112226/14/I-NB). For more information on the CCI programme of the European Space Agency (ESA) see <http://www.esa-cci.org/>.

Number of pages: 91

Authors:		William Lahoz, Jostein Blyverket and Paul Hamer with contributions from FMI, ETH, UCC teams	
Circulation (internal):		Project consortium and science partners	
External:		ESA	
Issue	Date	Details	Editor
1.1	September 2018	ETH included validation study of product v04.2 keeping similar analysis to PVIR revision 2. Removal of discussion on drought representation.	Martin Hirschi
1.2	September 2018	Addition of validation study from Geoville using GPCP, ERA-Land, and GIMMS NDVI products to assess product version v04.2 and v0.50	Franziska Albrecht
1.3	September 2018	Contribution from NILU removed study over Europe and now focuses on ENKF assimilation over the USA	Jostein Blyverket
1.4	September 2018	Contribution from UCC uses product version v03.2. Validation over Ireland is removed. Validation is done for areas over Austria, Denmark, and Italy	Walther Camaro
1.5	September 2018	Contribution from FMI uses product version v03.2, v04.1, and v05.0. Validation continued over the Sodankylä region.	Jaako Ikonen
1.8	1 September 2018	Complete document created	Randi Nordby Henriksen
1.9	20 September 2018	Contributions from ETH included and formatting	Randi Nordby Henriksen
2.0	21 September 2018	Contributions from UCC included and formatting	Randi Nordby Henriksen
2.1	22 September 2018	Contributions from FMI included and formatting	Randi Nordby Henriksen
2.2	1 October 2018	Contributions from Geoville included and formatted	Paul Hamer and Randi Nordby Henriksen



2.3	9 October 2018	Edited text, formatting, and bibliography	Paul Hamer
2.4	10 October 2018	Finalised formatting	Paul Hamer
2.5	11 October 2018	Internal review at NILU	Britt Ann Kåstad Høiskar, Jostein Blyverket
2.6	29 November 2018	Comments on v2.5 included, included product change log, and formatting in document	Paul Hamer; T. Scanlon, R. Kidd

For any clarifications please contact Paul Hamer (paul.hamer@nilu.no).



## Project Partners

<b>Prime Contractor, Scientific Lead</b>	<b>EODC</b> , Earth Observation Data Centre for Water Resources Monitoring (EODC) GmbH (Austria)
<b>Project Management</b>	<b>GeoVille</b> , GeoVille Information Systems GmbH (Austria)
<b>System Engineering Partners</b>	<b>AWST</b> , Angewandte Wissenschaft Software und Technologie GmbH (Austria)
<b>Earth Observation Partners</b>	<b>TU Wien</b> , Vienna University of Technology (Austria) <b>(Lead)</b> <b>TMS</b> , Transmissivity,(The Netherlands) <b>FMI</b> , Finnish Meteorological Institute, (Finland) <b>UCC</b> , University College Cork, (Ireland)
<b>Climate Research Partners</b>	<b>ETH</b> , Institute for Atmospheric and Climate Science, (Switzerland) <b>(Lead)</b> <b>NILU</b> - Norsk institutt for luftforskning (Norway)

## Table of Contents

<b>1</b>	<b>EXECUTIVE SUMMARY .....</b>	<b>14</b>
<b>2</b>	<b>DOCUMENTS .....</b>	<b>17</b>
2.1	APPLICABLE DOCUMENTS .....	17
2.2	REFERENCE DOCUMENTS .....	17
2.3	BIBLIOGRAPHY .....	17
<b>3</b>	<b>INTRODUCTION.....</b>	<b>18</b>
3.1	PURPOSE OF THE DOCUMENT .....	18
3.2	TARGET AUDIENCE .....	18
3.3	IMPORTANT DOCUMENTS .....	18
<b>4</b>	<b>DATASETS .....</b>	<b>23</b>
<b>5</b>	<b>VALIDATION STUDIES.....</b>	<b>24</b>
5.1	COMPARISON TO GLOBAL CLIMATE, LSM SIMULATIONS AND OTHER LARGE-SCALE ESTIMATES (ETH) .	24
5.1.1	<i>Datasets and data processing .....</i>	24
5.1.2	<i>Results in-situ comparisons .....</i>	26
5.2	VALIDATION WITH GPCP, ERA-LAND, AND GIMMS NDVI (GEOVILLE).....	31
5.2.1	<i>Data Sets .....</i>	31
5.2.2	<i>Methods .....</i>	31
5.2.3	<i>Results .....</i>	32
5.2.4	<i>Discussion and conclusion .....</i>	36
5.2.5	<i>Other Findings – Data Inconsistency .....</i>	37
5.3	ASSIMILATION OF THE ESA CCI ACTIVE AND PASSIVE PRODUCT INTO THE SURFEX LAND SURFACE MODEL USING THE ENKF (NILU).....	39
5.3.1	<i>Introduction.....</i>	39
5.3.2	<i>Data Sets .....</i>	40
5.3.3	<i>Methods .....</i>	41
5.3.4	<i>Results .....</i>	43
5.3.5	<i>Conclusions.....</i>	53
5.4	VALIDATION WITH SAR (UCC).....	53
5.4.1	<i>Data Sets and Methods .....</i>	53
5.4.2	<i>Results .....</i>	54
5.4.3	<i>Discussion and Conclusions .....</i>	66
5.5	VALIDATION OVER BOREAL AND SUB-ARCTIC ENVIRONMENTAL DATA (FMI).....	67
5.5.1	<i>Introduction.....</i>	67
5.5.2	<i>Single-pixel, In Situ Based Validation .....</i>	68



5.5.3	<i>Multi-pixel, SAC-SMA Model Configuration</i> .....	70
5.5.4	<i>Multi-pixel, Model Based Validation</i> .....	72
5.5.5	<i>Multi-pixel, Spatio-Statistical Pattern Analysis</i> .....	74
<b>6</b>	<b>CONCLUSIONS</b> .....	<b>78</b>
<b>7</b>	<b>BIBLIOGRAPHY</b> .....	<b>79</b>
<b>8</b>	<b>APPENDIX</b> .....	<b>82</b>

## List of Figures

Figure 1: Overview of the spatial coverage of the stations considered in this study, rectangles indicate the four focus areas of the comparison, i.e., the United States (US, red), Europe (EU, blue), Africa (AF, green), and Australia (AUS, purple). Stations are color coded by network, see Figure 2 for the legend. ....	25
Figure 2: Overview of the temporal coverage of the stations considered in this study, after masking for common data availability, split per region. The number of stations per region is indicated in brackets. ....	26
Figure 3: Correlation between in-situ soil moisture and CCI-SM for versions v0.1, v02.0, v02.2, v03.3, and v04.2, as well as ERA-SM layer 1 (ERA1, 0-7 cm), for absolute soil moisture (left) and the anomalies (right). ....	27
Figure 4: Correlation between in-situ measurements for CCI-SM v0.1, v02.0, v02.2, v03.3, and v04.2, as well as ERA-SM layer 1 and 2 for the absolute soil moisture values (top) and the anomalies (bottom). For each product, we distinguish between 3 regions US, EU, and AUS (red, blue and purple, AF has insufficient data), and the correlation at 5 cm depth (circles) and 10 cm depth (triangles). The black circles/triangles represent the respective median value. ....	29
Figure 5: Correlation between in-situ measurements at 5 cm depth and CCI-SM v0.1, v02.0, v02.2, v03.3, and v04.2, as well as ERA-SM layer 1, differentiating between grassland (orange) and forest (green) sites for absolute soil moisture values and anomalies. Again, the black dot denotes the median value. ....	30
Figure 6: Pearson correlation coefficient calculated for absolute values over the period 1997 to 2013 for a) CCI SM v05.0 and GPCP v1.2 precipitation estimates, b) CCI SM v05.0 and ERA-Land volumetric SM estimates and c) CCI SM v05.0 and GIMMS NDVI (x + 1 shift). ....	33
Figure 7: Pearson correlation coefficient calculated for anomaly values over the period 1997 to 2013 for a) CCI SM v05.0 and GPCP v1.2 precipitation estimates, b) CCI SM v05.0 and ERA-Land volumetric SM estimates and c) CCI SM v05.0 and GIMMS NDVI (x + 1 shift). ....	33
Figure 8: Differences of Pearson correlation coefficient calculated for absolute values over the period 1997 to 2013 for GPCP v1.2 precipitation estimates and CCI SM v04.2 and ESA CCI v05.0. ....	34
Figure 9: Differences of Pearson correlation coefficient calculated for absolute values over the period 1997 to 2013 for ERA-Land volumetric soil estimates and CCI SM v04.2 and ESA CCI v05.0. ....	35
Figure 10: Differences of Pearson correlation coefficient calculated for absolute values over the period 1997 to 2013 for GIMMS 3g NDVI estimates and CCI SM v04.2 and ESA CCI v05.0. ....	35



Figure 11: Theil Sen Slope estimator for ESA CCI SM v05.0 annual mean values calculated over the period 1997 to 2013..... 36

Figure 12: Theil Sen Slope estimator for ESA CCI SM v05.0 annual anomaly values calculated over the period 1997 to 2013. .... 36

Figure 13: Data inconsistency in Mongolia for daily, half-monthly, monthly and annual means of ESA CCI SM ..... 37

Figure 14: Data inconsistency in Mongolia for daily, half-monthly, monthly and annual FLAG of ESA CCI SM ..... 37

Figure 15: Annual means for ESA CCI SM v05.0 from 1979 to 2017 ..... 38

Figure 16: Comparison between the combined and the passive product for the annual mean of 1979..... 39

Figure 17: Comparison between combines, active and passive product means for 1991 and 2002. 39

Figure 18: (a) Daily counts of ESA CCI ACTIVE and PASSIVE observations assimilated into the ESA CCI L4 system from April 2015 to January 2017. (b) Spatial extent of number of total assimilated observations from the ESA CCI ACTIVE and PASSIVE product. Some regions are not covered because the ESA CCI ACTIVE or PASSIVE product were an arithmetic average of two observations observed at different times. In our sequential DA system these observations were therefore masked out. .... 44

Figure 19: (a) Mean of O-F and O-A residuals, the mean values are computed separately for each 3h window by averaging over the land domain, and then averaging the resulting values over the 8 analysis times for each day. (b) Same as in (a) but for standard deviation. .... 45

Figure 20: (a) Mean and (b) standard deviation of the O-F residuals from April 2015 to 1 January 2017. .... 46

Figure 21: Standard deviation of the normalized O-F residuals from April 2015 to 1 January 2017..... 48

Figure 22: Standard deviation of the surface (a) and root-zone (b) increments from April 2015 to 1 January 2017. Not the different color scale in (a) and (b)..... 49

Figure 23: Pearson correlation coefficient surface soil moisture, ensemble open-loop run vs USCRN in situ stations. Mean R = 0.72, std R = 0.11. Median R = 0.73..... 50

Figure 24: Difference between the analysis and the open-loop correlation with USCRN in situ stations, surface soil moisture. .... 51

Figure 25: The same as for Figure 23, but for root-zone soil moisture. Mean R = 0.76, std = 0.11. Median R = 0.78. .... 51

Figure 26: The same as for Figure 24, but for root-zone soil moisture. .... 52

Figure 27: ubRMSE for the open-loop vs USCRN in situ stations, root-zone. Median = 0.038 m<sup>3</sup> m<sup>-3</sup>. Mean = 0.040 m<sup>3</sup>/m<sup>3</sup>..... 52

Figure 28: CORINE Land Cover classes in Austrian area of interest. (<https://land.copernicus.eu/pan-european/corine-land-cover/clc-2012/view>). .... 55



Figure 29: Time series of in-situ, ASAR and ECV SM v03.2 time series for stations in the Austrian regions under investigation. The units are $m^3m^{-3}$ .....	56
Figure 30: Spatial correlation between ASAR SM and ESA CCI SM v03.2 datasets in the Austrian regions under investigation.....	58
Figure 31: CORINE Land Cover classes in the Danish area of interest. ( <a href="https://land.copernicus.eu/pan-european/corine-land-cover/clc-2012/view">https://land.copernicus.eu/pan-european/corine-land-cover/clc-2012/view</a> ).....	59
Figure 32: Time series of in-situ, ASAR and ECV SM v03.2 time stations in the Danish regions under investigation. The units are $m^3m^{-3}$ . ....	60
Figure 33: Spatial correlation between ASAR SM and ESA CCI SM v03.2 datasets in the Danish regions under investigation. ....	62
Figure 34: CORINE Land Cover classes in the Italian areas of interest. a) Umbria, b) Calabria ( <a href="https://land.copernicus.eu/pan-european/corine-land-cover/clc-2012/view">https://land.copernicus.eu/pan-european/corine-land-cover/clc-2012/view</a> ).....	63
Figure 35: Time series of in-situ, ASAR and ECV SM v03.2 time stations in the Italian regions under investigation. The units are $m^3m^{-3}$ .....	64
Figure 36: Spatial correlation between ASAR SM and ESA CCI SM v03.2 datasets in the Calabrian (Italy) regions under investigation. ....	66
<i>Figure 37: Location of the Sodankylä study domain, the 70 ESA CCI SM product pixels and distribution of FMI's soil moisture observation sites. ....</i>	<i>68</i>
<i>Figure 38: Left; ESA CCI SM ACTIVE, PASSIVE and COMBINED v04.1 and v05.0 products' correlations with daily weighted in situ measurements. Right; number of observation days for ESA CCI SM ACTIVE, PASSIVE and COMBINED v04.1 and v05.0 products during the summer period of each year. ....</i>	<i>69</i>
<i>Figure 39: A conceptualization of the SAC-SMA model. Each SAC-SMA model grid cell is divided into a maximum of 14 soil / vegetation density type tiles representing cross combinations of the 4 main mineral soil types. Semi-organic and organic soils are modelled with a separate scheme.....</i>	<i>71</i>
<i>Figure 40: ESA CCI SM COMBINED SM v03.2 v04.1 and v05.0 product 70 pixel average correlation with. SAC-SMA Model top layer SM estimates .....</i>	<i>72</i>
<i>Figure 41: ESA CCI SM PASSIVE SM v03.2 v04.1 and v05.0 product 70 pixel average correlation with. SAC-SMA Model top layer SM estimates. ....</i>	<i>72</i>
<i>Figure 42: ESA CCI SM ACTIVE SM v03.2 v04.1 and v05.0 product 70 pixel average correlation with. SAC-SMA Model top layer SM estimates. ....</i>	<i>73</i>
<i>Figure 43: Number of pixels (out of 70) containing PASSIVE SM observations in version v05.0 (right). Number of pixels (out of 70) containing PASSIVE SM observations in version v04.1 (right). ....</i>	<i>73</i>
<i>Figure 44: ESA CCI SM ACTIVE product correlation with SAC-SMA model top layer soil moisture dependency on pixel-wise major soil/vegetation type fraction size. ....</i>	<i>74</i>
<i>Figure 45: ESA CCI SM PASSIVE product correlation with SAC-SMA model top layer soil moisture dependency on pixel-wise major soil/vegetation type fraction size. ....</i>	<i>75</i>

Figure 46: Distance-based decay of inter-pixel soil moisture cross-correlation for ESA CCI ACTIVE and PASSIVE soil moisture data and SAC-SMA top layer model soil moisture data, as well as spatial autocorrelation for FMI interpolated precipitation observations. .... 77

Figure 47: Pearson correlation coefficient R for GPCP v1.2 precipitation estimates and a) CCI SM v0.1, b) CCI v02.1, c) CCI v02.2, d) CCI v03.2, e) CCI v04.0, f) CCI v04.1, g) CCI v04.2 and h) CCI v05.0 for the period 1997 to 2010. Calculations are based on half-monthly absolute values. .... 82

Figure 48: Pearson correlation coefficient R for GPCP v1.2 precipitation estimates and a) CCI SM v0.1, b) CCI v02.1, c) CCI v02.2, d) CCI v03.2, e) CCI v04.0, f) CCI v04.1, g) CCI v04.2 and h) CCI v05.0 for the period 1997 to 2010. Calculations are based on half-monthly anomaly values. .... 83

Figure 49: Pearson correlation coefficient R for ERA-Land soil moisture estimates a) CCI v02.1, b) CCI v02.2, c) CCI v03.2, d) CCI v04.0, e) CCI v04.1, f) CCI v04.2 and g) CCI v05.0 for the period 1997 to 2013. Calculations are based on half-monthly absolute values. .... 84

Figure 50: Pearson correlation coefficient R for ERA-Land soil moisture estimates and a) CCI v02.1, b) CCI v02.2, c) CCI v03.2, d) CCI v04.0, e) CCI v04.1, f) CCI v04.2 and g) CCI v05.0 for the period 1997 to 2013. Calculations are based on half-monthly anomaly values. .... 85

Figure 51: Pearson correlation coefficient R for GIMMS NDVI3g estimates and a) CCI v02.1, b) CCI v02.2, c) CCI v03.2, d) CCI v04.0, e) CCI v04.1, f) CCI v04.2 and g) CCI v05.0 for the period 1997 to 2013. Calculations are based on half-monthly absolute values and a shift of one half-month was applied. .... 86

Figure 52: Pearson correlation coefficient R for GIMMS NDVI3g estimates and a) CCI v02.1, b) CCI v02.2, c) CCI v03.2, d) CCI v04.0, e) CCI v04.1, f) CCI v04.2 and g) CCI v05.0 for the period 1997 to 2013. Calculations are based on half-monthly anomaly values and a shift of one half-month was applied. .... 87

Figure 53: Difference between Pearson correlation coefficient R derived for GPCP v1.2 precipitation estimates and different versions of CCI SM for the period 1997 to 2013. Calculations are based on half-monthly absolute values. .... 88

Figure 54: Difference between Pearson correlation coefficient R derived for GPCP v1.2 precipitation estimates and different versions of CCI SM for the period 1997 to 2013. Calculations are based on half-monthly anomaly values. .... 89

Figure 55: Difference between Pearson correlation coefficient R derived for ERA Land estimates and different versions of CCI SM for the period 1997 to 2013. Calculations are based on half-monthly absolute values. .... 90

Figure 56: Difference between Pearson correlation coefficient R derived for ERA Land estimates and different versions of CCI SM for the period 1997 to 2013. Calculations are based on half-monthly anomaly values. .... 91



Figure 57: Difference between Pearson correlation coefficient  $R$  derived for GIMMS NDVI3g estimates and different versions of CCI SM for the period 1997 to 2013. Calculations are based on half-monthly absolute values and a shift of one half-month was applied for deriving  $R$ . . 92

Figure 58: Difference between Pearson correlation coefficient  $R$  derived for GIMMS NDVI3g estimates and different versions of CCI SM for the period 1997 to 2013. Calculations are based on half-monthly anomaly values and a shift of one half-month was applied for deriving  $R$ . . 93



## List of Tables

Table 1: Overview of the products used for the different ECV validation studies. The data are available in different temporal resolution and applied in daily resolution (except for the NILU time series, where they are applied at 6 hr resolution). ..... 23

Table 2: Pearson correlation coefficient calculated for each pair of soil moisture datasets, including ESA CCI ECV v03.2. Correlation levels are all statistically significant (p-values < 0.05). Austrian regions under investigation. .... 57

Table 3: Pearson correlation coefficient calculated for each pair of soil moisture datasets, including ESA CCI ECV v03.2. Correlation levels are all statistically significant (p-values < 0.05). Danish regions under investigation..... 61

Table 4: Pearson correlation coefficient calculated for each pair of soil moisture datasets, including ESA CCI ECV v03.2. Correlation levels are all statistically significant (p-values < 0.05). Italian regions under investigation. .... 65

*Table 5: ESA CCI SM product yearly correlations with daily weighted in situ observations .... 69*

*Table 6: ESA CCI SM product summer period number of days with observations ..... 69*

*Table 7: Yearly, study domain wide average inter-pixel soil moisture cross-correlation and inter-pixel soil moisture cross-correlation dependency on (correlation with) distance between pixel-pairs for ESA CCI ACTIVE and PASSIVE soil moisture data and SAC-SMA top layer model soil moisture data, as well as spatial autocorrelation for FMI interpolated precipitation observations. .... 77*

## Acronyms

ABS	Absolute soil moisture
AMSR-E	Advanced Microwave Scanning Radiometer - Earth Observing System
ASAR	Advanced Synthetic Aperture Radar
ASCAT	Advanced SCATterometer
ATBD	Algorithm Development Document
CAL-VAL	Calibration and validation
CDF	Cumulative Distribution Function
CCI	Climate Change Initiative
DA	Data Assimilation
ECMWF	European Centre for Medium Range Weather Forecasts Environmental Satellite
ENVISAT	
ECV	Essential Climate Variable
ECV SM	Soil moisture time series developed in framework of ESA CCI
EnKF	Ensemble Kalman Filter
EO	Earth Observation
ERA	European Centre for Medium-Range Weather Forecasts (ECMWF) Re-Analysis
ESA	European Space Agency
ISMN	International soil moisture network
LSM	Land surface model
LTA	Long-term anomaly of soil moisture
NASA	National Aeronautics and Space Administration
NCAR	National Center for Atmospheric Research
NH	Northern Hemisphere
PSD	Product Specification Document
PVIR	Product Validation and Intercomparison Report
RMSD	Root mean square difference
RMSE	Root mean square error
SAC-SMA	Sacramento Soil Moisture Accounting model
SM	Soil moisture
SMOS	Soil Moisture and Ocean Salinity
SSM	Surface soil moisture
STA	Short-term anomaly of soil moisture
TUW	Vienna University of Technology
ubRMSD	Unbiased root mean square difference
VITO	Vlaamse Instelling voor Technologisch Onderzoek
VWC	Volumetric water content
WMO	World Meteorological Office
WRF	Weather Research and Forecasting model

## 1 Executive Summary

Within the framework of the European Space Agency (ESA) Climate Change Initiative (CCI) soil moisture project we developed a 40-year (1978-2018) soil moisture time series (ECV SMv04.2), which consists of three products: an active data set, a passive data set and a combined data set. It provides daily surface soil moisture with a spatial resolution of 0.25 °. The merged product as well as its active and passive sources are publicly available to the user on the project webpage (<http://www.esa-soilmoisture-cci.org>). Furthermore, the detailed description of its development (ATBD, RD-02), the product specification (PSD, RD-03), and a product user guide (PUG, RD-04) are publicly available on the project webpage (<http://www.esa-soilmoisture-cci.org>).

The validation of the final merged data set ECV SMv04.2 is an important mechanism within the production process. The validation is conducted by project partners, who are independent from the development of the ECV SMv04.2 data set. Five different validation and intercomparison studies are conducted from project partners, which are collected and described in detail in Section 5 of this document, the Product Validation and Intercomparison Report (PVIR). The studies provide various comparisons, including time series at the point-scale using soil moisture observations and soil moisture estimates from different data sources: in-situ measurements, land surface models, land surface data assimilation systems, land surface reanalyses as well as alternatively available remotely sensed products. Details of each individual study follow.

**ETH:** The first study evaluates the ECV SM products (from v0.1 up to the latest ECV SM product release, v04.2) over four regions (North America, Europe, Sub-Saharan Africa, and Australia) using in-situ observations from the ISMN and using the ERA-land soil moisture reanalysis at 0.25 degree resolution. This evaluation uses the three top layers of the ERA-land soil moisture reanalysis to compare the ECV SM products.

The evaluation shows no clear regions where the ECV SM products agree very well or very poorly with in-situ observations. However, the highest and most consistent correlations were found over Australia where the in-situ observations were located in the same climatic region. The CCI SM products correlate higher with the observed in-situ soil moisture at 5 cm than at 10 cm depth. This distinction in moisture at different depths was less clear for the comparison with ERA-land. Over the US, the ESA CCI CM products did show consistently higher correlation with the in-situ observations in areas of grassland than compared to areas of forest vegetation cover. This distinction for different vegetation types was less clear for the comparison with the ERA-land reanalysis.

**GEOVILLE:** The second study carries out an evaluation of the ESA CCI SM products (v04.2 and v05.0) using the ERA-land soil moisture reanalysis, the GPCP v1.2 precipitation product, and the GIMMS 3g NDVI between 1997 and 2013. All of the evaluation datasets are aggregated to a spatial resolution of 0.25° at half-monthly intervals. The evaluation is based on calculated anomalies, correlation coefficients, trend analysis, and the differences between the correlations obtained from the two ESA CCI SM product version examined.

The ESA CCI SM v05.0 product correlates well with the GPCP precipitation observations and the ERA-land soil moisture reanalysis. Although the ESA SM v05.0 product correlates with

NDVI over many areas of the globe, there are important instances where the soil moisture product negatively correlates with NDVI observations, i.e., over the Sahara and over the Boreal forest regions. There are also important differences between the v04.2 and v05.0 versions of the ESA CCI SM product. Most notably, less pronounced negative correlation coefficients in the boreal forest regions when correlating ESA CCI SM and ERA-Land volumetric soil moisture.

In addition to these quantitative evaluations of the products, this second study also carries out a qualitative verification of the v05.0 product and identifies inconsistencies in the data.

**NILU:** The third study addresses the assimilation of the ESA CCI SM v04.2 product over the US. The ESA CCI SM v04.2 product is assimilated into the SURFEX land surface model. Both the SURFEX land surface model and the assimilation analysis are compared to in-situ observations from the USCRN network. The SURFEX model performs extremely well over the US as it is forced by a combined radar and rain gauge precipitation product and correlates very well with in-situ observations of surface layer and root zone soil moisture. The assimilation of the ESA-CCI SM v04.2 product into SURFEX only makes marginal improvements to the analysis over and above the land surface model. This is an effect of assimilating satellite observations of soil moisture into a very high quality land surface model. Nevertheless, there is a clear signal of irrigated moisture in the data assimilation diagnostics that shows clearly the presence of additional information in the ESA CCI SM product potentially improving the SURFEX analysis.

**UCC:** The fourth study is based on the validation of the ECV CCI SM v03.2 time series with soil moisture (SM) estimates from Synthetic Aperture Radar (SAR) data retrieved from ENVISAT ASAR Wide Swath (WS) images using the change detection algorithm developed by TU-Wien (Wagner et al., 2007; Pathe et al., 2009). In-situ measurements are also used to assess the quality of the satellite soil moisture products. This study focuses on three regions, which differ according to climate zone, land cover, and topographic conditions (Austria, Denmark and Italy). The temporal behaviour of the scaled absolute soil moisture is analysed through the comparisons between the time series provided by the ECV CCI SM v03.2 and ASAR WS products. The results achieved in Denmark and in flat areas of Italy showed high correlations values during the inter-comparison of the SM time series. On the contrary, extensive forest coverage and/or high topographic complexity could possibly be the reasons why in hilly or mountains areas of Austria and Italy we find poor agreement between the soil moisture datasets. The ASAR SM and ESA CCI SM datasets are also compared spatially, aiming to improve our understanding of the capability of ESA CCI SM v03.2 to represent soil moisture dynamics over a relatively large area (0.25 x 0.25 degrees). The presence of high and reasonably homogeneous correlation patterns within the observed areas supports the reliability of the ESA CCI SM v03.2 product.

**FMI:** The fifth study performs an in-depth evaluation/validation of the ESA CCI soil moisture products over a typical northern boreal forest/taiga environment, namely within and around the multidisciplinary research centre of Sodankylä, in Northern Finland. The validation study focuses on comparing the different versions of the ESA CCI soil moisture datasets, including ACTIVE and PASSIVE soil moisture retrievals, released during 2017 and 2018; namely versions v03.2, v04.1 and v05.0. Weighted in situ observation based validation and comparisons are performed in a single ESA CCI SM pixel for snow free summer periods (June–September)



between the years 2012 and 2017. A spatially distributed soil moisture model (SAC-SMA) is used to assess both sub-pixel variability and multi-pixel, spatially distributed variability of ESA CCI soil moisture datasets with simulated soil moisture time series. The multi-pixel, spatially distributed, validation study domain covers an area of 155 km by 140 km and encloses 70 ESA CCI soil moisture product pixels/SAC-SMA model grid cells.

The overall validation results provided in this study show far better ESA CCI SM product correlation to the used reference soil moisture datasets than previous studies have shown for boreal environment sites. Average multi-pixel correlation between v05.0 and v04.1 with SAC-SMA model estimates are relatively similar, i.e. years during which the v04.1 product exhibits good or poor correlation, the newest v05.0 product exhibits similar patterns. A clear improvement from version v03.2 can however be observed, against both newer product versions. As other studies have found, there exists a clear positive trend in improved soil moisture retrieval accuracy towards the later part of the analysis period for all examined product versions and with both ACTIVE and PASSIVE products. The COMNIED product clearly offers the most stable performance when compared to both PASSIVE and ACTIVE retrievals, although it contains the least amount of observations. This may, however, also be a key factor in achieving the more stable performance. A major shortcoming in all of the ESA CCI soil moisture products and versions is the amount of missing data. This renders both validation and applicability in any type of end user applications challenging. In particular with the newest (v05.0) ESA CCI PASSIVE product; between 2010 and 2014 only half of the 70 pixels investigated contained PASSIVE observations and before 2010 only 16% of the pixels had any data at all.

The ACTIVE product exhibits high correlations with SAC-SMA soil moisture estimates during most analyzed years. The presence of high inter-pixel soil moisture time series cross-correlation, even between pixels with very different soil/vegetation type distributions, as well as the inconsistent performance between analyzed years, is however problematic. A more detailed spatial analysis of the ESA CCI v.04.1 product's performance shows that the ESA CCI PASSIVE soil moisture product tends to perform well in pixels containing large organic soil fractions. Organic soils (bogs) tend to react slowly to precipitation and represent soil moisture change as a smooth trend. Since soil moisture in organic soils tend to represent a trend, correlation to this is as a positive thing. In contrast, the PASSIVE product exhibits poor correlation with pixels containing large fractions of shallow soils, i.e., rapidly responding type soils. This suggests that the ESA CCI PASSIVE product is able to, in most cases, capture the temporal trend in soil moisture variation. Although the trend is seemingly captured, rapid response to precipitation events is less accurate. With the ACTIVE product there is a very significant dependency on shallow soils fraction size with SAC-SMA model based soil moisture correlation. This, and the presence of high inter-pixel soil moisture time series cross-correlation, as well as the known rapid response of these soil types to both precipitation and evaporation, raises the question that the relatively good performance of the ACTIVE product with SAC-SMA model top soil estimates may be good "for the wrong reasons". We therefore argue that it is possible that ACTIVE soil moisture retrievals likely respond mainly to direct changes in precipitation and possibly to moisture on vegetation surfaces rather than to actual moisture in the top soil layer.



## 2 Documents

### 2.1 Applicable documents

The documents outlined below detail the scope and focus for the work reported in this document.

[AD-1] Phase 2 of the ESA Climate Change Initiative Soil- Moisture CCI. ESA Contract No: 4000112226/14/I-NB.

[AD-2] ESA Climate Change Initiative Phase 2, Statement of Work, European Space Agency, CCI-PRGM-EOPS-SW-12-0012.

### 2.2 Reference documents

[RD-01] Product Validation and Intercomparison Report (PVIR) v2.0, Nov. 2014

[RD-02] Algorithm Theoretical Basis Document (ATBD) v4.2 (Executive Summary), Dec. 2015 – the ESA CCI website also includes ATBD documents describing the merging procedure, and the active and the passive elements of the combined ECV product

[RD-03] Product Specification Document (PSD), v4.2, Jul. 2015

[RD-04] Soil Moisture ECV Product User Guide (PUG), v1.0, Dec 2015

[RD-05] Climate Research Data Package (CRDP), v4.2, Dec. 2015

### 2.3 Bibliography

A complete bibliographic list, detailing scientific texts or publications that support arguments or statements made in this document is provided in Section 8.



## **3 Introduction**

### **3.1 Purpose of the document**

The purpose of the PVIR is the final validation of the soil moisture time series, which is developed in the framework of the ESA CCI soil moisture project. It includes five independent validation studies, which were conducted by the project partners as well as presented and discussed during several project meetings.

### **3.2 Target audience**

This document targets users of the soil moisture time series produced, as well as the scientific community. It demonstrates the value of an intercomparison between the ECV SM product and other available soil moisture products.

### **3.3 Important documents**


Detailed information on the ECV SMv04.2 time series is provided in the Product Specification Document (PSDv4.2), the Algorithm Development Document (ATBDv4.2), as well as the Product Validation and Intercomparison Report (PVIRv2), produced in the framework of the ESA CCI soil moisture project. These documents are listed in Section 2 and are publicly available on the project webpage (<http://www.esa-soilmoisture-cci.org>).

### 3.4 Product Change Log

Table 1 Summary ESA CCI SM Versions

Dataset Version	Release date	Public	Key Users	Project Partners	Major Changes Since Previous Versions	ATBD Version
v05.0	2018-04-09			X	<p>Major algorithmic change. The datasets are now decomposed into climatologies and anomalies before scaling and triple collocation. At the end of the processing, these are recombined to provide the bulk soil moisture signal.</p> <p>Datasets updated. SMAP now included from 2015 onwards. LPRM version 6 data used for all passive sensors. H113 ASCAT product is included for A and B sensors. GLDAS v2.1 is now used for the scaling of data (previously v1 was used).</p>	5.0 (not yet produced)
v04.4	2018-11-12	X			No algorithm changes since v04.1. Temporal extension to 2018-06-30.	4.4
v04.3	2018-04-17				<p>No algorithm changes since v04.1. Temporal extension to 2017-12-31.</p> <p>Not released, but used for State of the Climate BAMS report 2018.</p>	4.3
v04.2	2018-01-12	X			No algorithm changes since v04.1.	4.2
v04.1	2017-08-02		X	X	Masking of unreliable retrievals is undertaken prior to merging.	-

Dataset Version	Release date	Public	Key Users	Project Partners	Major Changes Since Previous Versions	ATBD Version
v04.0	2017-03-20			X	The combined product is now generated by merging all active and passive L2 products directly, rather than merging the generated active and passive products. Spatial gaps in TC-based SNR estimates now filled using a polynomial SNR-VOD regression. sm_uncertainties now available globally for all sensors except SMMR. The p-value based mask to exclude unreliable input data sets in the COMBINED product has been modified and is also applied to the passive product.	-
v03.3	2017-11-13	X			Temporal extension of ACTIVE, PASSIVE and COMBINED datasets to 2016-12-31.	3.3
v03.2	2017-02-14	X			SMOS temporal coverage extended. Uncertainty estimates for soil moisture now provided from 1991-08-05 onwards (ACTIVE), and from 1987-07-10 onwards (PASSIVE, and COMBINED). Two new quality flags introduced.	3.2
v03.1	2016-11-02		X	X	Blending made more conservative concerning the inclusion of single low-accuracy observations (on the cost of temporal coverage). Integration of Metop-B ASCAT. Error estimates which are used for relative weight estimation now provided alongside with the merged soil moisture observations.	-

 <b>soil moisture</b> cci	Product Validation and Intercomparison Report (PVIR) Revision 3	Version 2.6 Date 29 November 2018
---	--	--------------------------------------

Dataset Version	Release date	Public	Key Users	Project Partners	Major Changes Since Previous Versions	ATBD Version
v03.0	2016-04-25			X	Introduction of new weighted-average based merging scheme. Miras SMOS (LPRM) now integrated into the data products. Blending weights provided as ancillary data files.	-
v02.3	2016-02-08	X			Temporal extension to 2015-12-31. Valid_range in netCDF files now set to the packed data range.	-
v02.2	2015-12-17	X			No changes.	-
	2015-08-06		X	X	In ancillary files latitudes now goes from positive to negative values.	-
	2015-07-31		X	X	Email address added to metadata.	-
	2015-03-17			X	Temporal coverage extended (Nov-1978 to Dec-2014). Improvement in the flagging of the active data where extreme high and low values are filtered.	-
v02.1	2014-12-03			X	Change of product name to ESA CCI SM. Soil moisture values (flagged with values other than 0) are now set to NaN.	-
v02.0	2014-07-10	X			Provision of ancillary datasets (land mask, porosity map, soil texture data, AMSR-E VUA-NASA Vegetation Optical Depth averaged over the period 2002-2011, global topographic complexity and Global Wetland fraction.	-

Dataset Version	Release date	Public	Key Users	Project Partners	Major Changes Since Previous Versions	ATBD Version
v01.2	2014-03-03			X	All datasets updated to include days where no observations are available.	-
v01.1	2014-02-19			X	Active, passive and combined products made available. Dataset time span: 1978-11-01 to 2013-12-13 (passive and combined) and 1991-08-05 to 2013-12-13 (active). Using new land mask based on GSHHG 2.2.2. WindSat and preliminary AMSR2 included. ERS2 included in AMI-WS dataset. Active data resampled with Hamming window function. Improved rescaling algorithm. Data gaps in 2003-02-16 to 2006-12-31 filled with AMSR-E data.	-
v 0.1	2012-06-18			X	Combined product only including passive sensors (SMMR, SSM/I, TMI, AMSR-E; active: AMI-WS, ASCAT) with time span: 1978-11-01 to 2010-12-31. NetCDF-3 classic CF1.5 compliant.	-

## 4 Datasets

The following table shows an overview of the datasets used for the validation of the ECV product. For details on the single products identified please refer to the CDRP [RD-05].

*Table 2: Overview of the products used for the different ECV validation studies. The data are available in different temporal resolution and applied in daily resolution (except for the NILU time series, where they are applied at 6 hr resolution).*

Product	Producer	Data class	Description	Period	Coverage
ISMN	TU Wien	In-situ	In-situ soil moisture measurements	January 1950-present and continuing	Global
Soil Moisture retrieved from ENVISAT Advanced Synthetic Aperture Radar	European Space Agency (ESA)	Earth Observation	ASAR Wide Swath data acquired over three test sites in VV and HH polarization and 150 m spatial resolution	27/11/2002 – 12/04/2012	Regional (Austria, Denmark, Italy)
ERA-Land	ECMWF	Land surface model reanalysis	Reanalysis data for volumetric soil water at different levels of the soil profile	1979-2010	Global
Global precipitation climatology project v1.2(GPCP)	NCAR	Earth observation	Satellite and rain gauge based observation dataset of precipitation	10/1996-11/2015	Global
GIMMS 3g Normalized Difference Vegetation Index (NDVI)	VITO	Earth observation	NOAA AVHRR GIMMS NDVI3g data cover the period from 1981 to 2013 and constitute the latest release (third generation) of this unique long term NDVI time series of the GIMMS research group. The data is available in 0.07 x 0.07° ground resolution and half-monthly time intervals.	1981-2013	Global
SURFEX land surface model	NILU	Land surface model	Soil moisture at a spatial resolution of about 9 km	April 2015 – December 2016	United States (lower 48 states)
Soil moisture analyses, surface and root zone	NILU	Land data assimilation (EnKF) using the SURFEX LSM	Soil moisture at a spatial resolution of about 25 km	April 2015 – December 2016	United States (lower 48 states)
Land Surface Model (SAC-SMA)	FMI	Land Surface Model	Soil moisture estimate	2003 to 2013	Regional
Point scale soil moisture in-situ observations	FMI	In-situ	In-situ soil moisture measurements	2005 to 2012	Regional
Point scale snow depth in-situ observations	FMI	In-situ	In-situ snow depth measurements	2007 to 2013	Regional



## 5 Validation studies

The following section includes five validation studies conducted by project partners who are independent from the development of the ECV SM data sets.

### 5.1 Comparison to global climate, LSM simulations and other large-scale estimates (ETH)

Contributors: N. Nicolai-Shaw, M. Hirschi and Sonia I. Seneviratne (ETH Zürich)

#### 5.1.1 Datasets and data processing

##### CCI-SM

To date various versions of the CCI soil moisture product are available. We use here v0.1, v02.0, v02.2, v03.3, and v04.2 of the combined product derived from the collocated C-band scatterometer data set and the collocated multi-frequency radiometer data set. The spatial resolution is 0.25 degree, and coverage is global. Data is presented in  $\text{m}^3\text{m}^{-3}$  and represents soil moisture in the top few millimeters to centimeters of the soil [Kuria *et al.*, 2007]. Data is daily, but the quality and availability of the data has increased over time, as the number of available satellites has increased [Dorigo *et al.*, 2017, 2015, 2010].

##### ISMN

In-situ soil moisture measurements are obtained from the International Soil Moisture Network (ISMN). The ISMN database consists of measurements from various networks. If needed the data is transformed so that it is consistent in units ( $\text{m}^3 \text{m}^{-3}$ ), then quality checked and flagged [Dorigo *et al.*, 2011]. The analyses are based on a recent download from 12 April 2018.

##### ERA-Land

To determine the influence of soil depth on soil moisture variability we use ECMWF's ERA-Interim/Land soil moisture (ERA-Land) [Balsamo *et al.*, 2012, 2015; Dee *et al.*, 2011]. ERA-SM is available as a re-gridded 0.25 degree soil moisture product, corresponding to the CCI-SM resolution, and has global coverage. Here we use the top three layers, which represent 0-7 cm, 7-28 cm, and 28-100 cm soil depths. Data is aggregated to daily averages.

##### Data processing

We consider ISMN soil moisture measurements from 5 and 10 cm depth that have at least one year of data and focus on the US, Europe, Africa and Australia, see Figure 1. This selection results in 363 individual soil moisture time series from 18 different networks. Of these, 290 time series are available for 5 cm depth, and 73 for 10 cm depth. Soil moisture time series from the grid cells in which the stations fall are extracted from CCI-SM, and ERA-SM for this comparison.



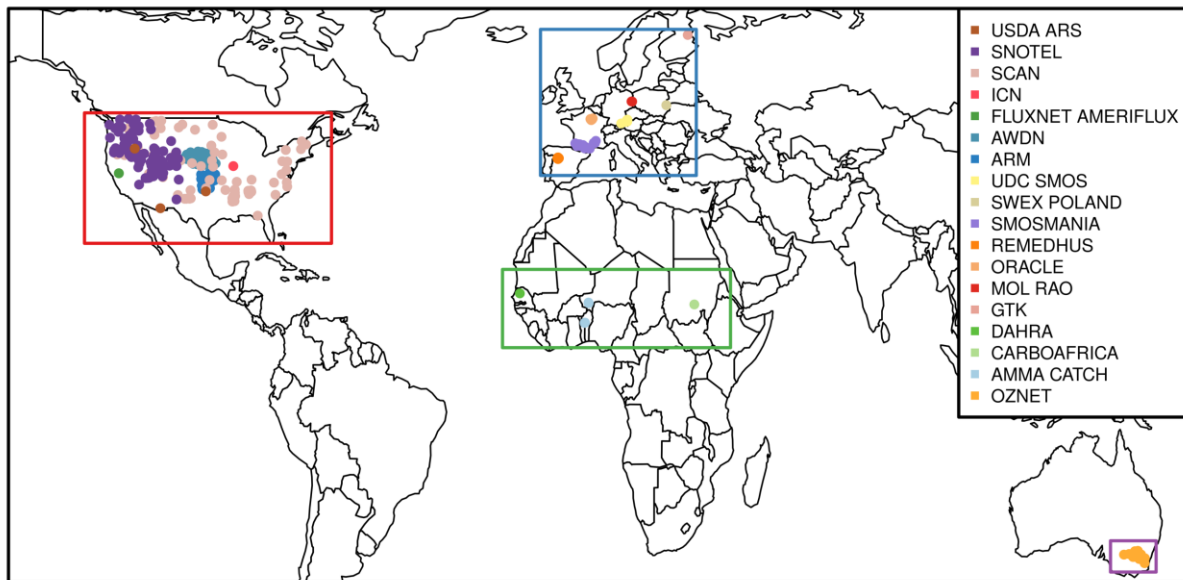


Figure 1: Overview of the spatial coverage of the stations considered in this study, rectangles indicate the four focus areas of the comparison, i.e., the United States (US, red), Europe (EU, blue), Africa (AF, green), and Australia (AUS, purple). Stations are color coded by network, see Figure 2 for the legend.

### **Comparisons of the products**

In this study, we focus on the evaluation of CCI-SM v04.2 and compare it to its forerunners v0.1, v02.0, v02.2, and v03.3, as well as to ERA-Land layer 1 and layer 2 soil moisture. All considered data sets have a different temporal coverage, and we account for this by masking for common data availability and constraining our investigation to the period 1996-2010, see Figure 2.

To account for the different units and dynamic ranges of the products, and to remove systematic differences between the products, the CCI-SM, and ERA-Land soil moisture data are linearly scaled with respect to the mean and standard deviation of the ISMN in-situ data [Brocca *et al.*, 2010]. Then, the long-term inter-annual anomalies are calculated based on subtracting the long-term mean using a 5-day window.

Agreement between in-situ data and CCI-SM, and ERA-SM is determined by the Pearson correlation between time series. Note that because data availability varies among locations, the time period (and amount of data) used to calculate the correlation differs between locations. Also, most of the available data is from the US, so a general global conclusion cannot be made. All investigations are performed on mean daily soil moisture, and results are shown for both the absolute scaled data, as well as the anomalies.

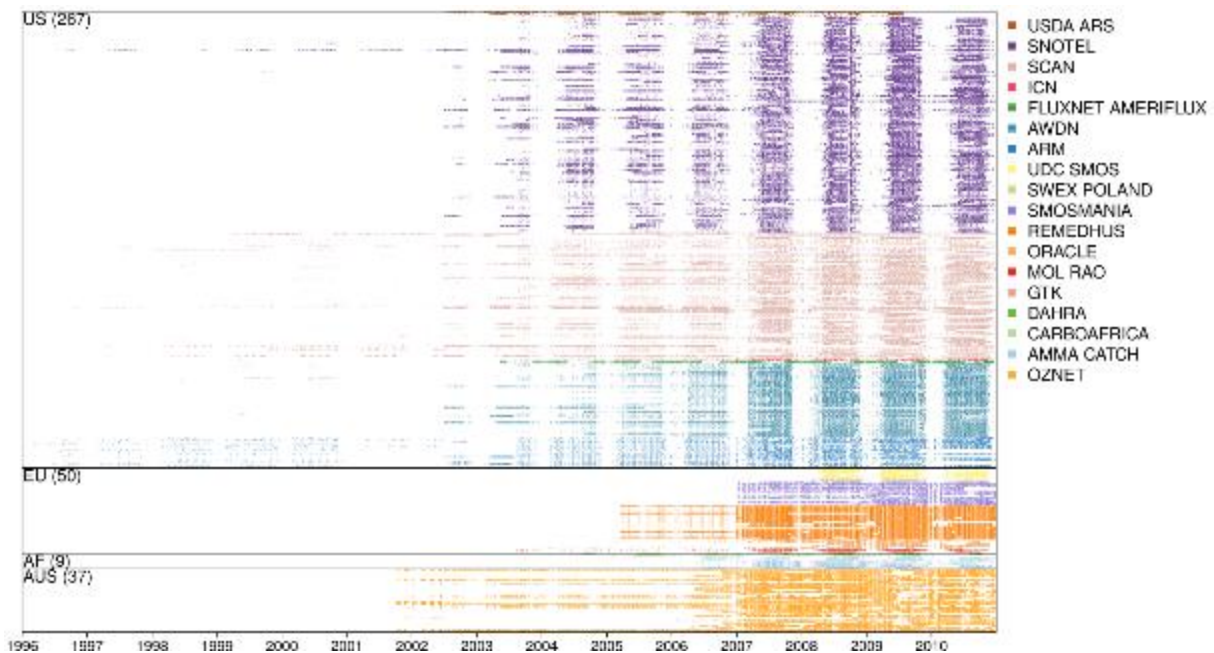


Figure 2: Overview of the temporal coverage of the stations considered in this study, after masking for common data availability, split per region. The number of stations per region is indicated in brackets.

## 5.1.2 Results in-situ comparisons

### General findings

We first focus on the correlations in the US only, see Figure 3. Correlation is highest for the absolute values and drops considerably for the anomalies. We find that the spatial pattern of the correlations is rather scattered, and there are no clear areas in which the products agree either very well or very poorly with in-situ soil moisture. Also, no pronounced difference in performance can be found between networks (not shown).

There is a slight increase in correlation for each subsequent CCI-SM product, most notable when comparing v0.1 to v04.2. ERA-SM layer 1 shows better agreement with in-situ soil moisture than CCI-SM, especially for the anomalies.

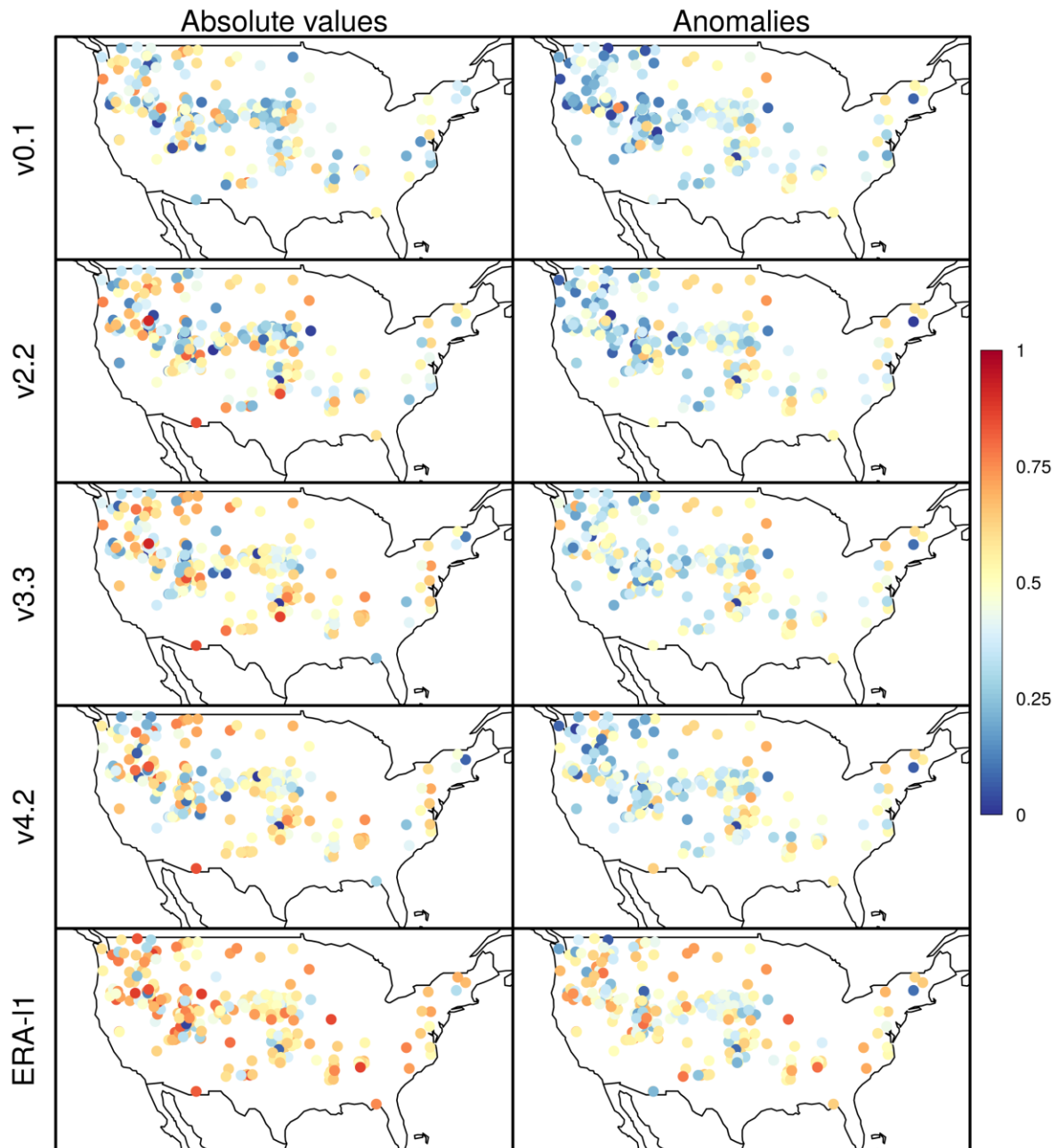


Figure 3: Correlation between in-situ soil moisture and CCI-SM for versions v0.1, v02.0, v02.2, v03.3, and v04.2, as well as ERA-SM layer 1 (ERA1, 0-7 cm), for absolute soil moisture (left) and the anomalies (right).



### **The influence of measuring depth**

CCI-SM represents soil moisture in only the top few millimeters to centimeters of the soil [Kuria *et al.*, 2007]. To determine the influence of measuring depth on the correlation we differentiate between measurements at 5 and 10 cm depth, see Figure 4. For each product, we distinguish between three different regions (US, EU, and AUS) and show the results for the absolute values (top) as well as the anomalies (bottom). Circles denote correlations with in-situ measurements taken at 5 cm depth, and triangles at 10 cm depth.

**CCI-SM:** For the US and Europe, there is a large spread in the derived correlations, likely due to the large spread in climate conditions that the stations are located in. For Australia, the spread is much smaller, there are far fewer stations here and they are all located in the south-eastern part of the continent. For the US, the absolute values show correlations ranging between 0.1 to 0.8 for 5 cm, and 0.1 to 0.6 for 10 cm, with the median correlation for the shallower 5 cm in-situ measurements being consistently higher. For Europe, the correlation is higher with a median value around 0.6 for 5 cm depth for the first three versions, and over 0.7 for v04.2. Again, the correlation with in-situ measurements at 10 cm depth is lower, though there are also far less measurements at this depth. The highest correlations are found in Australia, with up to 0.8 for the median. Again, here the correlation is lower for 10 cm depth.

For the anomalies, there is no clear difference in performance between consecutive products. And for the US, results are similar irrespective of the measuring depth.

**ERA-Land:** Absolute values of ERA-Land layer 1 (ERA-I1) and layer 2 (ERA-I2) show a higher correlation with in-situ measurements at 5 cm depth than at 10 cm depth for the US and Europe. For Australia though, the correlation is less dependent of the measuring depth, both for absolute values and the anomalies. For ERA-I2, there is even a slightly improved correlation with measurements taken at 10 cm. For the anomalies, the results are comparable, though here the median correlation for 10 cm is also higher over Europe. The range of the correlations is similar to CCI-SM but goes up to 0.9 for the absolute values. The median value is around 0.65, thus slightly higher than that of CCI-SM which is around 0.6 for v04.2.

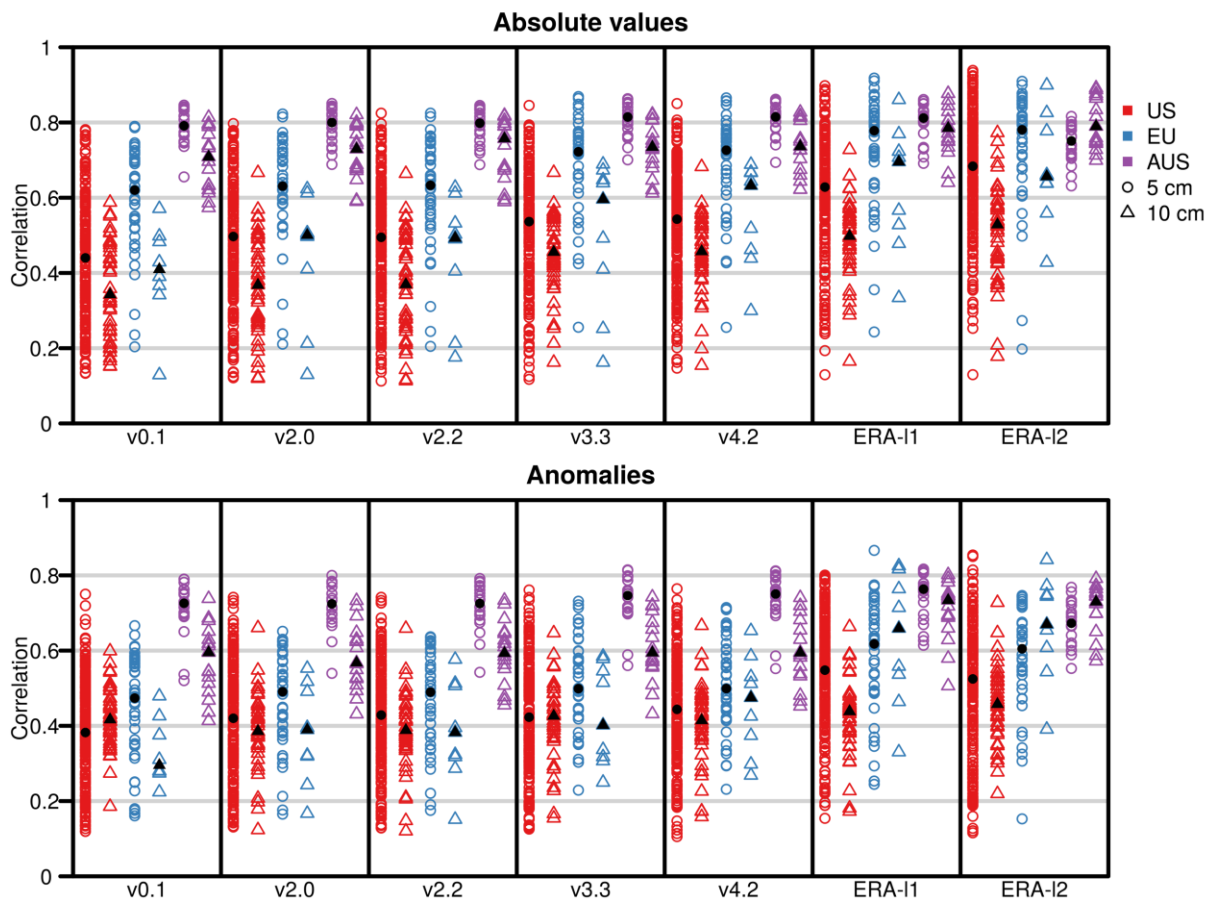


Figure 4: Correlation between in-situ measurements for CCI-SM v0.1, v02.0, v02.2, v03.3, and v04.2, as well as ERA-SM layer 1 and 2 for the absolute soil moisture values (top) and the anomalies (bottom). For each product, we distinguish between 3 regions US, EU, and AUS (red, blue and purple, AF has insufficient data), and the correlation at 5 cm depth (circles) and 10 cm depth (triangles). The black circles/triangles represent the respective median value.

### The influence of land cover

Figure 5 shows the correlations for CCI-SM v0.1, v02.0, v02.2, v03.3, and v04.2, as well as ERA-SM layer 1 over the US for absolute values and their anomalies, differentiating between grassland (orange) and forest (green) sites. As before, we see a decrease in correlation for the anomalies compared to the absolute values for all products. For all versions of CCI-SM there is a notably higher correlation for grassland sites than for forest sites, both for the absolute values as well as the anomalies. For ERA-Land this difference is much smaller.

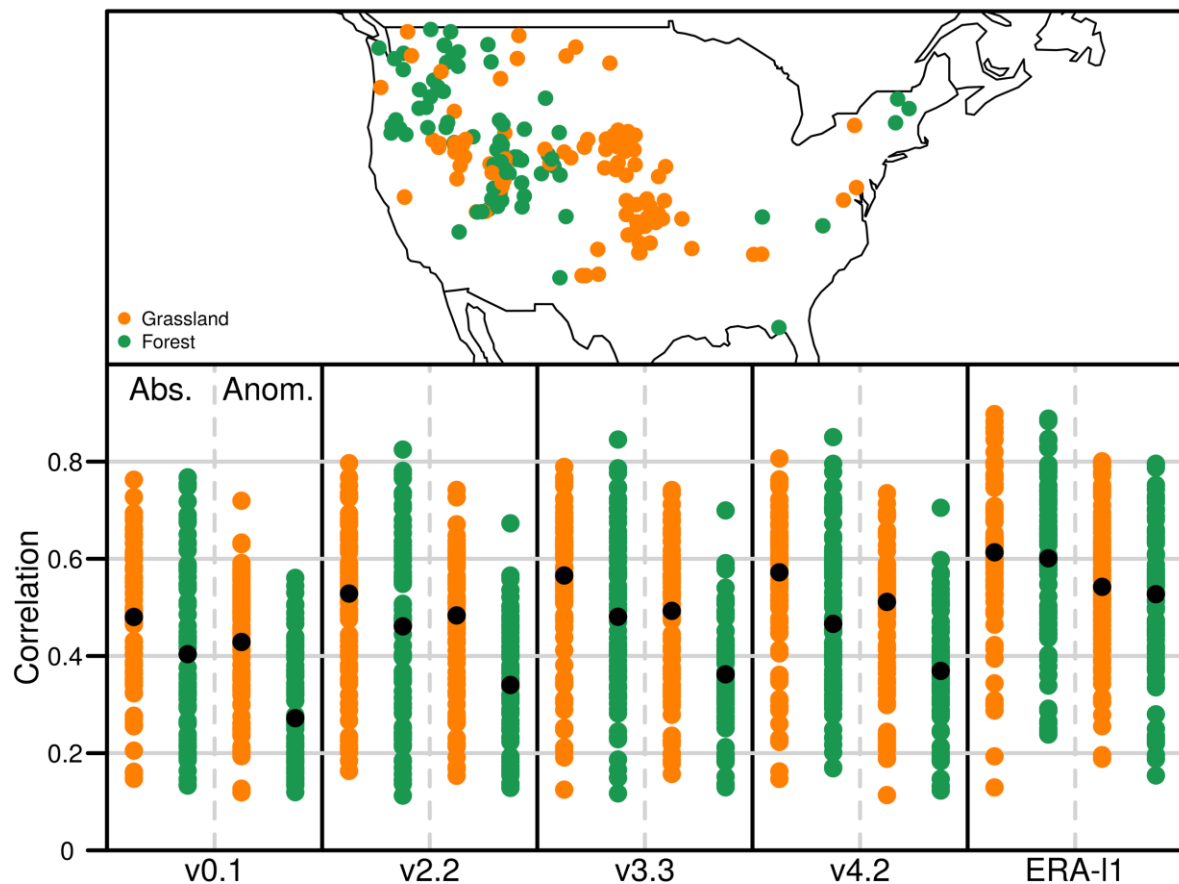


Figure 5: Correlation between in-situ measurements at 5 cm depth and CCI-SM v0.1, v02.0, v02.2, v03.3, and v04.2, as well as ERA-SM layer 1, differentiating between grassland (orange) and forest (green) sites for absolute soil moisture values and anomalies. Again, the black dot denotes the median value.

### Summary

- Spatially scattered pattern in correlations, no clear areas in which the products agree either very well or very poorly with in-situ soil moisture. Though, highest correlations are found in Australia.
- CCI-SM clearly shows a higher correlation with in-situ measurements at 5 cm depth than at 10 cm depth. For ERA-Land this distinction is less clear.
- CCI-SM clearly shows higher correlation with in-situ measurements over grassland sites than over forest sites. For ERA-Land this difference is much smaller.



## 5.2 Validation with GPCP, ERA-Land, and GIMMS NDVI (Geoville)

### 5.2.1 Data Sets

Biophysical and vegetation productivity parameters, namely precipitation (GPCP v1.2), ERA volumetric soil moisture (ERA-Land) and GIMMS 3g Normalized Difference Vegetation Index (NDVI), are used to analyse the relationships to existing ESA CCI soil moisture datasets (v04.2 and v05.0). All datasets are aggregated to a spatial resolution of 0.25° to correspond with the ESA CCI soil moisture and are converted to represent half-monthly observations to align with the temporal resolution of the GIMMS 3g NDVI dataset<sup>1</sup>.

An overview presenting the main characteristics for the biophysical datasets and vegetation index data used is given in Table 2.

### 5.2.2 Methods

#### 5.2.2.1 Anomaly calculation

Time series of anomalies are calculated at half-monthly steps ( $t$ ) for each bio-physical parameter across the reference period 1997 to 2010 as well as 1997 to 2013. The average value ( $\mu$ ) and the standard deviation ( $\sigma$ ) are calculated and the dimensionless anomaly is given by:

$$Anomaly = \frac{\mu_t - \mu_{1997-(2010)2013}}{\sigma_{1997-(2010)2013}}$$

#### 5.2.2.2 Pearson Correlation coefficient

The Pearson correlation coefficient  $r$  is calculated to analyze the relationship between the ESA CCI soil moisture data and the other bio-physical parameters as well as the vegetation productivity index. Correlation analysis is done separately for each of the ESA CCI soil moisture datasets, respectively. This way it is possible to identify potential changes in the relationship on a global scale that might be a consequence of the further development and improvements of the ESA CCI soil moisture data (v05.0).

We calculated the Pearson correlation coefficient for half-monthly estimates of the respective parameters for two time intervals: a) 1997 to 2010 and b) 1997 to 2013 for i) half-monthly values of GPCP v1.2 rainfall estimates, ESA CCI soil moisture, ERA Land and GIMMS NDVI3g, respectively. We applied time shifts up to one half-month to account for the variability in temporal response of rainfall and vegetation to soil moisture. The significance ( $p$ -value) was set at  $p \leq 0.05$ .

---

<sup>1</sup> The first half-month consists of the 1<sup>st</sup> to the 15<sup>th</sup> day of a month and the second half-month from the 16<sup>th</sup> to the end of each month of the year, respectively.



### 5.2.2.3 Differences between correlation coefficients

In a next step we compared the results of the Pearson correlation coefficient analysis by subtracting the Pearson  $r$  values obtained by correlating the biophysical parameters with the earlier CCI version from the ones obtained with the latest version.

$$Diff = Pearson R_{CCI\ v5.0} - Pearson R_{CCI\ vX.X}$$

This allowed us to see changes in the global relationships as a consequence of the further development of the latest CCI SM version (v05.0).

### 5.2.2.4 Trend Analysis

A two-folded trend analysis was performed on the annual sum of GPCP v1.2 precipitations as well as annual means of ESA CCI soil moisture (v0.1 to v05.0), ERA Land and GIMMS NDVI3g using the Theil Sen slope estimator<sup>2</sup> in combination with the Mann-Kendall significance test<sup>3,4</sup>. Calculations are done for both reference period 1997 to 2010 and 1997 to 2013, respectively.

Further, the differences between the global trend maps of the different ESA CCI soil moisture versions are calculated to identify areas with significant changes. This is done for all significant trend results at  $p \leq 0.05$ .

## 5.2.3 Results

### 5.2.3.1 Global relationships for the period 1997 to 2013

#### **Absolute values:**

In general, a strongly positive relationship between GPCP v1.2 precipitation data and CCI SM v05.0 is obtained across the globe, with exceptions of desert areas (e.g. Sahara desert), high elevations (e.g. Himalayas) and the far northern boreal regions of the globe showing negative correlations in some small areas (Figure 6a). These results align with the patterns revealed for the correlation between GPCP v1.2 precipitation and earlier versions of ESA CCI SM (see Appendix, Figure 47), in which especially the Sahelian band showed strong positive correlations.

A similar picture is revealed for the correlation between ESA CCI v05.0 and ERA Land volumetric soil moisture measurements, indicating strong positive correlations, which can be observed across the Sahelian band, North and South America, Europe, South East Asia and Australia (Figure 6b). However, the northern boreal regions of Canada, Europe and Russia are showing strongly negative correlated relationships. But, compared to correlation results with earlier versions of ESA CCI SM, these areas have become less pronounced and are decreased in the latest ESA CCI SM version (see Appendix, Figure 49).

For the correlation between ESA CCI SM v05.0 and GIMMS NDVI3g strong positive correlations are revealed in particular for areas of the Sahelian band, Brazil, East Russia, West Canada and

---

<sup>2</sup> Gilbert, Richard O. (1987), "6.5 Sen's Nonparametric Estimator of Slope", Statistical Methods for Environmental Pollution Monitoring, John Wiley and Sons, pp. 217–219, ISBN 978-0-471-28878-7.

<sup>3</sup> Mann, H.B. 1945. Non-parametric tests against trend, *Econometrica* 13:163-171.

<sup>4</sup> Kendall, M.G. 1975. Rank Correlation Methods, 4th edition, Charles Griffin, London.





parts of India and Australia. However, negative correlations are obtained for the United States, Europe and West Asia (e.g. Kazakhstan), which might be a consequence of large scale intensive agricultural activities in these regions. These areas are persistent throughout the correlation results with earlier versions of ESA CCI SM (see Appendix, Figure 51).

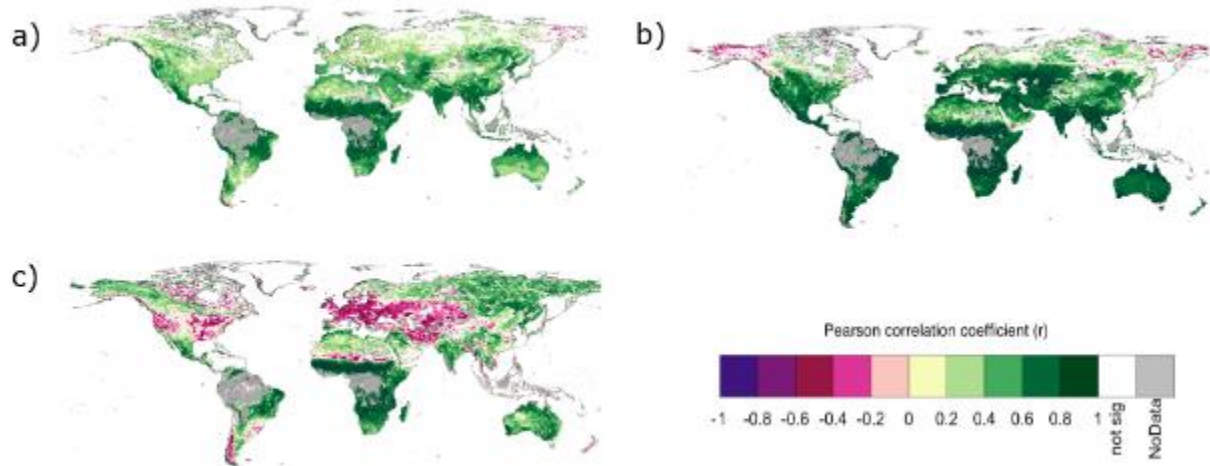


Figure 6: Pearson correlation coefficient calculated for absolute values over the period 1997 to 2013 for a) CCI SM v05.0 and GPCP v1.2 precipitation estimates, b) CCI SM v05.0 and ERA-Land volumetric SM estimates and c) CCI SM v05.0 and GIMMS NDVI ( $x + 1$  shift).

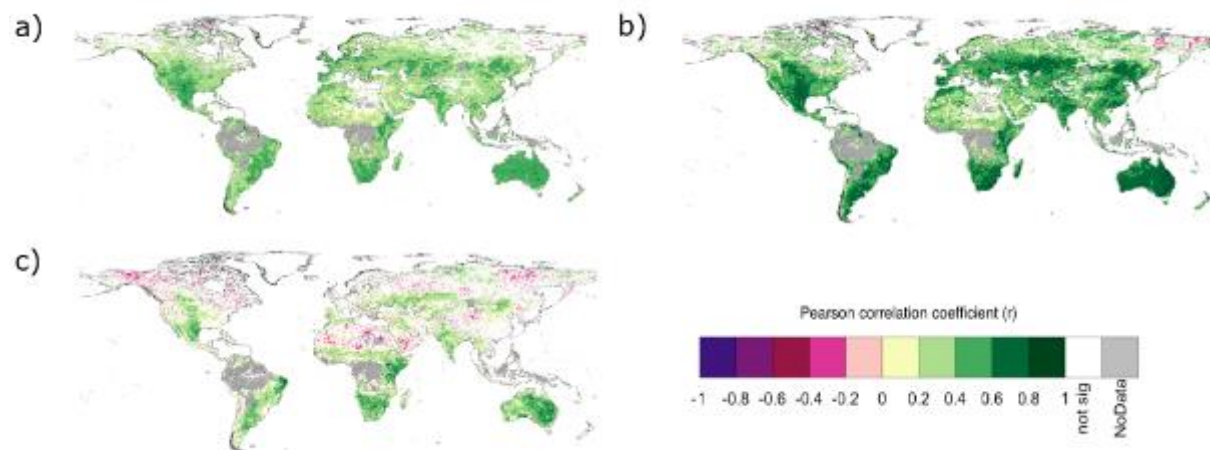


Figure 7: Pearson correlation coefficient calculated for anomaly values over the period 1997 to 2013 for a) CCI SM v05.0 and GPCP v1.2 precipitation estimates, b) CCI SM v05.0 and ERA-Land volumetric SM estimates and c) CCI SM v05.0 and GIMMS NDVI ( $x + 1$  shift).

**Anomaly values:**

Similar Pearson correlation coefficients are obtained when anomaly values are applied, however, R-values are in general lower compared to the result of the half-monthly averages of the bio-physical measurements (Figure 7). Again strong positive correlations are obtained across the globe for CCI SM v05.0 and GPCP v1.2 precipitation estimates (Figure 7a) as well as

CCI SM v05.0 and ERA-Land volumetric SM estimates (Figure 7b). For the correlation between CCI SM v05.0 and GIMMS NDVI3g (x + 1 shift), lower correlation coefficients are obtained with a changing pattern. In fact, negative correlations in North America are less pronounced or slightly positive compared to the absolute values. A similar behaviour is shown in the North Eastern parts of Russia (Figure 7c). The results for the anomaly correlations with earlier versions of ESA CCI SM are provided in Figure 48, Figure 50 and Figure 52 of the Appendix.

### 5.2.3.2 Analysis of the differences

Figure 8 illustrates the differences in the Pearson correlation coefficients for GPCP v1.2 precipitation and ESA CCI SM v04.2 and v05.0, respectively. On a global scale the differences are rather small, especially in areas like the Sahelian band, North America, Europe and Australia for which correlation results have been persistent over the different ESA CCI SM versions. However, larger differences are revealed for the regions in Scandinavia, the eastern parts of Russia, China as well as the Sahara desert (Figure 8). When looking at the differences between the correlation results of earlier versions of ESA CCI SM, a less pronounced pattern is revealed with differences being rather small, except for v02.1 and v02.2 (see Appendix, Figure 53).

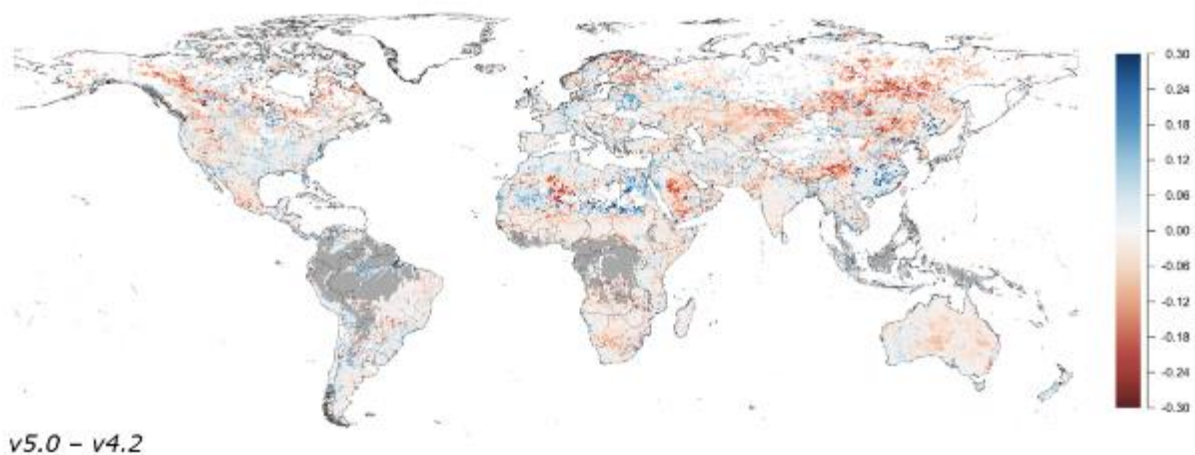
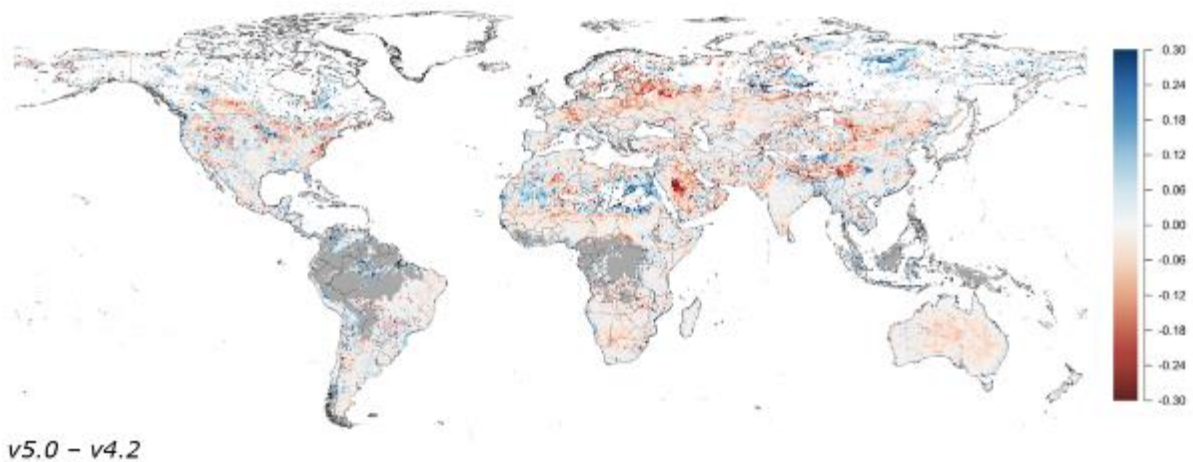


Figure 8: Differences of Pearson correlation coefficient calculated for absolute values over the period 1997 to 2013 for GPCP v1.2 precipitation estimates and CCI SM v04.2 and ESA CCI v05.0.

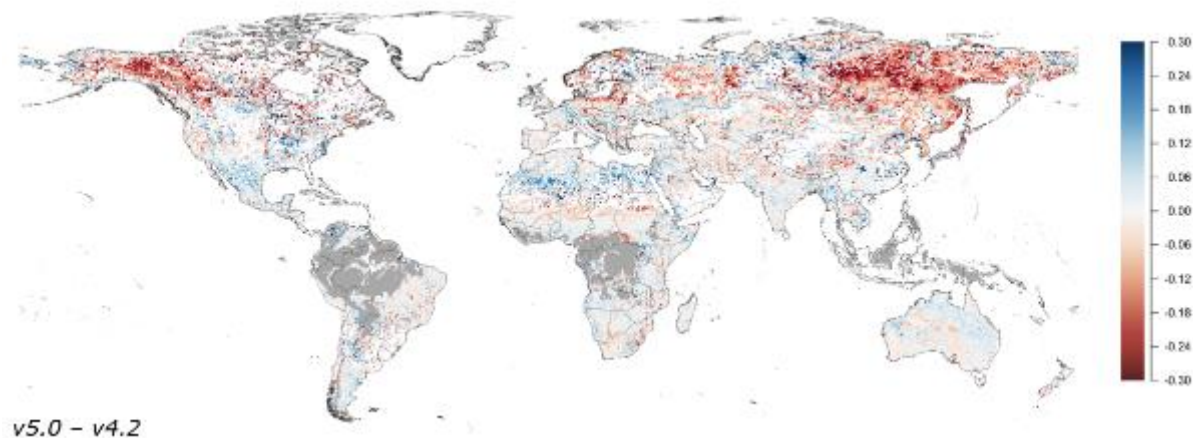
When considering the correlation coefficients between ERA Land volumetric soil moisture and ESA CCI SM v04.2 and v05.0, larger differences are identified in the Sahelian band, as well as the northern parts of North America and the boreal regions of Europe and Russia (Figure 9). Rather negative differences are revealed for earlier versions of ESA CCI SM (see Appendix, Figure 55).



v5.0 - v4.2

Figure 9: Differences of Pearson correlation coefficient calculated for absolute values over the period 1997 to 2013 for ERA-Land volumetric soil estimates and CCI SM v04.2 and ESA CCI v05.0.

In contrast, the differences between the correlation coefficients of ESA CCI SM v04.2 and GIMMS NDVI3g and ESA CCI v05.0 and GIMMS 3g NDVI are rather large, with strong negative results revealed for the boreal regions of Russia and North America (Figure 10). When looking at the correlations between NDVI and earlier versions of ESA CCI SM, differences pronounced in the boreal regions of Eastern Russia as well as Alaska (see Appendix, Figure 57).



v5.0 - v4.2

Figure 10: Differences of Pearson correlation coefficient calculated for absolute values over the period 1997 to 2013 for GIMMS 3g NDVI estimates and CCI SM v04.2 and ESA CCI v05.0.

### 5.2.3.3 Trend Analysis

The Theil-Sen trend analysis revealed strong negative trends in the Northern boreal regions and positive trend results in the area of the Himalayas (Figure 11). Except for Mongolia, China and Saudi Arabia, trends are rather negative, indicating a declining trend in soil moisture.

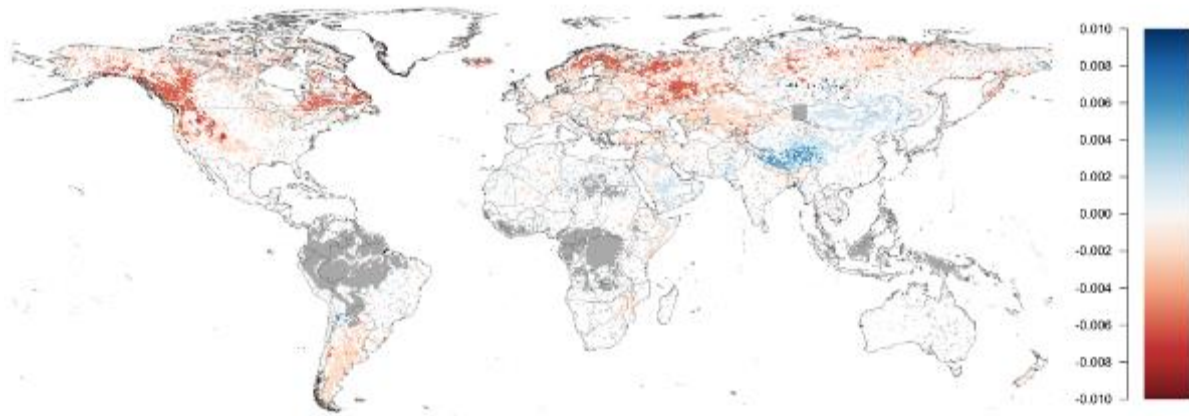


Figure 11: Theil Sen Slope estimator for ESA CCI SM v05.0 annual mean values calculated over the period 1997 to 2013.

A similar, but less pronounced picture is revealed for the Theil-Sen slopes calculated for the anomaly values over the same period (Figure 12).

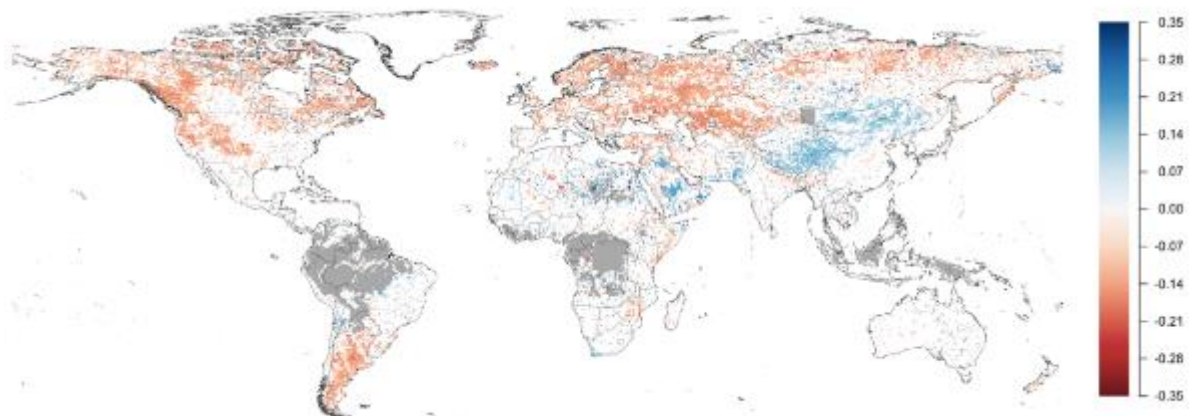


Figure 12: Theil Sen Slope estimator for ESA CCI SM v05.0 annual anomaly values calculated over the period 1997 to 2013.

#### 5.2.4 Discussion and conclusion

We investigated the global relationships between GPCP v1.2 precipitation, ESA CCI SM v05.0 as well as GIMMS NDVI3g across the reference period 1997 to 2013 and compared our results with findings obtained when applying the same method to previous versions of ESA CCI SM. We were able to identify differences in the global relationships, with the ESA CCI SM v05.0 dataset showing slightly different patterns. For example, less pronounced negative correlation coefficients in the boreal regions, when correlating ESA CCI SM and ERA-Land volumetric soil moisture.

As for the preceding versions, there are still inconsistencies in very dry regions like the Sahara desert or in mountainous regions like the Himalaya, which require further investigation.



### 5.2.5 Other Findings – Data Inconsistency

While performing the correlation analysis we came across some inconsistencies in the ESA CCI SM v05.0 dataset. In fact, a distinctive rectangle appeared in the Western part of Mongolia and is apparent in the soil moisture data (Figure 13) as well as the FLAG data (Figure 14).

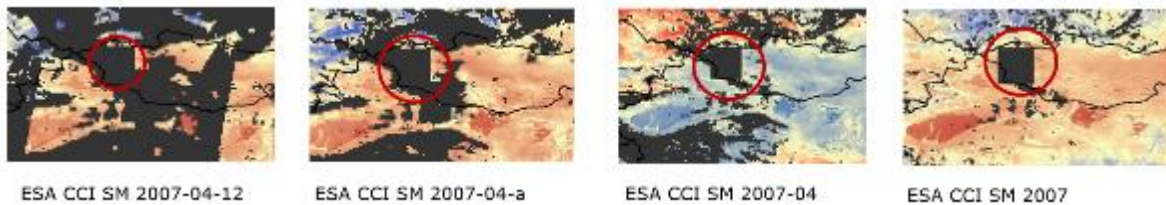


Figure 13: Data inconsistency in Mongolia for daily, half-monthly, monthly and annual means of ESA CCI SM

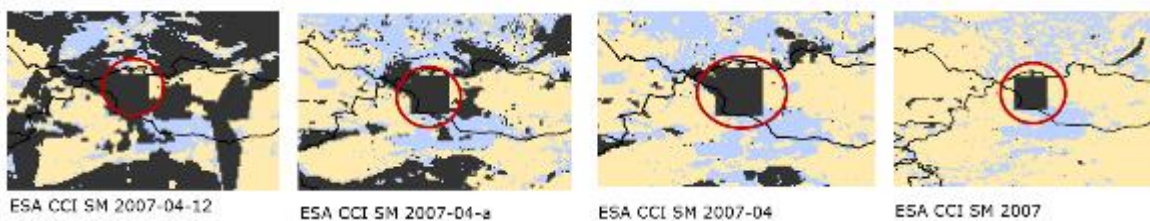
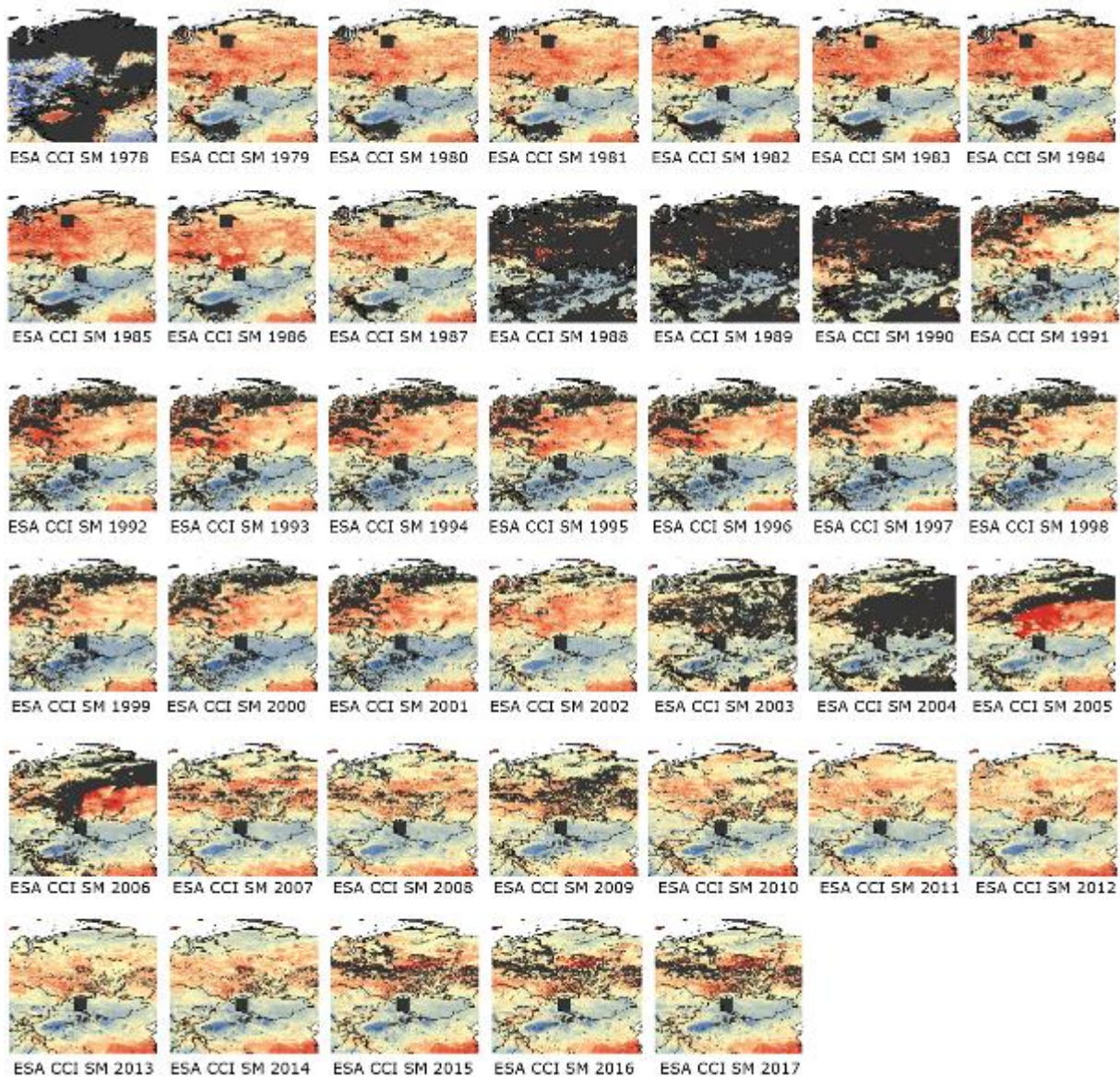


Figure 14: Data inconsistency in Mongolia for daily, half-monthly, monthly and annual FLAG of ESA CCI SM

We further investigated this data inconsistency or data gap over the entire ESA CCI SM v05.0 time series from 1979 to the year 2017 by computing annual means (Figure 15). Apart from the data gap in the eastern part of Mongolia, another rectangle appeared in the Northern part of Russia<sup>5</sup>. While both appear starting from the year 1979 and the one in Russia is slowly disappearing in 1991 and rather replaced by a distinct data pattern (“inverse rectangle”). The one in Mongolia is present throughout the data series.

<sup>5</sup> Note: No other data inconsistencies are found.



*Figure 15: Annual means for ESA CCI SM v05.0 from 1979 to 2017*

In a next step we analyzed the data separately. That is, we looked at the combined, the passive as well as the active product. We found that for the year 1979 the data gaps are visible in the passive as well as the combined product (Figure 16).



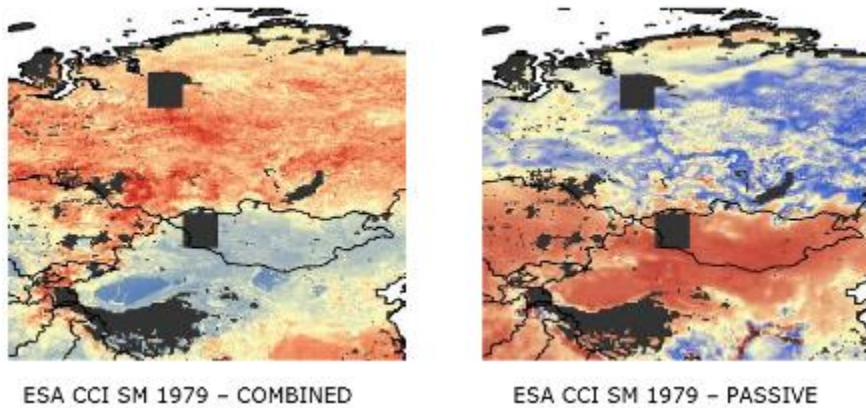


Figure 16: Comparison between the combined and the passive product for the annual mean of 1979

However, for the years 1991 and 2002 only the data gap in Mongolia is apparent ( )

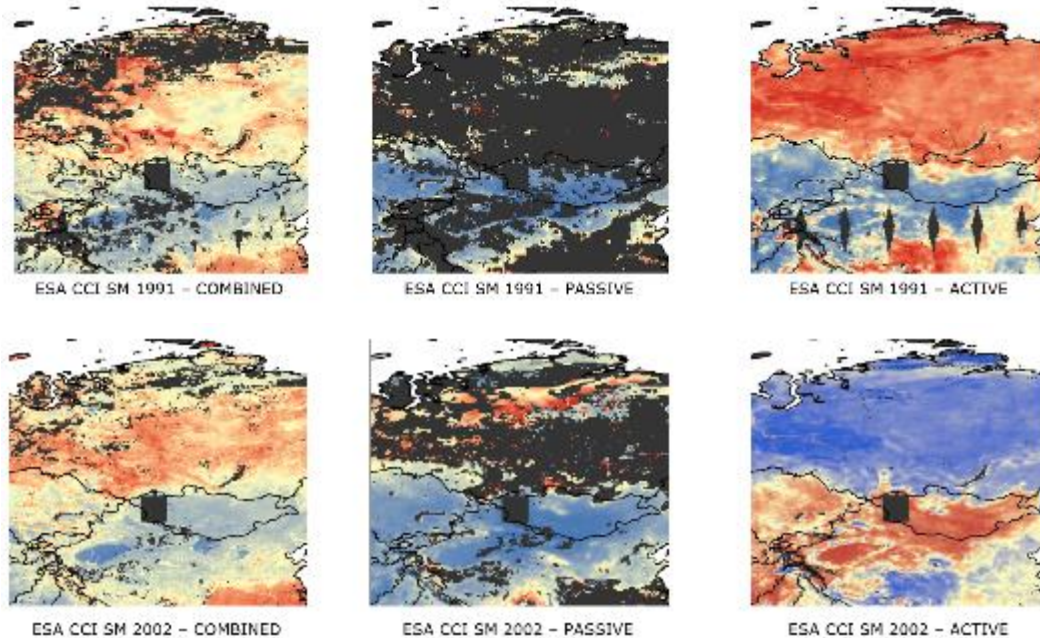


Figure 17: Comparison between combined, active and passive product means for 1991 and 2002.

### 5.3 Assimilation of the ESA CCI ACTIVE and PASSIVE product into the SURFEX land surface model using the EnKF (NILU)

Contributors: J. Blyverket, P. Hamer, W.A. Lahoz and T. Svendby

#### 5.3.1 Introduction

The ESA CCI for soil moisture project has been ongoing since 2012, the goal of the project was to create a global consistent soil moisture product using active and passive satellite sensors. As of 10.10.2018, the dataset spans from 1978 until the end of 2018. The ESA CCI SM product is divided into three different products, the ACTIVE product which consists of daily soil

moisture values from active sensors, using backscatter as a measure of soil moisture. The PASSIVE daily product, using passive observed brightness temperature as a measure of soil moisture and finally the COMBINED product, fusing the ACTIVE and PASSIVE product into one, and thus improving the spatial coverage by combining information from sensors in different orbits.

One of the strengths of the ESA CCI SM product is that it combines data from different sensors, which allows for higher spatial and temporal resolution of soil moisture. Even though the ESA CCI product should be superior in coverage compared to a stand-alone satellite, it has temporal and spatial gaps. The temporal gaps are mostly because of the revisit time of the satellites while the spatial gaps could be in the horizontal direction. Horizontal because not all parts of the globe will be covered every day. In addition to gaps in the horizontal, the ESA CCI product lacks information in the vertical dimension because the sensors are only sensitive to water in the top ~1-2 cm of the soil. The unobserved root-zone layer is important for, e.g., the partitioning of latent and sensible heat fluxes to the atmosphere, drainage and the available water for the biosphere. Root-zone soil moisture has a longer memory than atmospheric processes, which should imply that root-zone anomalies are important for subseasonal to seasonal climate predictions. Due to the limitations of satellite observations for the root-zone layer, land surface models are therefore required to estimate it.

By combining land surface modelling and observations using data assimilation (DA), we can create a product which combines the spatial and temporal coverage of a land surface model with observations of surface soil moisture. The land surface model controls the partitioning of rainfall into runoff, evapotranspiration, drainage and soil moisture, while the observations can compensate for model parameterizations and drift. Knowing the errors of the model and the observations, DA has the potential to create a superior product over model or satellite soil moisture alone. In this section we evaluate the potential for assimilating the ESA CCI ACTIVE and PASSIVE product into a land surface model, and evaluate the resulting analysis product against in situ stations over the U.S. This study is highly relevant for answering how and if assimilation of the ESA CCI product can improve model root-zone soil moisture.

### **5.3.2 Data Sets**

The ESA CCI soil moisture data product consists of an ACTIVE, PASSIVE and COMBINED product. The ACTIVE soil moisture retrieval product is based on the Change detection method developed at Vienna University of Technology (TU Wien). The change detection method is derived for C-band scatterometers. Soil moisture is retrieved directly using scatterometer measurements without the need for an iterative adjustment process. It is assumed that the relationship between the surface soil moisture and the backscatter coefficient  $\sigma_0$  is linear. For the time-period 31.3.2015 - 31.12.2016 used in our study the ACTIVE soil moisture observations comes from the METOP-A and B satellites (ASCAT-A and ASCAT-B). The PASSIVE soil moisture dataset is derived using the land surface brightness temperature which is related to the soil dielectric constant and hence the surface soil moisture content. The conversion from observed brightness temperature to soil moisture values are handled by the land parameter retrieval model (LPRM). The LPRM is a radiative transfer model that simultaneously retrieves vegetation density, soil moisture and surface temperature.



### 5.3.2.1 *Bias Correction*

In this section we describe the pre-processing needed of the ESA CCI soil moisture product, so that it can be assimilated using a sequential DA method into the ISBA land surface scheme. As mentioned above the ACTIVE and PASSIVE products are delivered as a daily product, a composite of different satellite overpasses at a given date. For a sequential DA algorithm to work, the timing of the forecast (model) and observation (satellite retrieval) need to coincide as much as possible, to avoid bias between the model and observations. We use a temporal gap of  $\pm 1.5$  hours centred at 00 UTC, 03 UTC, 06 UTC, 09 UTC and 18 UTC; satellite overpasses within this time window are mapped to the central time. The range of the ACTIVE product is given in percent, 0-100 %. The ACTIVE data are converted to volumetric soil moisture and are scaled to the model minimum and maximum for a given grid point, all data are mapped so that we only use model data when there are observation values available. The PASSIVE product is given in volumetric soil moisture and does not need any additional conversion. To handle the bias between the model and observation we rescale the observations using cumulative distribution function matching (CDF-matching). The CDF-matching is performed for each individual gridpoint, given that the gridpoint has more than 150 observations over the whole time-period. If there are less than 150 observations at a gridpoint, the values at that particular gridpoint are discarded. The CDF-matching works by ranking the observations and model values for an individual gridpoint at a specific time e.g., 9 am. By taking the difference between the two ranked datasets and fitting a 5th order polynomial to these points we can find the new observed value by adding this difference to the old observed value. The CDF-matched observations will then have a CDF which is matched with the CDF of the model for that gridpoint and time of the day.

## 5.3.3 *Methods*

### 5.3.3.1 *Modelling System*

Within the SURFEX land surface modelling platform (Le Moigne, 2012) we use the Interaction Between Atmosphere/Biosphere diffusion scheme (ISBA-DF). Vertical transport of water is solved using the mixed form of Richard's equations while the soil temperature is solved using the one-dimensional Fourier law. The ISBA model also includes soil freezing and an explicit snow scheme. The model uses 14 vertical layers over a depth of 12 m. The depth of the different layers are currently 0.001, 0.01, 0.04, 0.1, 0.2, 0.4, 0.6, 0.8, 1.0, 1.5, 2, 3, 5, 8, 12 m. Layer-1 is here a skin layer 1 mm in thickness, depending on the experiments we use layer-2 and layer-3 (0.01 and 0.04 m) as the observation layer. The time-step for the land model is 15 min, output is saved at 3 h intervals. The ISBA scheme can be run using sub-grid patches; the mass and energy balance are then computed in each individual tile/patch before a weighted average is performed. In this work we only use one patch where the parameters for the mass and energy balance are aggregated from the different land covers within the grid-cell. The sub-grid runoff is handled using the DT92 option. Water infiltration excess is computed using the Horton option. A homogeneous profile is used for the saturation coefficient K, the rainfall intensity is homogeneously distributed across the grid-cell. Snow processes are modelled using the built in 3L snow scheme in ISBA. More information about the model can be found in (Decharme et al., 2011). Land cover is extracted from ECOCLIMAP, a global database at 1 km



resolution for land surface parameters. For nature grid-cells surface parameters are computed using the fraction of 12 vegetation types from the 1 km resolution land cover map. The leaf area index (LAI) is derived from the ECOCLIMAP database and given as a climatology for each calendar month. The clay and sand fraction are extracted from the Harmonised World Soil Database (HWSD). In SURFEX several soil parameters are decided by the clay and sand fraction given by (Noilhan and Lacarrere 1995). The hydraulic conductivity and soil water potential are related to the liquid soil water content through the Clapp and Hornberger (1978) relations. Grid cell orography is computed using the GTOPO 1 km resolution digital elevation model (DEM).

#### 5.3.3.2 Data Assimilation System

The land surface DA system uses the Ensemble Square Root Filter (Sakov and Oke, 2008). In this work the state vector  $X$  consist of the top 8 model layers, i.e.,  $(\theta_1, \theta_2, \dots, \theta_8)$ . An observations vector  $d$  consists of the satellite observation  $(\theta_{obs})$ , the EnKF combines an ensemble of model states  $(x)$  with the observations  $d$ .

Models are simplified representations of the real world and have different sources of errors. For a land surface model some of these errors are: i) error of representativeness, ii) error in model parameters/parameterization of physical processes, iii) external errors such as atmospheric forcing, land cover classification and sand and clay fraction. These different errors can in theory be represented in the DA system. In the system we use we represent errors in the forcing (by perturbing the different forcing fields) and model parameter errors (by perturbing the state variables or model parameters).

Time series of cross-correlated forcing fields are generated using an autoregressive lag-1 model (AR(1)). These perturbations in the atmospheric forcing allow for an ensemble of model runs, where the spread represents the model uncertainty. Precipitation and shortwave radiation have a lower bound of zero, the perturbations of these variables are therefore multiplicative. Perturbations in longwave radiation and air temperature are additive. To avoid bias in the forcing files, the perturbations are constrained to zero for the additive variables and to one for the multiplicative. To ensure physical consistency in the perturbation parameters (e.g., increases in longwave radiation give decreases in shortwave radiation) we impose cross-correlations on the pseudorandom fields. To ensure sufficient spread in the ensemble for dry regions and in the deeper model layers we also perturb the clay and sand fraction by 10%. This will affect the hydraulic conductivity used in SURFEX, and hence works as a perturbation to the model parameters.

The setting of observation errors is based on the assumption of a linear relationship between the dynamic range of soil moisture values and the errors. This relationship is given as  $(wfc - wwilt)$ , where  $wfc$  is the field capacity and  $wwilt$  is the wilting point; they both depend on the soil texture and vegetation type for each grid point. This relationship is scaled with a dimensionless scaling coefficient  $\lambda_0$ , resulting in an observation error given by:  $\lambda_0 (wfc - wwilt) m^3 m^{-3}$ . The observational error is set to  $0.03 m^3 m^{-3}$ , and scaled according to the grid point characteristics as discussed above.



## 5.3.4 Results

### 5.3.4.1 Total Number of Observations

In a land surface DA system a land surface model is confronted with observations, which means that the resulting analysis product is weighted according to the model and observation errors. In our case the model error is the ensemble spread and the observation error is set to a constant which depends on the field capacity and wilting point for a specific grid cell. The analysis is an optimal weighting of the model and observation, giving a new initial condition for the whole soil moisture profile (not just the surface). Hence, correcting the model. For such a system driven by prescribed atmospheric forcing, knowing the number of assimilated observations from a given observation platform is useful, because this tells us how many corrections we can get from that platform in time and space.

In Figure 18 (a) we have plotted the total number of assimilated observations for each day of the time-period (by taking the sum over all the grid cells with an observation). We can clearly see a seasonal pattern, where the total number of assimilated observations decreases in DJF, because of the snow cover and frozen soil. In the summertime we note that around 6000 – 7000 observations are assimilated, which results in around 23-26 % of the total domain having an observation each day. Figure 18 (b) illustrates the spatial coverage of the total number of assimilated observations. Some regions are not covered because the ESA CCI ACTIVE or PASSIVE product were an arithmetic average of two observations observed at different times. In our sequential DA system these observations were therefore masked out. This decreases the spatial coverage of the ESA CCI product for sequential DA and perhaps ESA CCI product future versions should be delivered with sub-daily observations of individual observations or stick to one observation instead of taking the average.

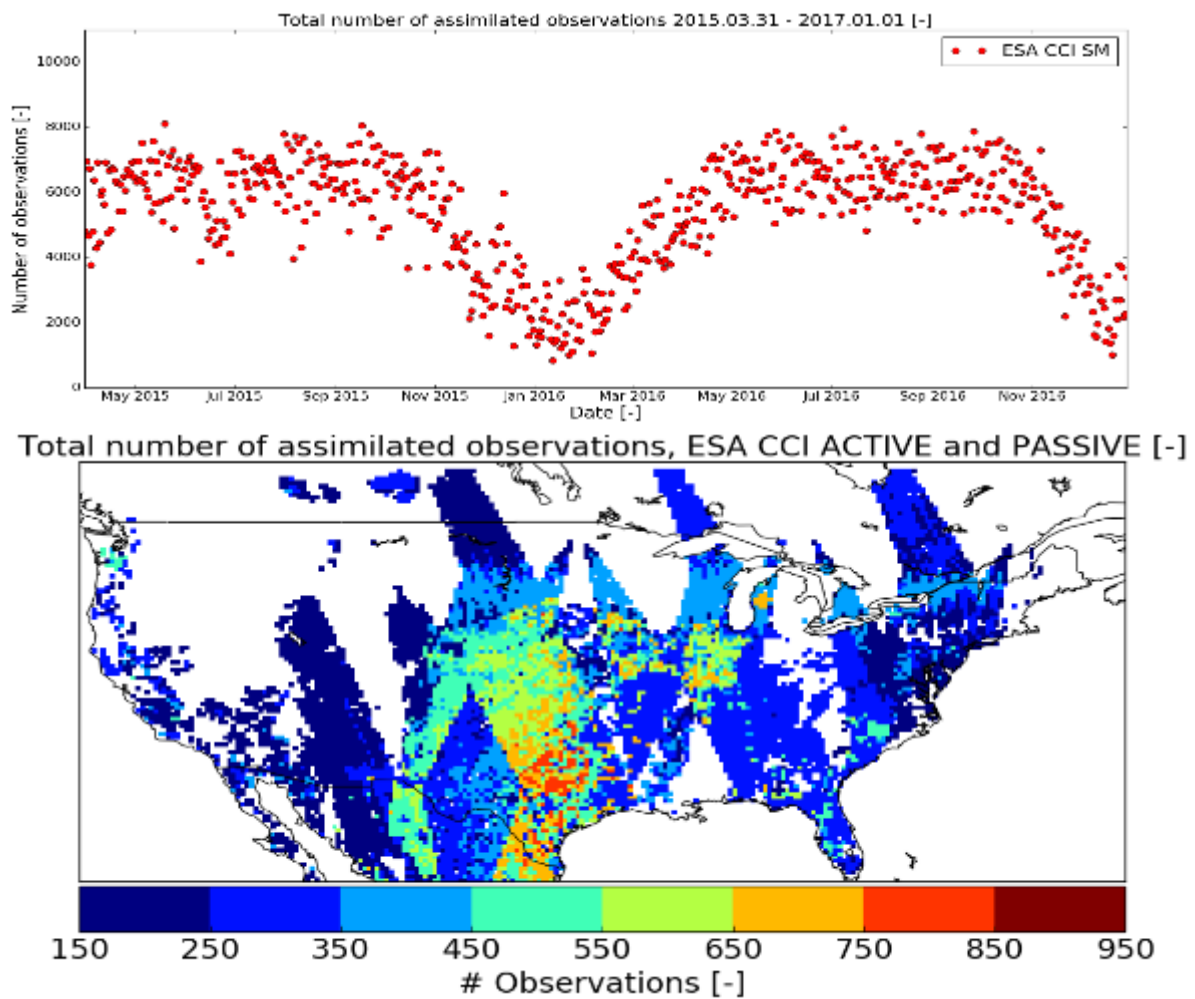


Figure 18: (a) Daily counts of ESA CCI ACTIVE and PASSIVE observations assimilated into the ESA CCI L4 system from April 2015 to January 2017. (b) Spatial extent of number of total assimilated observations from the ESA CCI ACTIVE and PASSIVE product. Some regions are not covered because the ESA CCI ACTIVE or PASSIVE product were an arithmetic average of two observations observed at different times. In our sequential DA system these observations were therefore masked out.

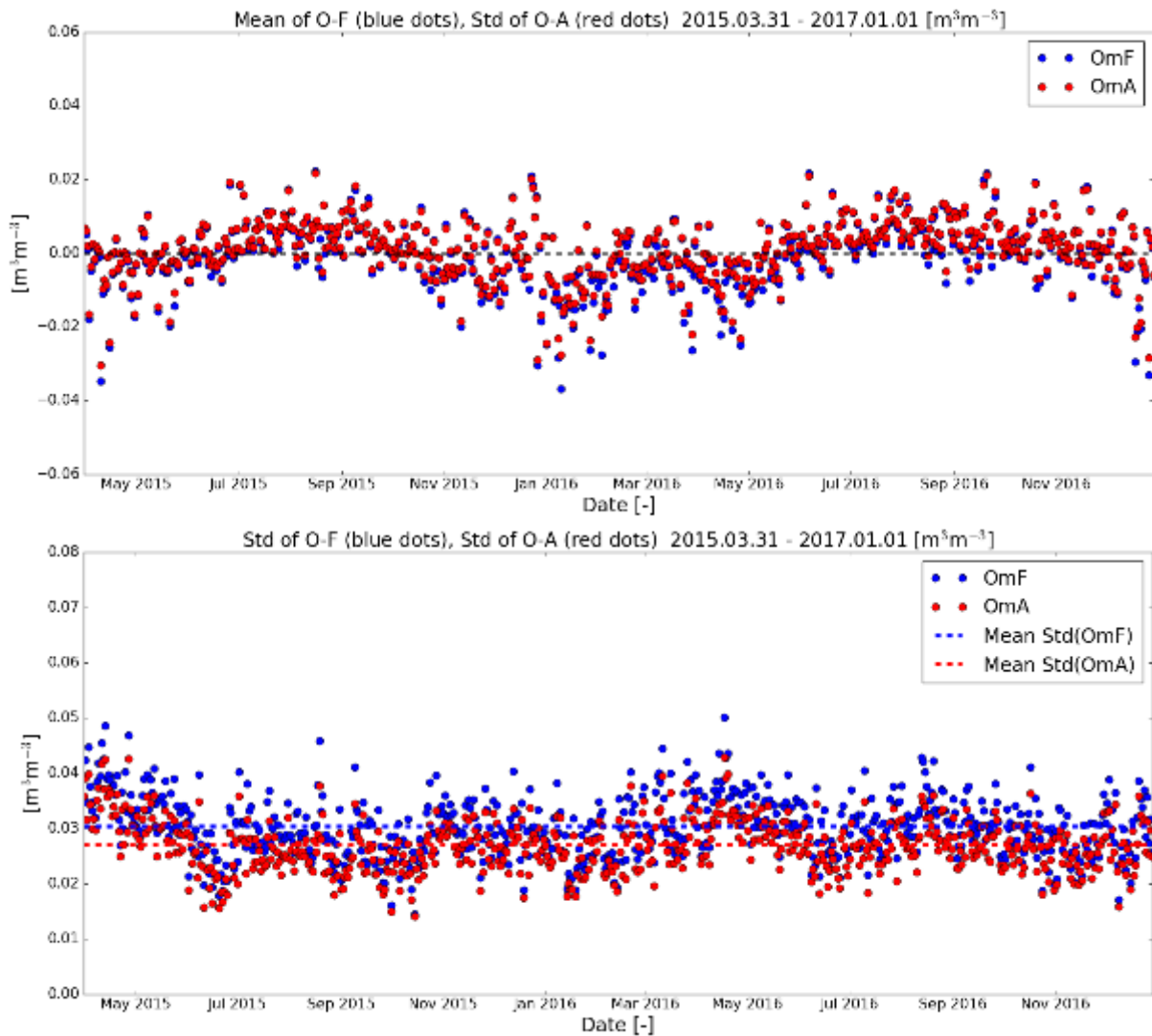


Figure 19: (a) Mean of O-F and O-A residuals, the mean values are computed separately for each 3h window by averaging over the land domain, and then averaging the resulting values over the 8 analysis times for each day. (b) Same as in (a) but for standard deviation.



### 5.3.4.2 O-F and O-A residuals

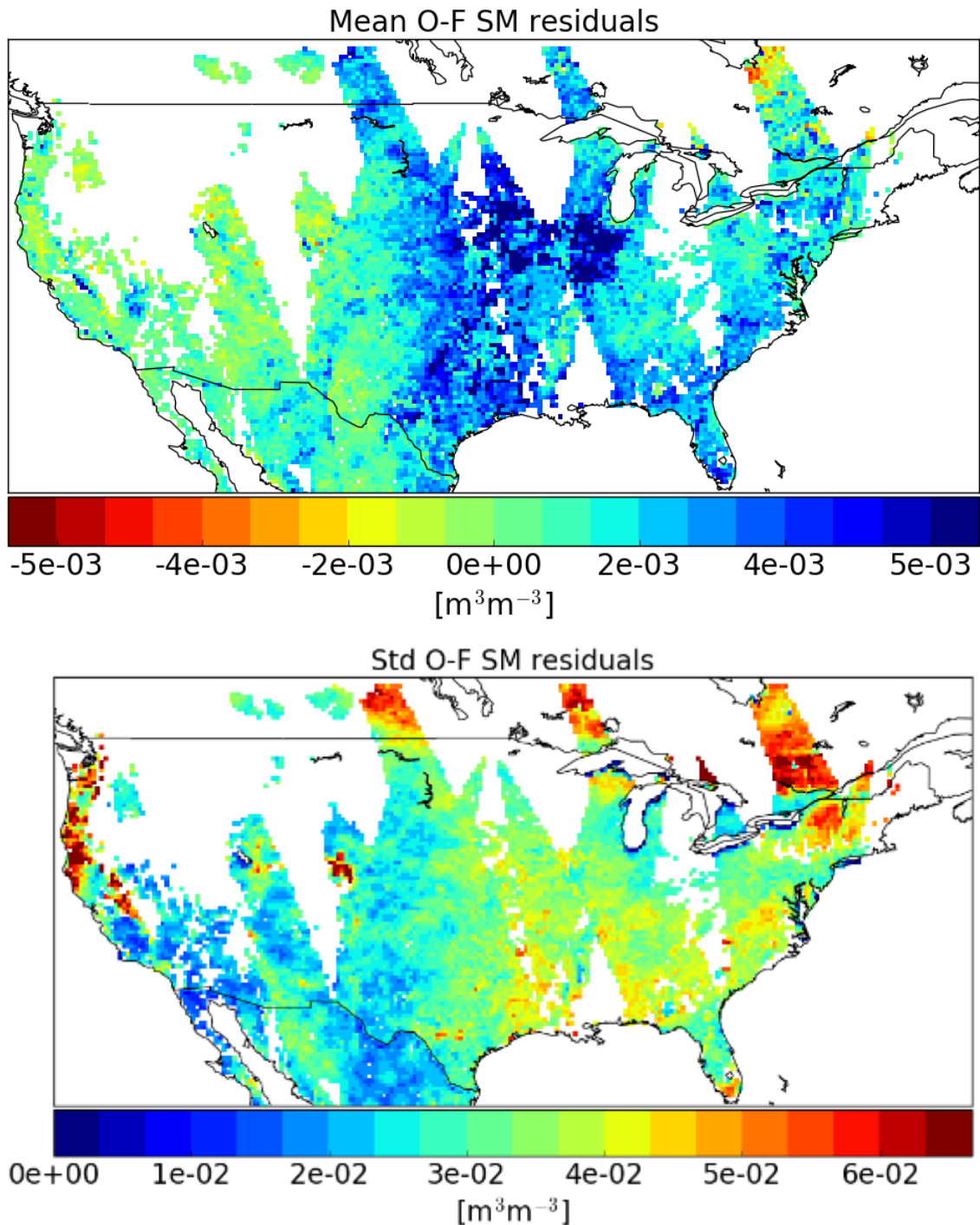


Figure 20: (a) Mean and (b) standard deviation of the O-F residuals from April 2015 to 1 January 2017.

The Observation-minus-Forecast (O-F) and Observation-minus-Analysis (O-A) statistics are valuable tools for checking how the DA system is performing. In a well calibrated DA system the O-F residuals have a zero-mean, white noise characteristic, reflecting an unbiased analysis that extracts all of the information from the observations. Figure 19 (a) shows that the long-term mean of the O-F residuals is close to zero, this is expected as we remove the long-term





bias between observations and model by matching the CDFs (see the methods section). We also note that for most of the data points the DA system moves the O-A closer to zero, hence the analysis moves the model closer to the observation without adding any bias to the system. While the DA system by construction is bias free, the long-term mean of the O-F in Figure 20 (a) shows regions with non-zero residuals. One possible reason for this bias might be irrigation. The model is driven by state-of-the-art atmospheric forcing that has a high skill, so the precipitation input should be of good quality. Since the  $O-F > 0$ , it means that the observations are consistently wetter than the model, indicating that the observations are sensitive to irrigation over this region of the U.S. This is again supported by the standard deviation of the O-F residuals in Figure 20 (b), which depicts the typical O-F differences. For the wet bias region in the central U.S, the O-F standard deviation is larger than in the surrounding region, which is an indication that the ESA CCI data contains independent information from that in the atmospheric forcing data.

#### 5.3.4.3 *Standard deviation of the normalized O-F residuals*

For a land surface DA system to work close to optimal, we need to correctly specify the model and observation errors. One way to check the consistency between model errors (spread of the ensemble) and observation errors is to compute the standard deviation of the normalized O-F residuals. This metric compares the actual errors in the system ( $cov(O-F)$ ) to the assumed errors (ensemble spread and observation error). Values greater than one indicate that the actual errors are underestimated, while a value smaller than one indicates that the actual errors are overestimated (the actual errors are less than the assumed errors). Figure 21 illustrates the spatial pattern of the  $norm(O-F)$  metric, showing large regions where the metric is close to unity (0.8 – 1.2). Eastern parts of the domain show regions where the actual errors are underestimated, especially regions in Canada show large underestimation of the actual errors. Further west over the western Great Plains, Eastern Rockies, and Great Basin, the errors show signs of being overestimated. While in the north west of the US the errors are again underestimated. Note the underestimation of errors in the Sierra Nevada mountain region in California.

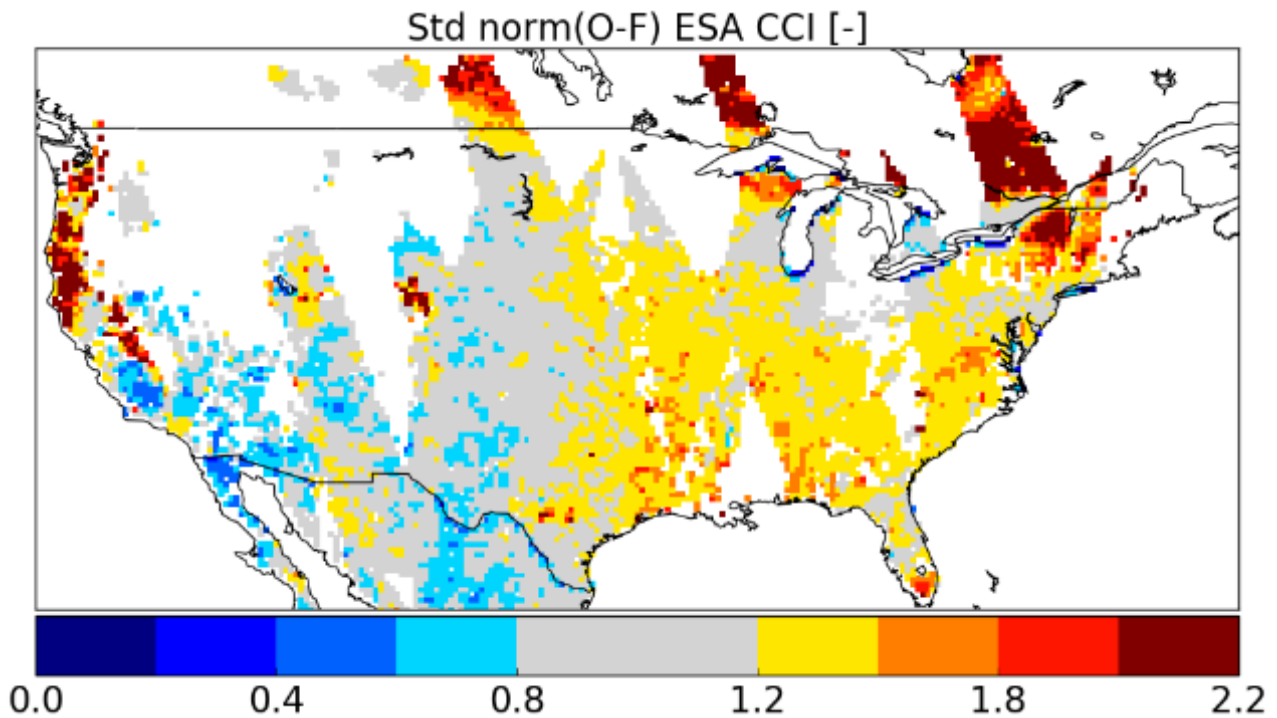


Figure 21: Standard deviation of the normalized O-F residuals from April 2015 to 1 January 2017.

#### 5.3.4.4 Mean and standard deviation of the analysis increments

Figure 22 (a) shows the standard deviation of the surface zone (computed as a weighted mean of the two top model layers) increments. This figure illustrates the typical size of the surface zone soil moisture increments in time. The largest increments ( $\sim 0.01$  m<sup>3</sup>/m<sup>3</sup>) are located in the central U.S, while the smallest increments are found in the western parts of the U.S. Figure 22 (b) shows the typical size of the root-zone increments, weighted from layer 1 (1 cm) to layer 8 ( $\sim 100$  cm). As for the surface zone we see that the increments are largest in the central U.S, and very close to zero in the western parts. The typical root-zone increments are smaller than the surface zone increments, this is because of the smaller ensemble spread in the root-zone (less affected by the perturbations in the atmospheric forcing). The typical size of the





root-zone increments  $\sim 0.003 \text{ m}^3/\text{m}^3$  in the central U.S. seems to follow what Reichle et al. (2018) show in their study.

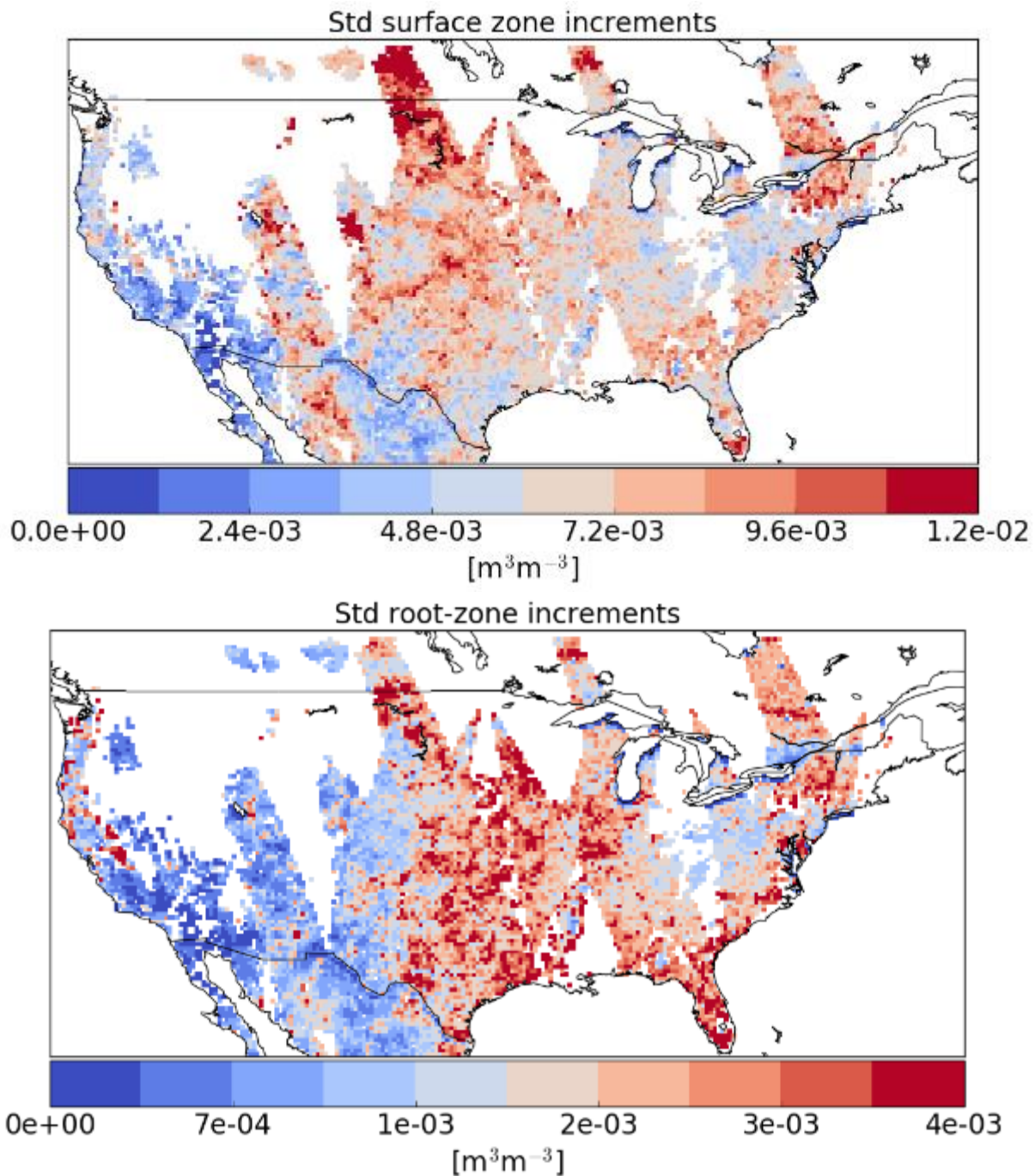


Figure 22: Standard deviation of the surface (a) and root-zone (b) increments from April 2015 to 1 January 2017. Note the different color scale in (a) and (b).

#### 5.3.4.5 Validation against the USCRN and SCAN in situ networks

For validation of surface and root-zone soil moisture data from the DA experiments we utilize in situ soil moisture data from the U.S. Climate Reference Network (USCRN) Diamond et al. 2013. The in situ data went through a quality control, discarding values lower than  $0.0 \text{ m}^3/\text{m}^3$ ,



higher than  $0.6 \text{ m}^3 \text{ m}^{-3}$  and measurements taken when the soil temperature was below 4 C. The hourly data were averaged using for example 2 pm, 3 pm and 4 pm data, to obtain the data at 3 pm. The skill metrics used are the Pearson correlation coefficient and unbiased root mean square error (ubRMSE). Figure 23 shows the Pearson correlation coefficient between the ensemble open-loop and the USCRN in situ stations for surface soil moisture. One thing to note is the high correlation of the open-loop ( $R = 0.72$ ), this is probably a result of the high quality forcing utilized and also the state-of-the-art land surface model. Figure 24 is the difference between the analysis correlation with the in situ stations and the open-loop correlation with the in situ. The changes in correlation are small for the whole domain, reasons for this might be that the information content in the land surface model and the ESA CCI ACTIVE and PASSIVE products are very similar. Little information is therefore added to the land surface model. It is also hard to improve on the already high correlation between the open-loop and the in situ soil moisture, utilizing a poorer forcing data set might have shown larger relative improvements from the open-loop to the analysis (at the cost of lower correlation between the open-loop and in situ stations).

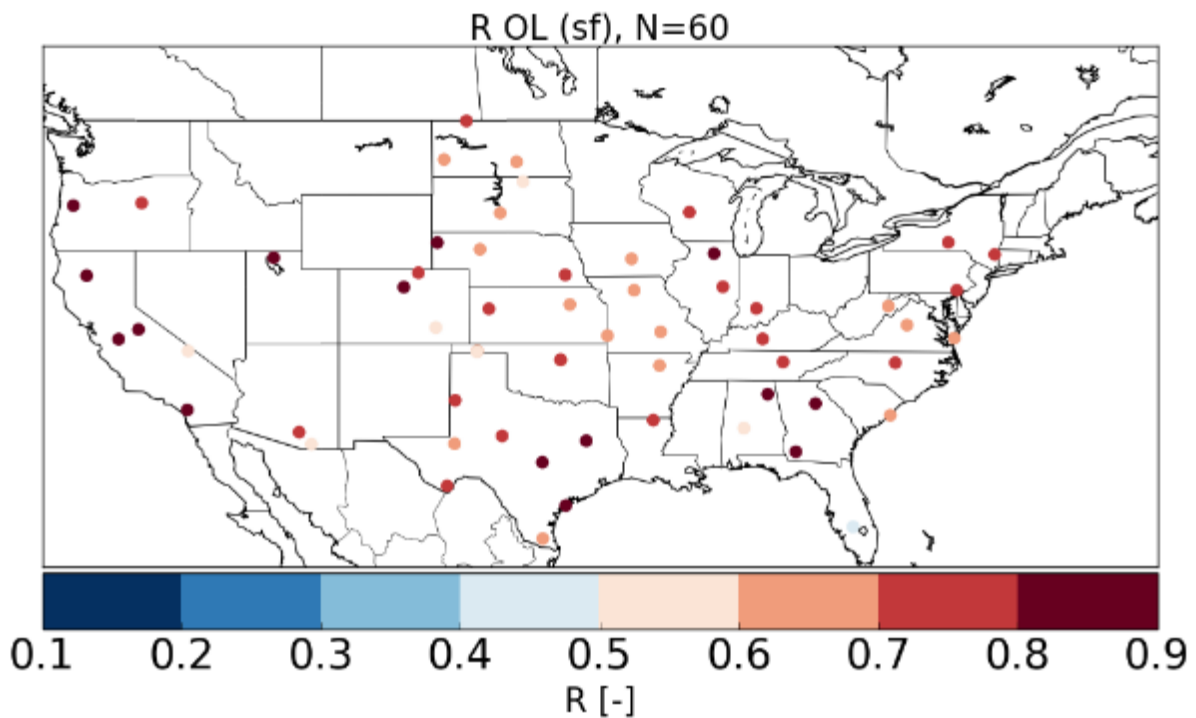


Figure 23: Pearson correlation coefficient surface soil moisture, ensemble open-loop run vs USCRN in situ stations. Mean  $R = 0.72$ , std  $R = 0.11$ . Median  $R = 0.73$ .

In Figure 25 the correlation between the open-loop and the root-zone soil moisture is plotted, again we note the high initial correlation between the model and the in situ stations (Mean  $R = 0.76$ , median  $R = 0.78$ ), this is even higher than for the surface zone. Figure 26 is the difference between the analysis and the open-loop correlations with the in situ, there is in general little change in the correlations, except for some points. The improvements can be seen in the central U.S, while most negative impacts of the assimilation are seen in Illinois and Missouri. This region has some of the largest O-F differences (see Figure 20), which most likely



were due to irrigation. If the satellite observations observes irrigation the DA system will add moisture

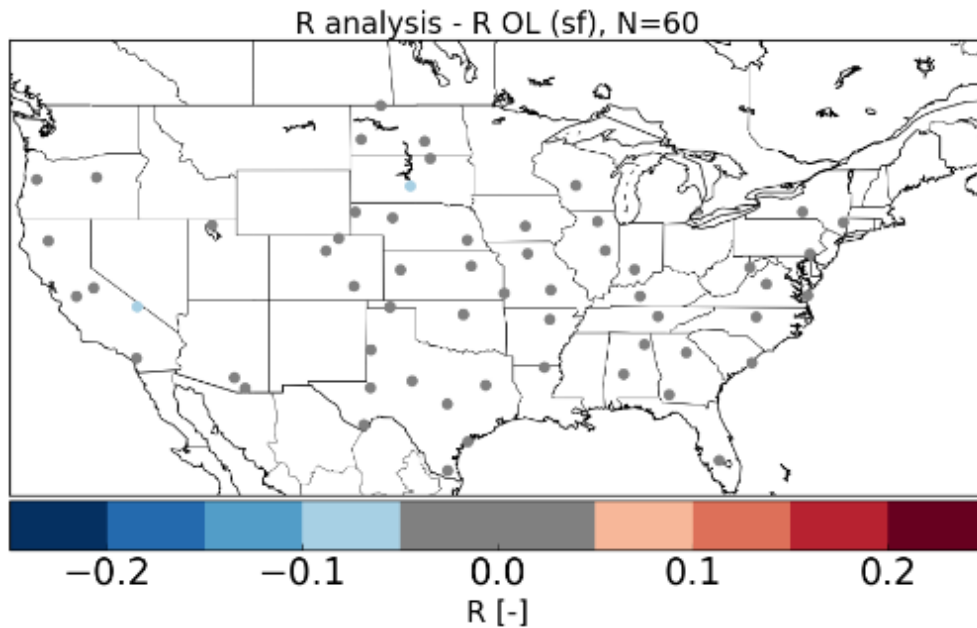


Figure 24: Difference between the analysis and the open-loop correlation with USCRN in situ stations, surface soil moisture.

to the model soil and correct for this, however, if the in situ station is not affected by the irrigation (it sits outside the irrigated field) we will be comparing two different things (probably degrading the analysis). This is seen more in the root-zone than in the surface zone because of the longer memory of the deeper layers, while the surface layer will be less sensitive to irrigation on a notable time scale.

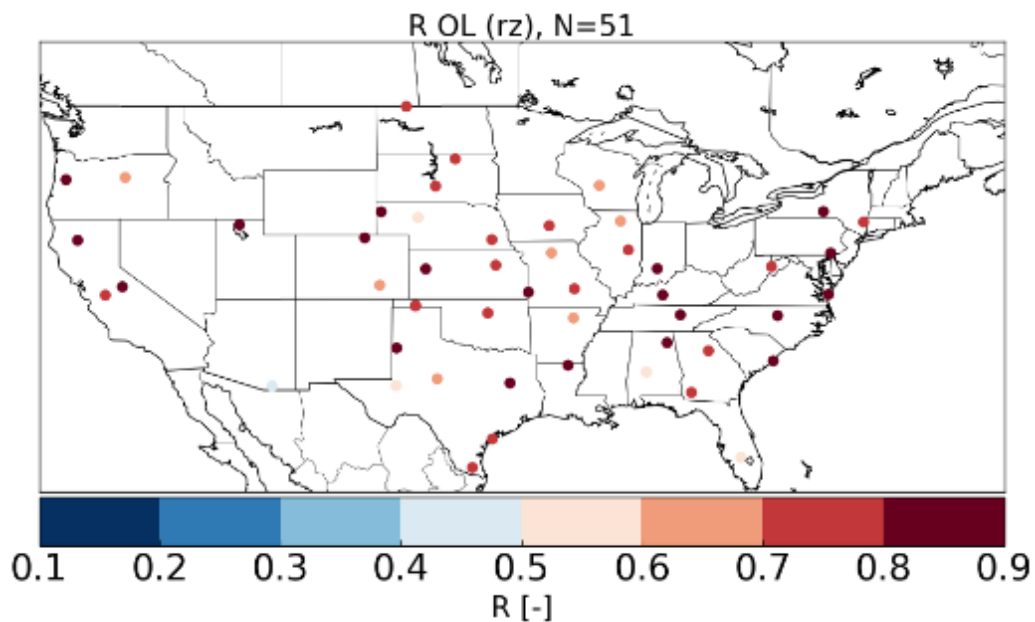


Figure 25: The same as for Figure 23, but for root-zone soil moisture. Mean  $R = 0.76$ ,  $std = 0.11$ . Median  $R = 0.78$ .



Figure 27 shows the ubRMSE for the open-loop vs in situ, for the root-zone soil moisture. Again there is little change between the open-loop and the analysis (not shown), we also note that the mean ubRMSE = 0.040 m<sup>3</sup>/m<sup>3</sup>, which is often a threshold used when creating a Level 4 product. The ubRMSE is highly variable with values ranging from 0.015 – 0.09 m<sup>3</sup>/m<sup>3</sup>.

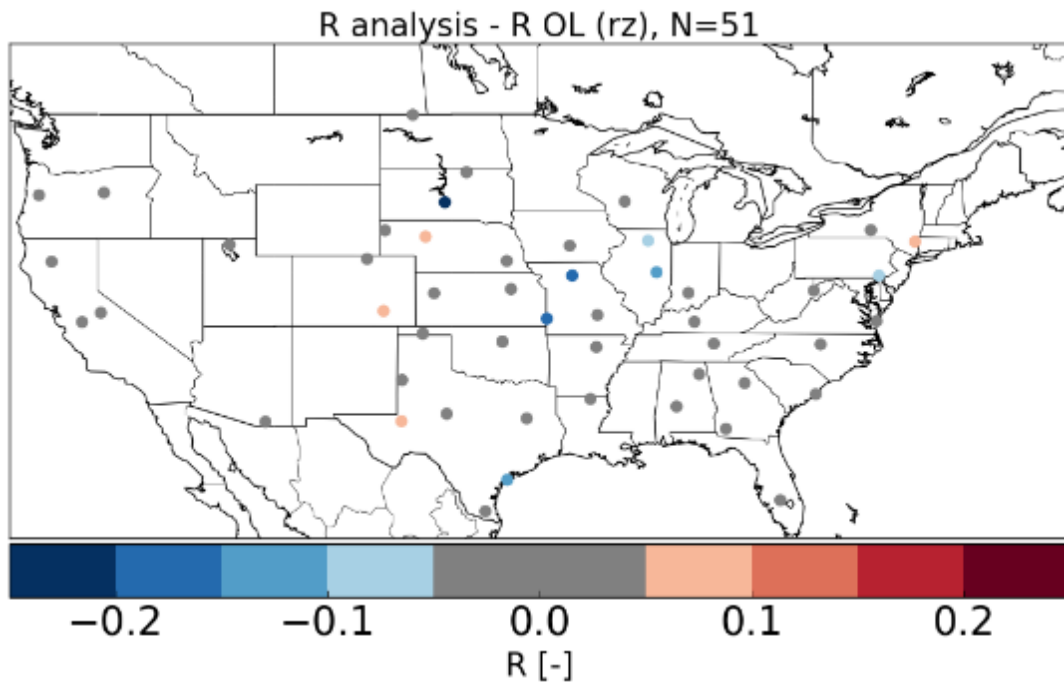


Figure 26: The same as for Figure 24, but for root-zone soil moisture.

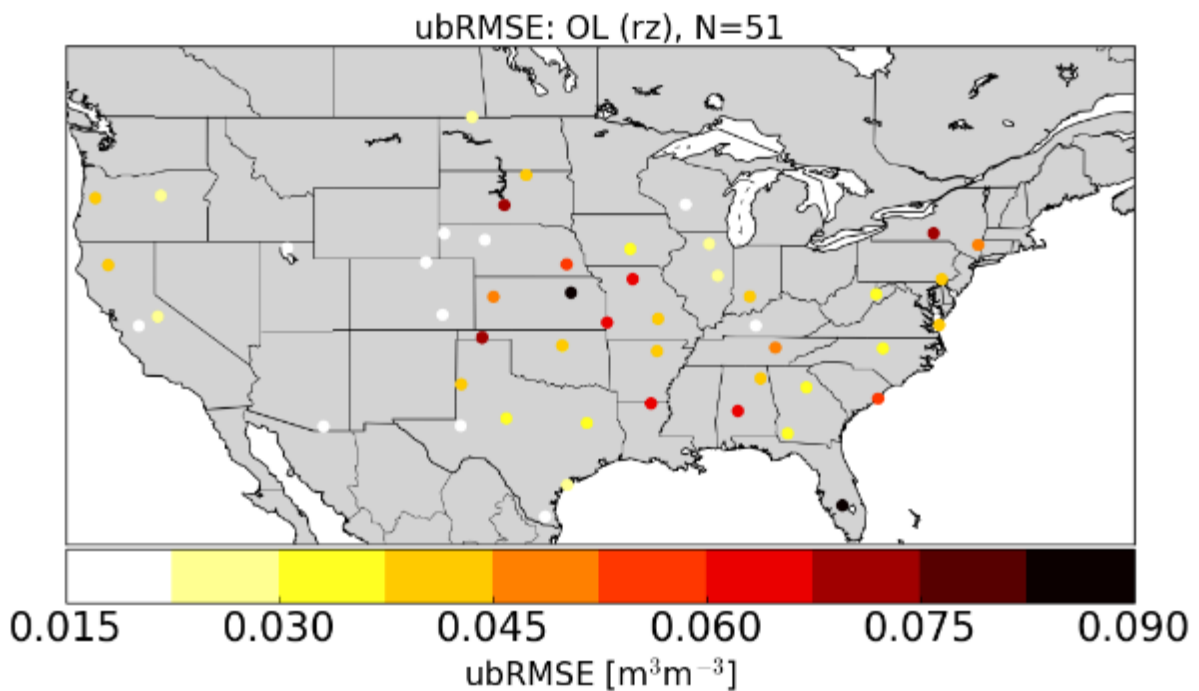


Figure 27: ubRMSE for the open-loop vs USCRN in situ stations, root-zone. Median = 0.038 m<sup>3</sup> m<sup>-3</sup>. Mean = 0.040 m<sup>3</sup>/m<sup>3</sup>.

### 5.3.5 Conclusions

The ESA CCI L4 soil moisture product is validated using DA diagnostics and in situ soil moisture measurements. The DA statistics shows that the land surface DA system is reasonably unbiased, even though the O-F residuals show some wet biases (mostly in irrigated regions). The model and observation errors are for large parts of the domain close to being reasonable, however the standard deviation of the normalized innovations show that there are some regions where the actual errors in the system are over or underestimated. Since this is an ensemble setup, the resulting surface and root-zone soil moisture can be delivered with uncertainty estimates, it is however difficult to tell whether these estimates reflects the actual uncertainties in soil moisture.

A final comment is that the skill of the assimilation system can be varying with season. By taking the skill metrics over the whole time-period (included winter season), where soil moisture retrieval is difficult and more profound to errors can degrade the analysis. This would have to be taken into account in the DA system in future studies.

Based on the comparison with in situ stations we saw that the assimilation had little impact on the skill of the model. There might be several reasons for this: i) the open-loop skill was already very high when compared to in situ stations ii) the representativeness of the in situ observation could be different than the model, not allowing information from the observations to impact the analysis and iii) the information content in the ESA CCI ACTIVE and PASSIVE product could be quite similar to the model, again reducing the impact the observations would have on the analysis.

## 5.4 Validation with SAR (UCC)

Contributor: W. Cámaro (UCC)

### 5.4.1 Data Sets and Methods

Soil moisture time series retrieved from ENVISAT ASAR Wide Swath images were used to evaluate the ESA CCI SM product version 03.2. The retrieval algorithm and approach followed are reported in Pratola *et al.* (2015). The study has been carried out by focusing on three regions, covering parts of Austria, Denmark and Italy, and which differ in climate zone, land cover, topographic conditions and soil type. In-situ soil moisture measurements have been compared with both ENVISAT ASAR WS and ESA CCI SM v03.2 datasets. The satellite-derived soil moisture products (ASAR SM and ESA CCI SM v03.2 datasets) have been scaled by adopting the CDF-matching technique (Liu *et al.* 2011), using the in-situ soil moisture dataset as a reference. Moreover, soil moisture short-term normalised anomalies have been evaluated using a 35-day moving average, adopting the approach by Albergel *et al.* (2009). However, the relatively lower temporal frequency of our soil moisture data has led to evaluation of the anomalies only when at least three values are available within this temporal interval. Temporal agreement between each pair of soil moisture time series was investigated using the Pearson correlation coefficient (R). The reliability of statistics was tested using Student's t-test, which estimates the probability (p-value) of the achieved correlation to be a



coincidence, i.e. not significant. The threshold for accepting such a hypothesis (the null hypothesis) is set to 0.05.

Note that even though many studies evaluate soil moisture products in terms of both the correlation coefficient (R) and the root mean square difference (RMSD) (e.g. Willmott *et al.*, 2005; Albergel *et al.*, 2013), we did not calculate RMSD in this study as this additional information would be redundant due to the deployment of the CDF-matching technique. In fact, the (unbiased) RMSD (ubRMSD) is solely determined by R, scaled with the variance of the reference dataset (Gupta *et al.*, 2009), which makes meaningful interpretation of spatial patterns a difficult task (Draper *et al.*, 2013; Gruber *et al.*, 2016).

## 5.4.2 Results

### AUSTRIA

The representativeness of the ESA CCI SM v03.2 product was explored through comparison of the satellite-derived and ground-measured soil moisture time series over the Eastern Styria region near to the city of Feldbach in Austria. In this region lowlands and hilly landscapes with comparably low altitudes represent the prevailing landforms. Half of the region is covered by agricultural lands, mainly distributed between non irrigated arable lands and complex cultivation patterns. The remaining areas are mainly forest and in small percentage urban activities areas. Two ECV pixels have been analysed, including a different number of in-situ stations belonging to the WEGENERNET network (<https://wegenernet.org/portal/>) (See Figure 28). The temporal trend of the most complete in situ stations in the pixels under investigation is shown in Figure 29.



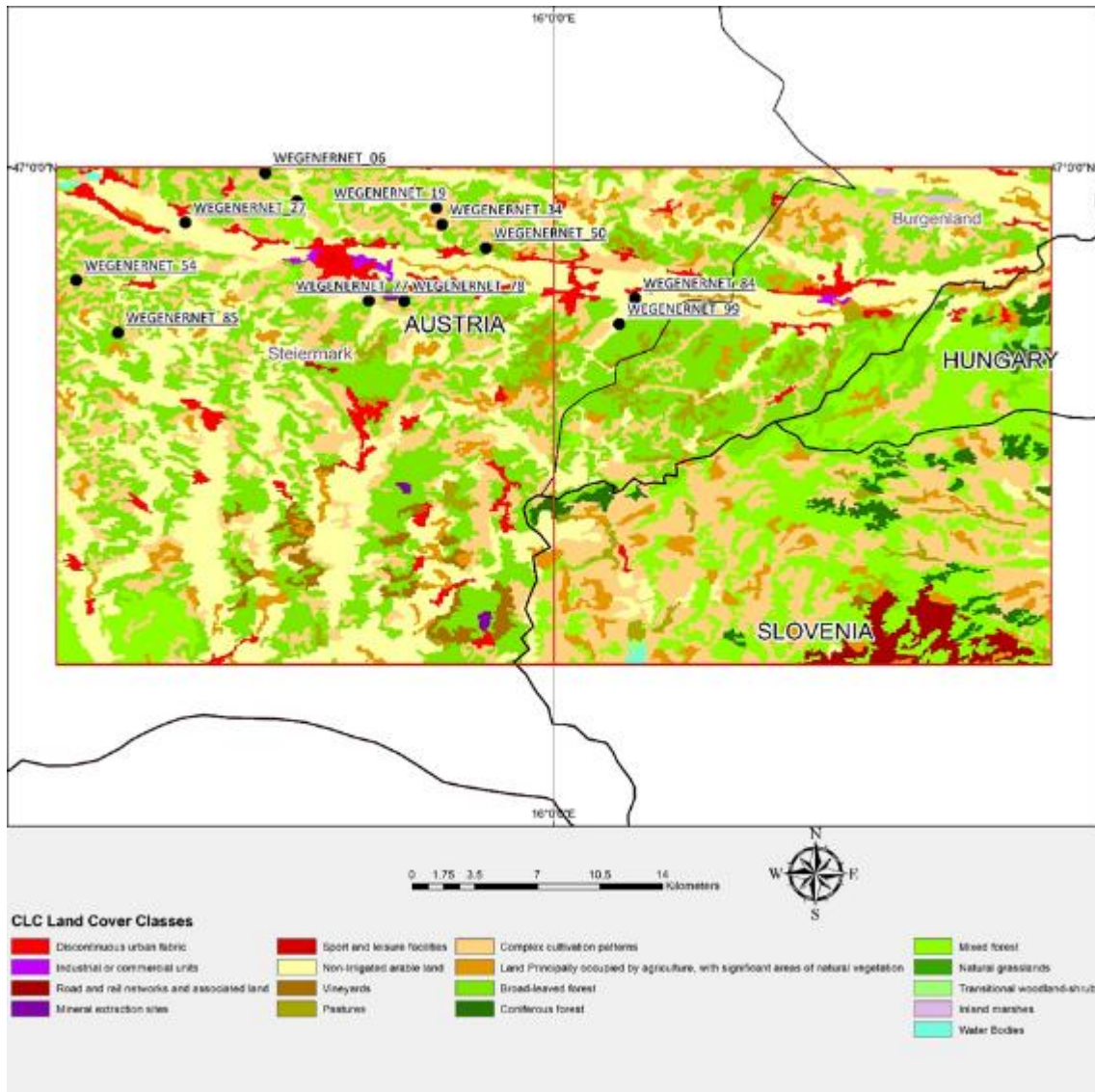


Figure 28: CORINE Land Cover classes in Austrian area of interest. (<https://land.copernicus.eu/pan-european/corine-land-cover/clc-2012/view>).



Figure 29: Time series of in-situ, ASAR and ECV SM v03.2 time series for stations in the Austrian regions under investigation. The units are  $m^3m^{-3}$ .

Generally, the highest in situ values tend to be well represented only by the ECV SM product. On the other side, the driest ground conditions are well represented by ASAR and ECV SM products, except by a few observations in summer 2009, when low soil moisture values in-situ are not well represented, where some anomalous high values have been retrieved.

The evaluation of the correlation between ASAR SM, ECV SM v03.2 and in situ SM time series does not exhibit very high correlations values in all the sites (Table 3). The best result in terms of correlation between the ASAR and ECV SM time series is observed in WEGENERNET 50, where  $R=0.607$ ; the lowest correlation occurs in WEGENERNET 06, where  $R=0.346$ . The comparison between the satellite SM dataset and ground measurements provided low correlations values. Concerning the short-term anomalies analysis, low correlation values are



observed in all the Austrian sites, in accordance with the correlation between the soil moisture datasets.

*Table 3: Pearson correlation coefficient calculated for each pair of soil moisture datasets, including ESA CCI ECV v03.2. Correlation levels are all statistically significant ( $p$ -values  $< 0.05$ ). Austrian regions under investigation.*

Site	ASAR vs. ECV		ASAR vs. <i>in situ</i>		ECV vs. <i>in situ</i>	
	R	p	R	p	R	p
WEGENERNET 06	0.34644	<0.001	0.1383	<b>0.110</b>	0.24953	<0.005
WEGENERNET 15	0.45641	<0.001	0.21792	<0.05	0.35451	<0.001
WEGENERNET 19	0.4744	<0.001	0.27741	<0.005	0.32076	<0.001
WEGENERNET 27	0.54297	<0.001	0.3865	<0.001	0.30666	<0.001
WEGENERNET 34	0.51253	<0.001	0.36071	<0.001	0.45623	<0.001
WEGENERNET 50	0.60771	<0.001	0.46107	<0.001	0.5522	<0.001
WEGENERNET 54	0.43916	<0.001	0.21821	<0.05	0.36367	<0.001
WEGENERNET 77	0.52817	<0.001	0.24604	<0.001	0.36454	<0.001
WEGENERNET 78	0.49443	<0.001	0.24329	<0.05	0.35007	<0.005
WEGENERNET 84	0.45876	<0.001	0.41143	<0.001	0.29966	<0.05
WEGENERNET 85	0.48213	<0.001	0.13265	<b>0.144</b>	0.36326	<0.001
WEGENERNET 99	0.35351	<0.001	0.29182	<0.01	0.21907	<0.05

In Figure 30 we present the correlation results between the ESA CCI SM dataset and the ASAR SM time series in each ASAR pixel within the ECV cells. We observed higher values of correlations in areas related to agricultural land covers. The areas belonged to forest land cover classes, tends to presented not significance or very low correlation values.

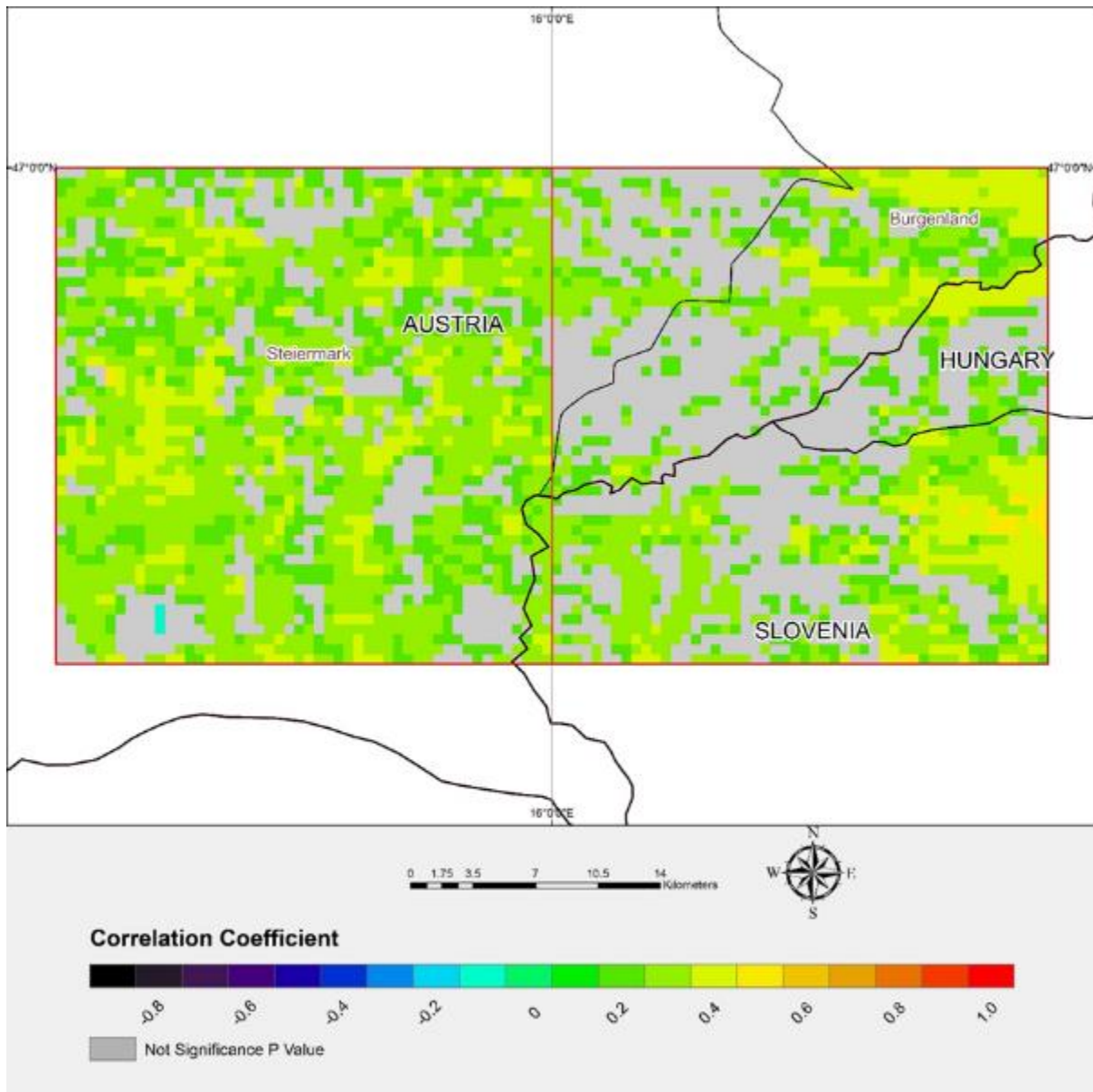


Figure 30: Spatial correlation between ASAR SM and ESA CCI SM v03.2 datasets in the Austrian regions under investigation

### DENMARK

The representativeness of the ESA CCI SM v03.2 product was explored through comparison of the satellite-derived and ground-measured soil moisture time series over the Skjern River Basin, located in the western part of Denmark. The Skjern basin presents a smooth topographic variation from west to east (0 till 125 m a.s.l). This flat region is covered mainly by agricultural areas, but patchy areas of forest and woodlands are also observed. Five ECV pixels have been analysed, including a different number of in-situ stations belonging to the HOBE network (<https://enoha.eu/network/hobe>) (See Figure 31). The temporal trend of the most complete in situ stations in the pixels under investigation is shown in Figure 32.

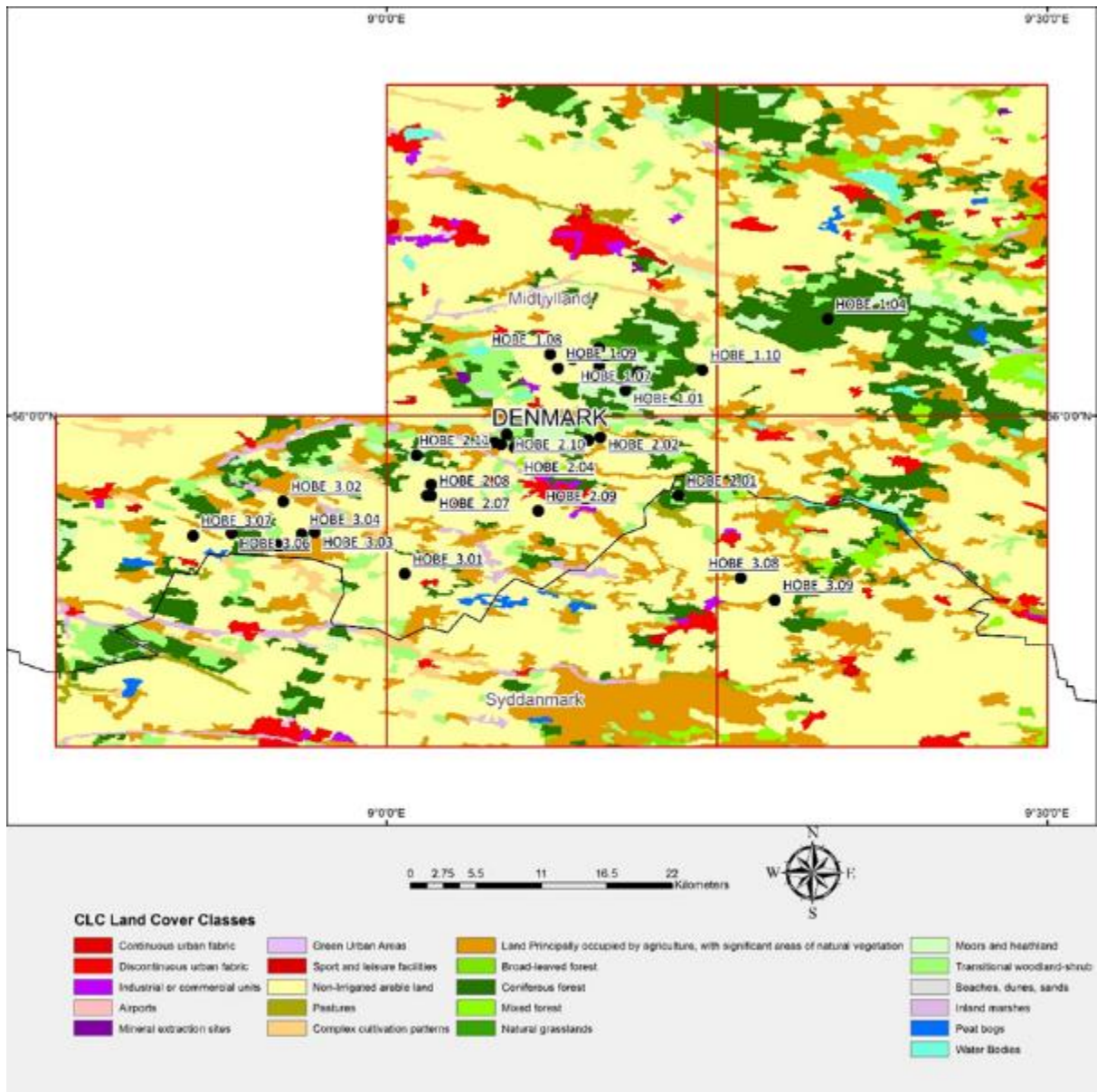


Figure 31: CORINE Land Cover classes in the Danish area of interest. (<https://land.copernicus.eu/pan-european/corine-land-cover/clc-2012/view>)



Figure 32: Time series of in-situ, ASAR and ECV SM v03.2 time stations in the Danish regions under investigation. The units are  $m^3 m^{-3}$ .

Table 4: Pearson correlation coefficient calculated for each pair of soil moisture datasets, including ESA CCI ECV v03.2. Correlation levels are all statistically significant ( $p$ -values  $< 0.05$ ). Danish regions under investigation.

Site	ASAR vs. ECV		ASAR vs. <i>in situ</i>		ECV vs. <i>in situ</i>	
	R	p	R	p	R	p
Hobe_1.01	0.69288	<0.001	0.48138	<0.001	0.726226	<0.001
Hobe_1.02	0.7327	<0.001	0.45866	<0.001	0.421416	<0.001
Hobe_1.03	0.62257	<0.001	0.70752	<0.001	0.648782	<0.001
Hobe_1.04	0.71919	<0.001	0.5828	<0.001	0.676535	<0.001
Hobe_1.05	0.657	<0.001	0.44777	<0.001	0.482671	<0.001
Hobe_1.06	0.70885	<0.001	0.59569	<0.001	0.539134	<0.001
Hobe_1.07	0.68843	<0.001	0.42721	<0.001	0.180475	<b>0.111</b>
Hobe_1.08	0.85573	<0.001	0.15133	<b>0.425</b>	0.014635	<b>0.939</b>
Hobe_1.09	0.71334	<0.001	0.02264	<b>0.873</b>	-0.010025	<b>0.944</b>
Hobe_1.10	0.62015	<0.001	0.4505	<0.001	0.592742	<0.001
Hobe_2.01	0.715	<0.001	0.42948	<0.001	0.44212	<0.001
Hobe_2.02	0.67911	<0.001	0.43303	<0.001	0.59289	<0.001
Hobe_2.03	0.72319	<0.001	-0.0597	<b>0.674</b>	-0.304251	<0.05
Hobe_2.04	0.66353	<0.001	0.37168	<0.05	0.232197	<b>0.125</b>
Hobe_2.05	0.71565	<0.001	0.26669	<0.05	0.405077	<0.005
Hobe_2.06	0.76147	<0.001	0.56439	<0.001	0.695674	<0.001
Hobe_2.07	0.7175	<0.001	0.13887	<b>0.363</b>	0.080072	<b>0.601</b>
Hobe_2.08	0.71856	<0.001	0.20279	<b>0.162</b>	0.20279	<b>0.162</b>
Hobe_2.09	0.68272	<0.001	-0.1455	<b>0.219</b>	-0.153958	<b>0.193</b>
Hobe_2.10	0.69729	<0.001	0.56066	<0.001	0.626417	<0.001
Hobe_2.11	0.77435	<0.001	0.16069	<b>0.281</b>	0.248788	<b>0.092</b>
Hobe_3.01	0.66847	<0.001	0.40138	<0.005	0.402692	<0.005
Hobe_3.02	0.84513	<0.001	0.24294	<b>0.057</b>	0.261357	<0.05
Hobe_3.03	0.75986	<0.001	0.23706	<0.05	0.292061	<0.05
Hobe_3.04	0.74358	<0.001	0.35049	<0.005	0.221412	<b>0.070</b>
Hobe_3.05	0.52566	<0.001	0.04693	<b>0.722</b>	-0.092301	<b>0.483</b>
Hobe_3.06	0.85772	<0.001	0.21179	<0.05	0.144942	<b>0.178</b>
Hobe_3.07	0.77222	<0.001	0.44459	<0.001	0.433369	<0.001
Hobe_3.08	0.71516	<0.001	0.33716	<0.001	0.452719	<0.001
Hobe_3.09	0.77633	<0.001	0.43492	<0.001	0.410793	<0.005

The adoption of the CDF-matching technique leads to reduction of bias between datasets which exhibit the same periodical behaviour, with wetter and drier conditions during specific periods of the year.



In the Danish regions under investigation, some in situ stations presented non periodical behaviour, affecting the temporal correlation between satellite and in-situ datasets. However, there are in situ stations distributed in all the region with periodical behaviour, where are observed high correlation values between satellite and in-situ datasets.

On the other hand, the correlation values between ASAR and ESA CCI SM v03.2 time series are fairly high in all the sites, generally ranging between 0.6 and 0.8. (See Table 4).

Concerning the short-term anomalies analysis, better results were found with respect to the Austrian sites. The correlation between ASAR and ESA CCI SM anomalies provides  $R > 0.6$  in all the sites. In addition, the correlation between satellite and in-situ datasets presented the same behaviour of the soil moisture correlation analysis, where a low correlation values were presented in stations with a non-periodical behaviour.

Analysis of the spatial variability in correlation between the ASAR SM time series and the ESA CCI SM v03.2 dataset (Figure 33) reveals the capability of the ECV SM to represent the moisture condition over the  $0.25 \times 0.25$  degree pixel used. There are many ASAR pixels within the analysed ECV cells, where  $R$  reaches values higher than 0.6. On the other side, there are low or not significance correlation values in some areas that are being part or are surrounded by forest classes defined in the CORINE Land Cover classification.

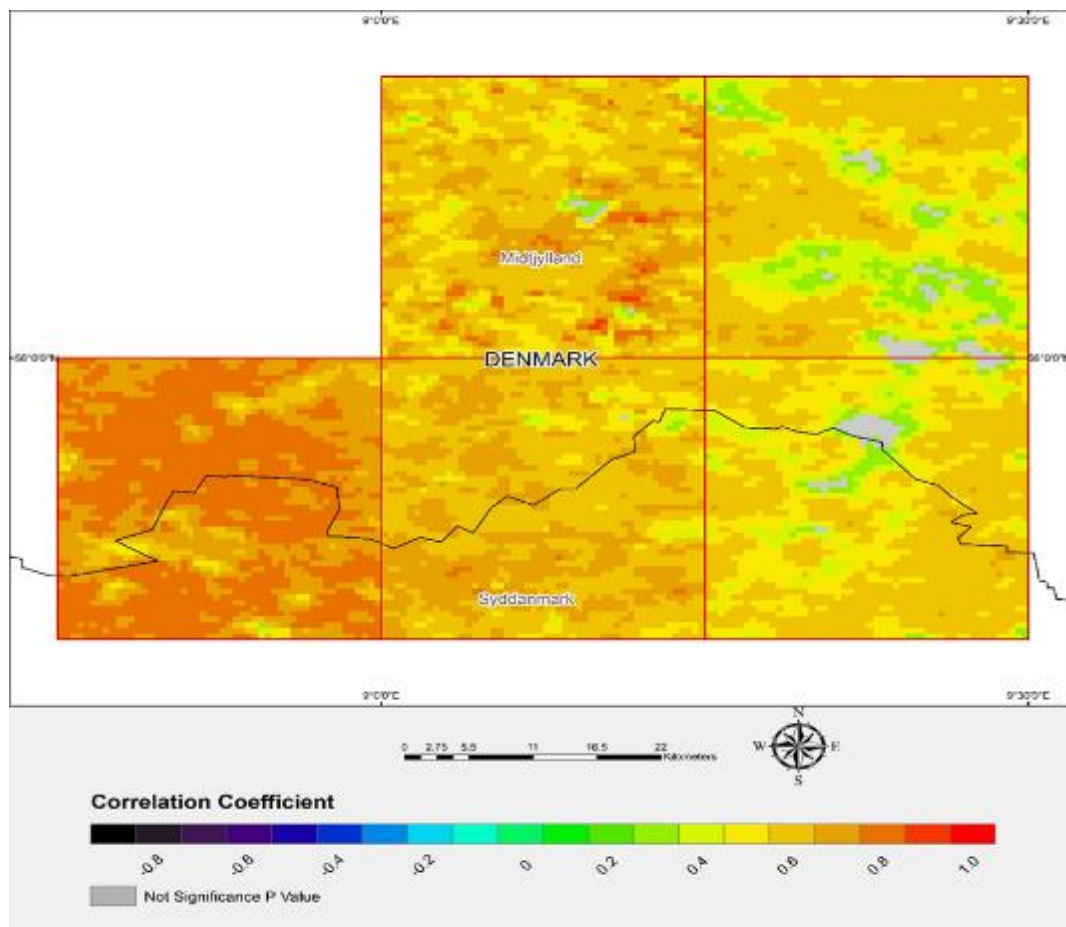


Figure 33: Spatial correlation between ASAR SM and ESA CCI SM v03.2 datasets in the Danish regions under investigation.



### ITALY

The representativeness of the ESA CCI SM v03.2 product was explored through comparison of the satellite-derived and ground-measured soil moisture time series over two different areas in Italy. The Calabria region presents a high topographic variation with altitudes between 0 and 2300 m a.s.l, this region is mainly covered by agricultural areas with a high percentage of non-irrigated lands and some vineyards areas. The remaining areas are mainly forest land covers. Finally, the Umbria presents a similar condition with a high topographic variation, most of this area is mountainous and hilly. Umbria presented an equality distributed land cover between agricultural and natural areas. The land cover distribution in accordance to the CORINE Land Cover dataset is showed in Figure 34.

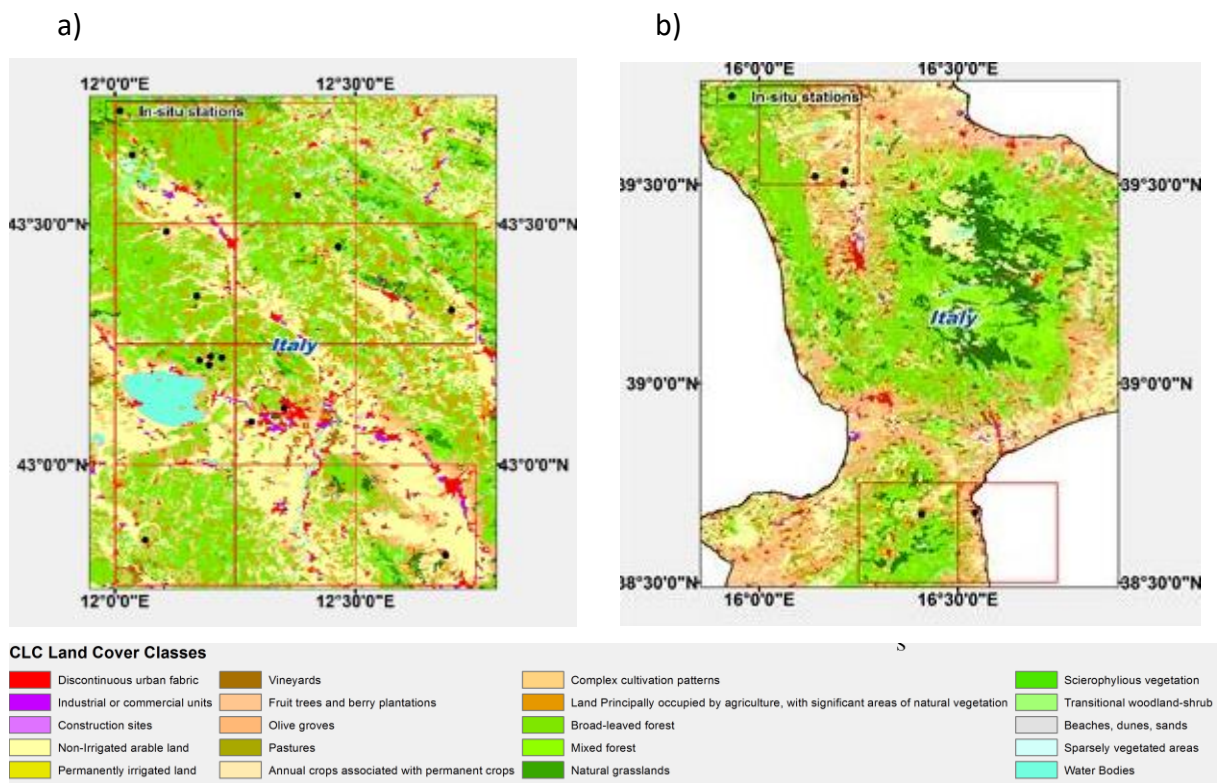


Figure 34: CORINE Land Cover classes in the Italian areas of interest. a) Umbria, b) Calabria (<https://land.copernicus.eu/pan-european/corine-land-cover/clc-2012/view>)

The temporal trend of the in situ stations with correlation values released is shown in Figure 35. It is observed that most of the temporally compatible data are collected from August 2008 until March 2012 due to a lack of ASAR data availability from 2006 to 2008.



Figure 35: Time series of in-situ, ASAR and ECV SM v03.2 time stations in the Italian regions under investigation. The units are  $m^3m^{-3}$ .



As mentioned before the CDF-matching technique leads to reduction of bias between datasets which exhibit the same periodical behaviour. In the Italian regions are observed wetter soil conditions in winter, and drier conditions in summer.

In the Calabrian region, two areas were analysed. The southern area presented two pixels with different topographic conditions. Most of the area of the western pixel is mountainous and hilly, the Chiaravalle Centrale in-situ station located in this area had not presented temporal compatible datasets. The same situation is presented in the second pixel where most of this area is part of the ocean, consequently the Satriano in-situ stations had not presented correlation values between the soil moisture datasets.

On the other hand, the second Calabrian area is located in the northern part of the region, mostly covered by flat agricultural lands with a piece of mountainous region located in the west of the ECV cell. There are three in-situ stations where Satellite derived and ground measurement datasets presented high correlation values ( $R > 0.7$ ) (See Table 5).

Finally, most of the Umbria region is mountainous or hilly with forest lands. In this area, most of the in-situ stations had not presented temporal compatible datasets. Likely, the presence of a very high topographic variation and forest lands affected the accuracy of the ASAR SM dataset. An exception, occurs in the Hydrol-Net-Perugia in-situ station, where we found temporal compatible datasets, but there are not significant or very low correlation values between satellite derived datasets

Table 5: Pearson correlation coefficient calculated for each pair of soil moisture datasets, including ESA CCI ECV v03.2. Correlation levels are all statistically significant ( $p$ -values  $< 0.05$ ). Italian regions under investigation.

Site		ASAR vs. ECV		ASAR vs. <i>in situ</i>		ECV vs. <i>in situ</i>	
Region	Station	R	p	R	p	R	p
Calabria	Chiaravalle Centrale	---	---	---	---	---	---
	Satriano	---	---	---	---	---	---
	Fitterizzi	0.762	<0.001	0.75783	<0.001	0.78641	<0.001
	Mongrassano	0.76323	<0.001	0.49783	<0.001	0.68763	<0.001
	Torano	0.77129	<0.001	0.74368	<0.001	0.78515	<0.001
Umbria	Hydrol-Net-Perugia	0.36582	<0.05	0.24546	<b>0.113</b>	0.75265	<0.001

Analysis of the spatial variability in correlation between the ASAR SM time series and the ESA CCI SM v03.2 dataset (Figure 36) reveals the capability of the ECV SM to represent the moisture condition over flat areas.

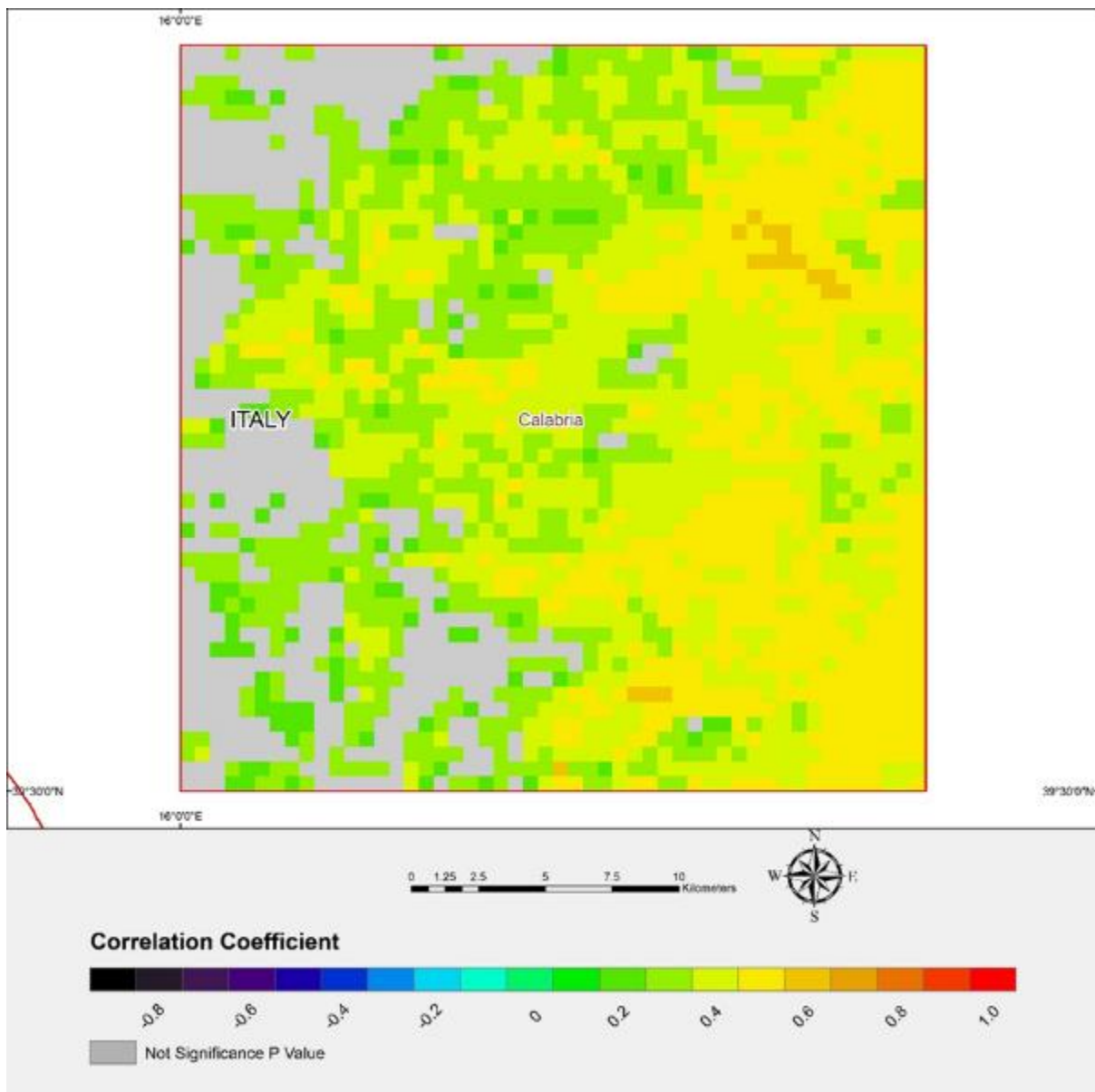


Figure 36: Spatial correlation between ASAR SM and ESA CCI SM v03.2 datasets in the Calabrian (Italy) regions under investigation.

### 5.4.3 Discussion and Conclusions

The representativeness of the global CCI ECV SM v.03.2 product is investigated through the use of finer spatial resolution ASAR Wide Swath (WS) data and ground measurements across three European regions: Austria, Denmark and Italy.

The results achieved by comparing the three soil moisture datasets temporally and spatially do not generally differ significantly from those found during the previous validation activities. Therefore, we can confirm the capability of the ECV SM v03.2 product to represent the soil moisture variability, despite its coarser spatial resolution.

The comparison of the ECV SM v03.2 product with the ASAR WS and in-situ time series confirms the capability of the former to capture the temporal dynamics of soil moisture in Denmark and in flat areas in Calabria, Italy, where a seasonal variation occurs.

On the contrary, very poor agreement are observed in the Eastern Styria region in Austria, where the correlation between ASAR SM, ECV SM v03.2 and in-situ dataset are generally lower than 0.5. Such a result is likely to be due to a loss of the SM product accuracy due to the forest coverage and the topographic complexity effect. An exception occurs in WEGENERNET 50 station, where was observed an acceptable correlation between satellite retrieved SM datasets and ground measurements.

A short-term anomalies study was also carried out by subtracting the average of at least three soil moisture measurements within a time interval of 35 days (17 days before and 17 days after each SM observation). The choice of evaluating the anomalies with respect to only three SM values is due to the limited number of data available in all the regions under investigation. However, we understand that such a small amount of observations provides unreliable results in terms of correlation between the datasets.

The comparison between soil moisture time series in each ASAR pixel and in the corresponding ECV cells shows high R values in flat areas. By studying the spatial distribution of the correlation between ASAR and ECV SM v03.2 in the Denmark sites, we find that higher correlation patterns occur in areas covered by less dense forest. In addition, the temporal distribution analysis showed higher correlation values in the time series with seasonal trends.

On the basis of the overall outcomes of this validation activity, we can state that the ECV SM v03.2 product is a good representation of the soil moisture condition over the  $0.25^\circ \times 0.25^\circ$  cell. However, although providing confidence in the use of the ECV SM product, results and observations presented in this study highlight also the need of further investigation of the source of error related to SM retrieval algorithms, particularly over forest coverage and complex topography. Therefore, it will be necessary to test the ECV SM quality with further studies in other regions worldwide, with the aim of comprehensively understanding this global soil moisture product. As the ECV SM dataset is updated, improved and temporally extended, Sentinel-1 data will replace the ASAR WS acquisitions for the quality assessment activity.

## 5.5 Validation over boreal and sub-arctic environmental data (FMI)

Contributors: J. Ikonen, T. Smolander, K. Rautiainen and J. Pulliainen (FMI)

### 5.5.1 Introduction

As with previous validation studies, validation of the ESA CCI soil moisture (SM) datasets in boreal and subarctic regions focuses on validation in the Sodankylä region, Northern Finland. The Sodankylä region represents a typical northern boreal forest / taiga environment hosting a multidisciplinary research centre operated by the Finnish Meteorological Institute (FMI).

Figure 37 depicts the location of the Sodankylä multidisciplinary research centre and the location of the validation study domain. A more detailed description of the Sodankylä region

and the in situ instrumentation located at the multidisciplinary research centre is provided in Ikonen et al. (2016).

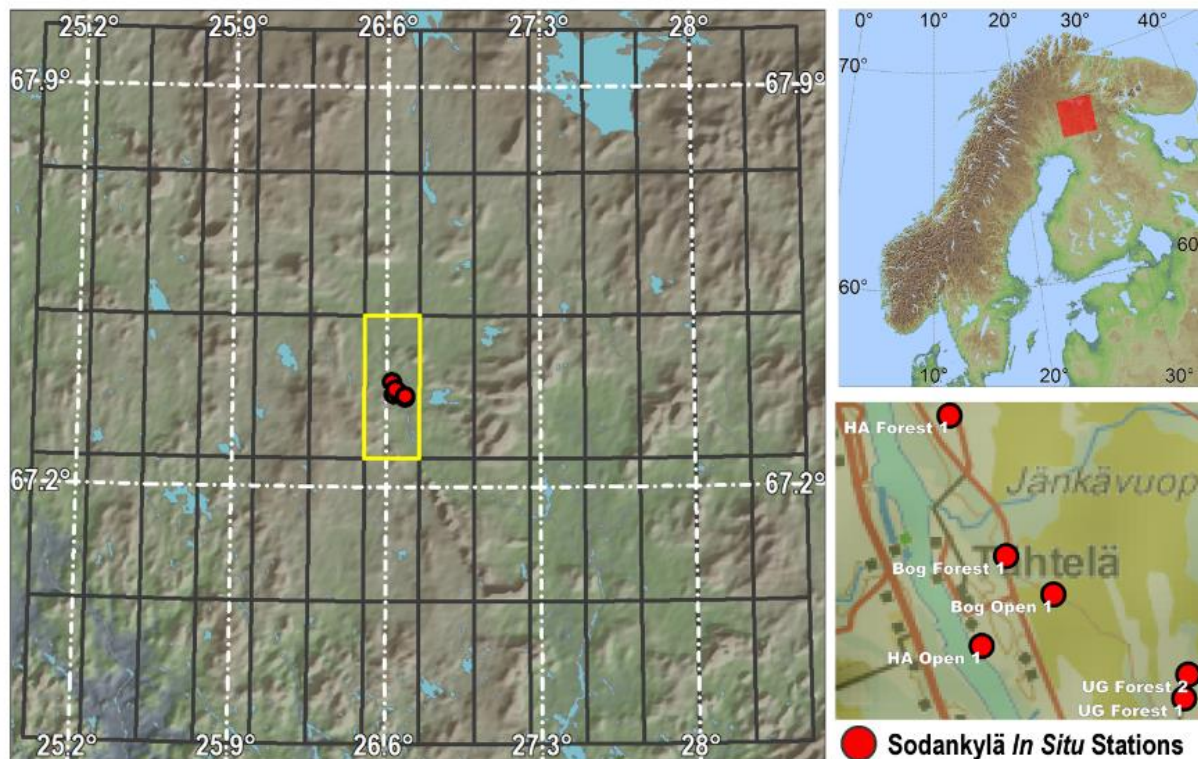


Figure 37: Location of the Sodankylä study domain, the 70 ESA CCI SM product pixels and distribution of FMI's soil moisture observation sites.

This validation study focuses on comparing the different versions of the ESA CCI soil moisture datasets released during 2017 and 2018, namely versions v03.2, v04.1 to v05.0. Weighted in situ observation based validation and comparisons are performed in a single ESA CCI SM pixel for snow free summer periods (June–September) between the years 2012 and 2017. A spatially distributed version of the "Sacramento Soil Moisture Accounting Model" (SAC-SMA; Burnash 1995) and a potential evapotranspiration model based on Hamon's approach in Oudin et. al (2005) forms the components of the modelling system used for multi-pixel, model based, validation and comparison. The model domain covers an area of 155 km by 140 km and encloses 70 ESA CCI soil moisture product pixels / SAC-SMA model grid cells. The Sodankylä multidisciplinary research centre is located roughly in the middle of the domain.

### 5.5.2 Single-pixel, In Situ Based Validation

As done previously in PVIR studies, in situ based validation is conducted in one ESA CCI soil moisture pixel, covering an area of 26 km (north-south) by 10 km (west-east), encapsulating the Sodankylä multidisciplinary research centre. In situ soil moisture observations are taken from sensors at a depth of 5 cm except for stations on semi-organic soils. For these stations, top soil moisture measurements are taken at a depth of 10 cm. A total of 6 stations are used to produce a single soil moisture value representing the ESA CCI SM pixel. The list of stations, their descriptions and weights used ("Weighting Scheme 1") are provided in the previous PVIR

document [RD-01]. In situ validation and comparisons are conducted for the ESA CCI SM COMBINED version v04.1 and v05.0 products and against their component products; ACTIVE and PASSIVE soil moisture retrievals separately. Validation and comparisons for all products versions are conducted for, snow free, summer periods (June–September) between the years 2012 and 2017.

Table 6: ESA CCI SM product yearly correlations with daily weighted in situ observations

YEAR	COMBINED	COMBINED	ACTIVE	ACTIVE	PASSIVE	PASSIVE
	v04.1	v05.0	v04.1	v05.0	v04.1	v05.0
2012	0.57	0.69	0.60	0.66	0.64	-
2013	0.64	0.72	0.66	0.66	0.75	-
2014	0.26	-0.05	0.09	0.12	0.59	-
2015	0.57	0.40	0.42	0.42	0.66	0.72
2016	0.17	-0.08	-0.04	-0.04	0.28	0.68
2017	-	0.14	-	0.07	-	0.65

Table 7: ESA CCI SM product summer period number of days with observations

YEAR	COMBINED	COMBINED	ACTIVE	ACTIVE	PASSIVE	PASSIVE
	v04.1	v05.0	v04.1	v05.0	v04.1	v05.0
2012	110	104	110	104	39	-
2013	95	95	95	95	58	-
2014	81	81	81	81	43	-
2015	94	94	94	94	55	75
2016	96	96	96	96	43	71
2017	-	95	-	95	-	45

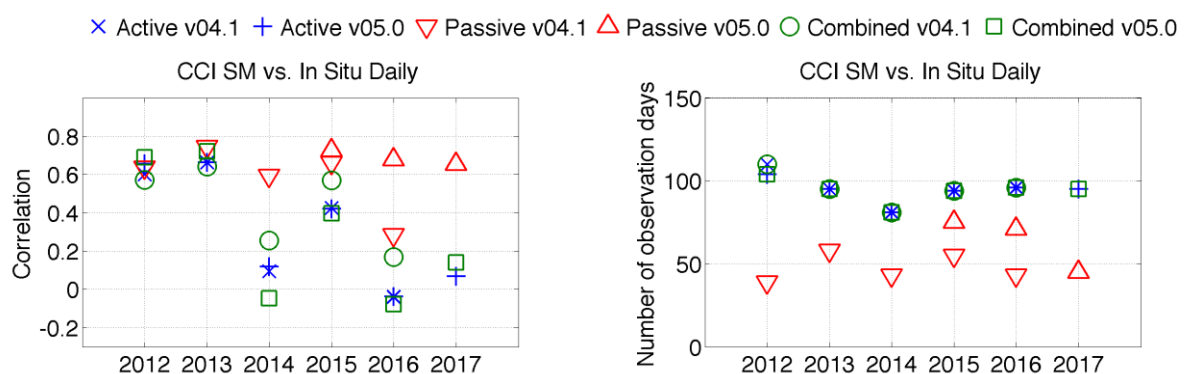


Figure 38: Left; ESA CCI SM ACTIVE, PASSIVE and COMBINED v04.1 and v05.0 products' correlations with daily weighted in situ measurements. Right; number of observation days for ESA CCI SM ACTIVE, PASSIVE and COMBINED v04.1 and v05.0 products during the summer period of each year.

A comparisons of yearly (summer period, 2012 to 2017) correlations with weighted in situ observations for ESA CCI SM COMBINED products (version v04.1 and v05.0) were conducted as part of the in situ, single pixel, based validation study. The statistical metrics for the



corresponding validation results are provided in Table 6 and Table 7. A comparison of ESA CCI SM product version v04.1 and v05.0 component correlations with weighted in situ observations is provided in Figure 38 (left).

Although the PASSIVE product exhibits the best performance against weighted in situ observations, the amount of missing data is a clear disadvantage in terms of applicability in any type of end user applications. With both the v04.1 and v05.0 versions of the ESA CCI SM product, the ACTIVE and COMBINED components contain an equal amount of observations, and between the two versions there is only a small difference for the year 2012. With the v04.1 version the PASSIVE component only has half of the observations compared to the ACTIVE and COMBINED components, or even less during 2012. The v05.0 version of the PASSIVE component has more observations than the version v04.1 for the years 2015 and 2016, but still less than ACTIVE and COMBINED components in both product versions, and in 2017 the v05.0 PASSIVE component has less than half of the observations compared to v05.0 ACTIVE and COMBINED components. Further, PASSIVE v05.0 observations were only available for 2015, 2016 and 2017 for the Sodankylä pixel, see Figure 38 (right).

The overall daily correlation with in situ observations between 2012 and 2016 is around the same in COMBINED product versions v04.1 and v05.0 (0.43 vs. 0.42). Weekly correlation between weighted in situ and the v04.1 version is clearly higher (0.57 vs. 0.46) than with the v05.0 version. The COMBINED product v0.50 exhibits higher daily correlation with in situ observations in 2012 (0.69 vs. 0.57) and 2013 (0.72 vs. 0.64) than COMBINED v0.41 product. The previous product version (v0.41) exhibits higher daily correlations in 2015 than the latest version (v0.50), while during 2014 and 2016 both product versions exhibit low correlation with daily in situ observations. The latest product v0.50 also exhibits low correlation at 2017 (which is not available in v04.1). The COMBINED v05.0 product provides more similar climatology to the weighted average level of in situ observations than the previous v04.1 version, i.e. smaller bias.

The ACTIVE v05.0 product exhibits nearly the same performance as the previous product version (v04.1), however daily correlation with in situ observations in 2012 were slightly higher, although with slightly fewer observations. The daily correlation between PASSIVE v05.0 and in situ observations were satisfactory (ranging between 0.65 and 0.72) for the entire analysis period of 2015 and 2017. The daily correlation between PASSIVE v05.0 and in situ observations for 2016 was clearly higher and for 2015 slightly higher than with the previous PASSIVE v04.1 version. There were also significantly more data available in the v05.0 version for both both 2015 and 2016 in the Sodankylä pixel. Although, the PASSIVE v05.0 version performed significantly better than the COMBINED v05.0 version for the years 2015-2017, there was significantly less data available. Further, PASSIVE v05.0 observations were only available for 2015, 2016 and 2017 for the Sodankylä pixel.

### **5.5.3 Multi-pixel, SAC-SMA Model Configuration**

The multi-pixel validation domain covers an area of 155 km by 140 km and encloses 70 ESA CCI soil moisture product pixels / SAC-SMA model grid cells. Multi-pixel validation is conducted for a period of 13 years covering the summer periods (June 1<sup>st</sup> to September 30<sup>th</sup>), between the years 2003 and 2015. The multi-pixel, model based, validation study focuses on ESA CCI





SM COMBINED product versions v03.2 v04.1 and v0.50 including their component ACTIVE and PASSIVE products.

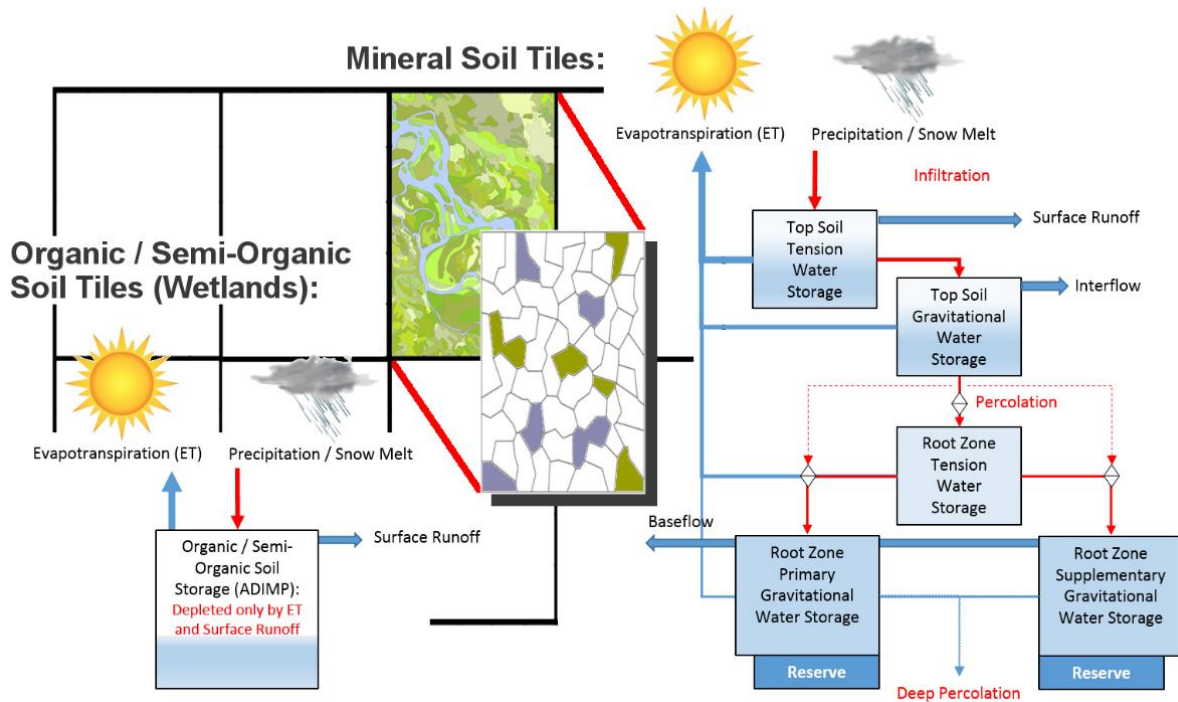


Figure 39: A conceptualization of the SAC-SMA model. Each SAC-SMA model grid cell is divided into a maximum of 14 soil / vegetation density type tiles representing cross combinations of the 4 main mineral soil types. Semi-organic and organic soils are modelled with a separate scheme.

Each SAC-SMA model grid cell is divided into a maximum of 14 soil / vegetation density type tiles representing cross combinations of the 4 main mineral soil types (Fine Haplic Podzol, Coarse Haplic Podzol, Haplic Arenosol, Eutric Regosol) and three primary vegetation density types (dense, sparse and open) as well as separate tiles for semi-organic and organic soil as well as shallow rocky soils. The spatial coverage (size) of each individual tile varies from grid cell to grid cell based on the distribution of soil types within each grid cell.

With the SAC-SMA model, we calculate mineral soil and shallow rocky soil tile soil moisture through two conceptual vertical soil zones; an upper zone representing short-term surface soil and interception storage, and a lower zone representing deeper root zone soil moisture storages. The zones have free water and tension water elements, where the free water (fast flow component) is predominantly driven by gravitation forces, but may also be depleted by evapotranspiration, percolation and horizontal flow, while the tension water (slow flow component) is driven by evapotranspiration and diffusion. Organic and semi-organic soil tile soil moisture is calculated with a single conceptual soil moisture storage (represented by an impervious area fraction parameter “ADIMP” in the model) that can only be depleted by evapotranspiration and horizontal flow. A conceptualization of the SAC-SMA model and our implementation is provided in Figure 39. The SAC-SMA model used in this study has been extensively validated with in situ observations in the previous PVIR report [RD-01].

### 5.5.4 Multi-pixel, Model Based Validation

Overall the 70 pixel average daily ESA CCI COMBINED SM product's correlation between v05.0 and v04.1 with SAC-SMA model estimates are relatively similar, i.e. years during which the v04.1 product exhibits good or poor correlation, the newest v05.0 product exhibits similar patterns. A clear improvement from version v03.2 can however be observed, for both products (see Figure 40). The main difference is that with the newest product version (v05.0) the deviations tend to be more extreme; when the ESA CCI COMBINED SM product performs poorly, the v05.0 product tends to perform significantly more poorly, conversely when the ESA CCI COMBINED SM product exhibits better performance, version v05.0 tends to exhibit somewhat better overall performance. With the ESA CCI COMBINED SM v05.0 product, the 70 pixel average daily correlation during 2004, 2007, 2014 and 2016 exhibit very poor performance, with even negative average correlations for 2004. Both the previous ESA CCI COMBINED SM, v04.1 product version and v05.0 version exhibit high correlation with SAC-SMA model estimates, clearly exceeding the 0.5 value mark, during 2012, 2013 and 2015. With the v05.0 version providing improved correlations over version v04.1.

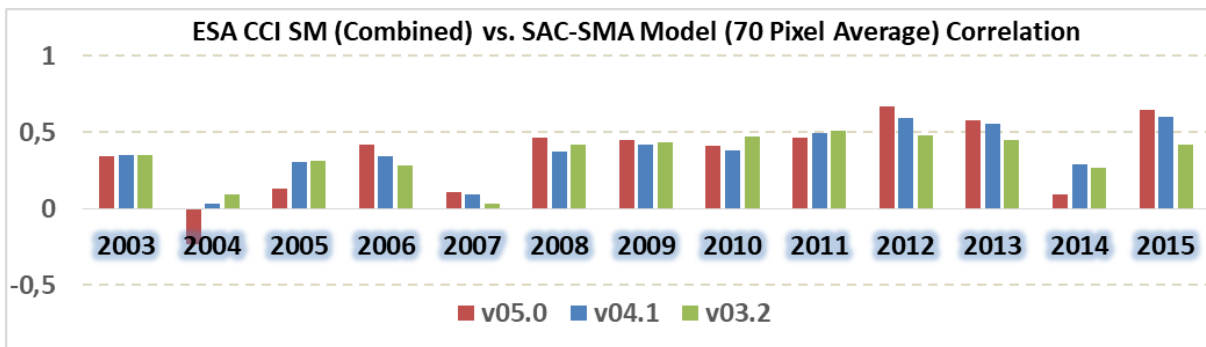


Figure 40: ESA CCI SM COMBINED SM v03.2 v04.1 and v05.0 product 70 pixel average correlation with. SAC-SMA Model top layer SM estimates

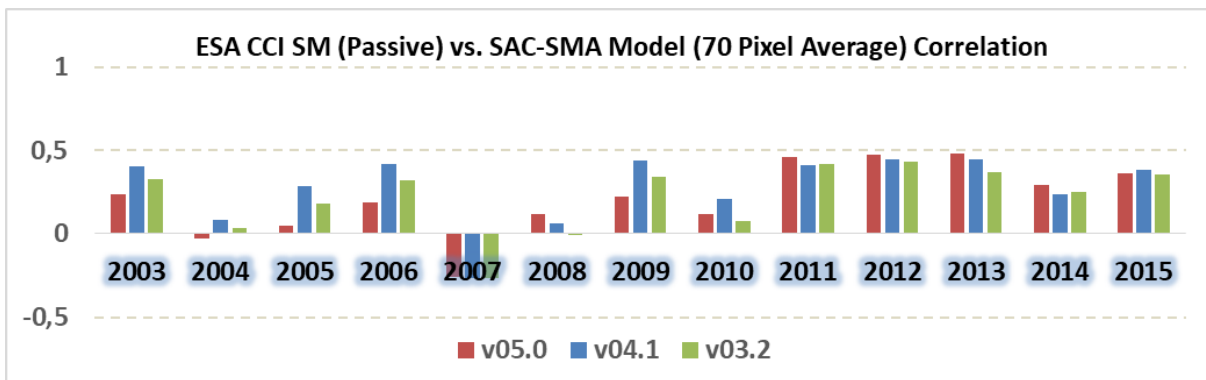


Figure 41: ESA CCI SM PASSIVE SM v03.2 v04.1 and v05.0 product 70 pixel average correlation with. SAC-SMA Model top layer SM estimates.

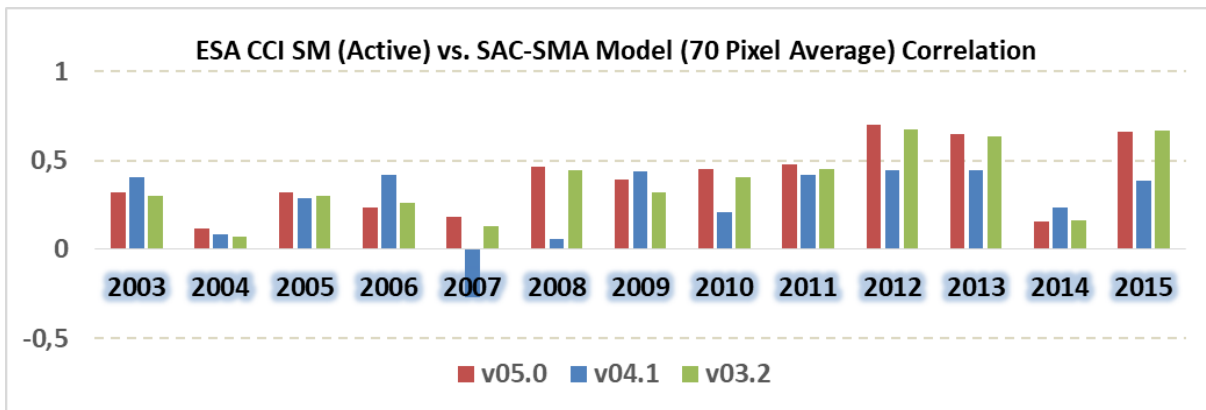


Figure 42: ESA CCI SM ACTIVE SM v03.2 v04.1 and v05.0 product 70 pixel average correlation with SAC-SMA Model top layer SM estimates.

The average ESA CCI PASSIVE SM (2003-2017) 70 pixel average daily correlation between v05.0 (0.22) and v04.1 (0.26) with SAC-SMA model estimates are nearly the same. However, there is a clear improvement in daily correlation with SAC-SMA model estimates after 2010 with the v05.0 product. Prior to 2011, however, there is a significant decrease in correlation with SAC-SMA model estimates (see Figure 41). A major shortcoming of the newest (v05.0) ESA CCI PASSIVE product is the amount of missing data; between 2010 and 2014 only half of the 70 pixels investigated contained PASSIVE observations with the v05.0 product version and before 2010 only 16% of the pixels had any data, which was less than in v04.1 (see Figure 43).

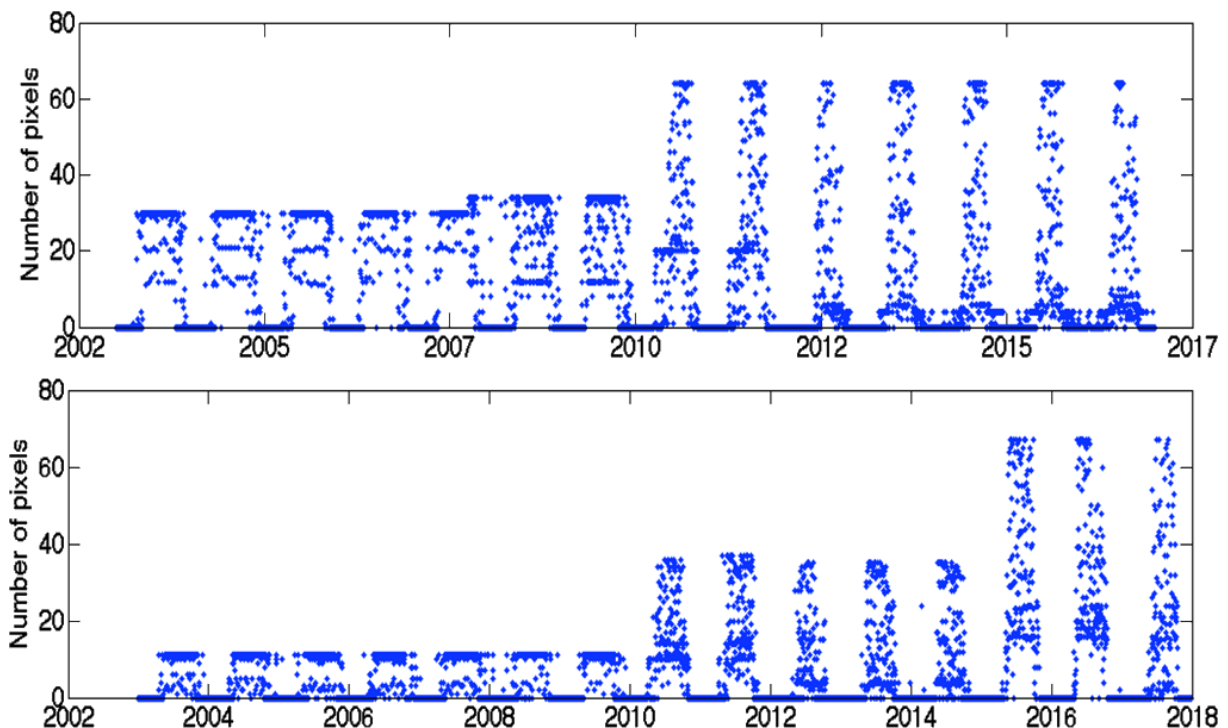


Figure 43: Number of pixels (out of 70) containing PASSIVE SM observations in version v05.0 (right). Number of pixels (out of 70) containing PASSIVE SM observations in version v04.1 (right).

The 70 pixel average ESA CCI ACTIVE SM v05.0 version clearly exhibits an improvement in daily correlation with SAC-SMA model estimates. In particular there is a clear improvement in average correlation after 2006. The only exception is 2014 (as well as 2009, although to a much lesser degree), which has been problematic for the ESA CCI SM products through-out the previous versions (see Figure 42). In general the ESA CCI ACTIVE SM products for all validated versions outperform the COMBINED and PASSIVE SM products.

### 5.5.5 Multi-pixel, Spatio-Statistical Pattern Analysis

As part of the multi-pixel, model based, validation we explore the dependency of PASSIVE and ACTIVE soil moisture retrieval performance to differences in soil/vegetation type tile coverage within each SAC-SMA model grid cell (i.e., ESA CCI SM product pixel). This is explored in order to determine if any specific soil/vegetation combination(s) are a factor in determining ESA CCI SM product correlation with SAC-SMA model soil moisture, i.e., does the domination of some soil/vegetation type combination within a pixel increase or decrease ESA CCI SM data product performance. Due to the large amount of missing data for the newest (v.05.0) ESA CCI SM product, particularly the large amount of missing PASSIVE observations, this analysis is only conducted for v.04.1 PASSIVE and ACTIVE components. With this assessment, for simplicity and since mineral soil/vegetation tile soil moisture correlate strongly with each other, all mineral soil/vegetation tiles (excluding shallow soils) are merged into a single “mineral soils” tile.

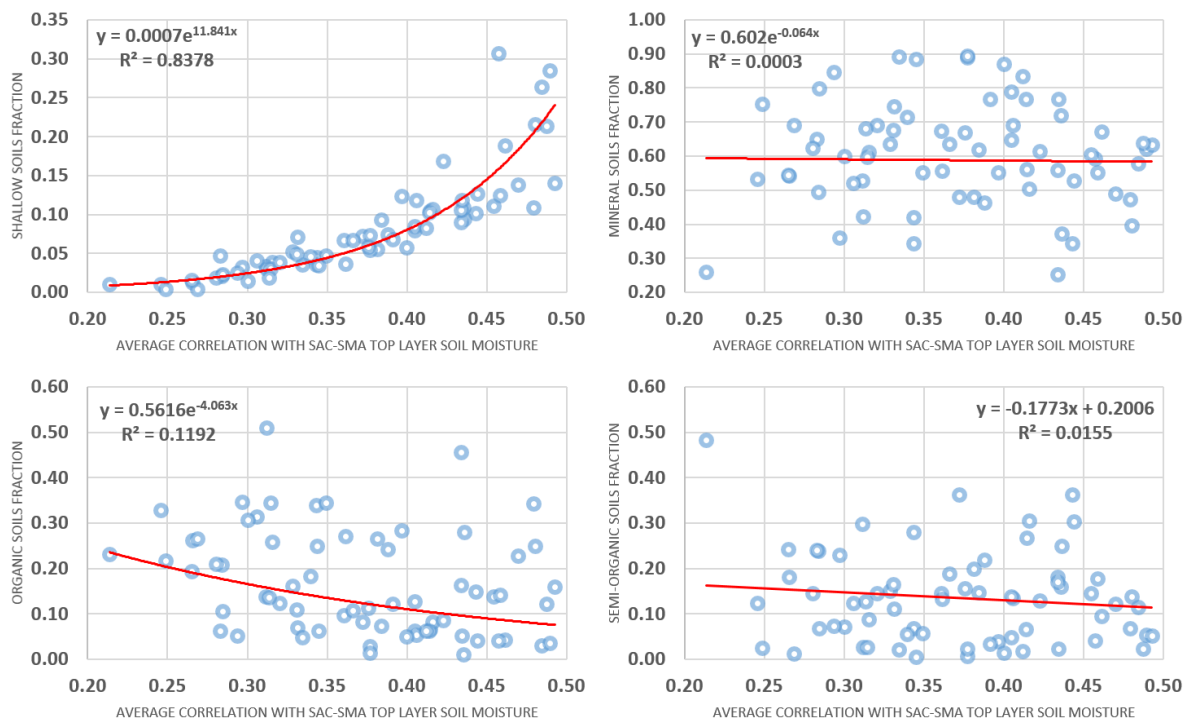


Figure 44: ESA CCI SM ACTIVE product correlation with SAC-SMA model top layer soil moisture dependency on pixel-wise major soil/vegetation type fraction size.

In Figure 44, we provide diagrams of major soil/vegetation type fraction sizes against ACTIVE soil moisture retrieval correlation with SAC-SMA model top layer soil moisture estimates. A best fit trend line along with the equation describing the relationship and the R-squared value is also provided. From Figure 44, we can deduce that there exists a significant exponential relationship (R-squared value of 0.8378) between ACTIVE soil moisture retrieval correlations with SAC-SMA model top layer soil moisture estimates and the size of the shallow soils fraction in a pixel. The relationship is given as:

$$y = 0.0007e^{11.841x}$$

where, y is the correlation of ACTIVE soil moisture retrieval with SAC-SMA model top layer soil moisture and x is the size of shallow soils fraction within a pixel. The other major soil/vegetation type fractions do not exhibit significant relationships with ACTIVE soil moisture retrieval and SAC-SMA model top layer soil moisture estimate correlations. Further, it is not possible to define a statistically significant multiple linear regression model describing the dependency of major soil type fractions and ACTIVE soil moisture retrieval correlation with SAC-SMA model top layer soil moisture estimates. As such, the exponential relationship between shallow soil fraction size and correlation with SAC-SMA model estimates is the single best predictor.

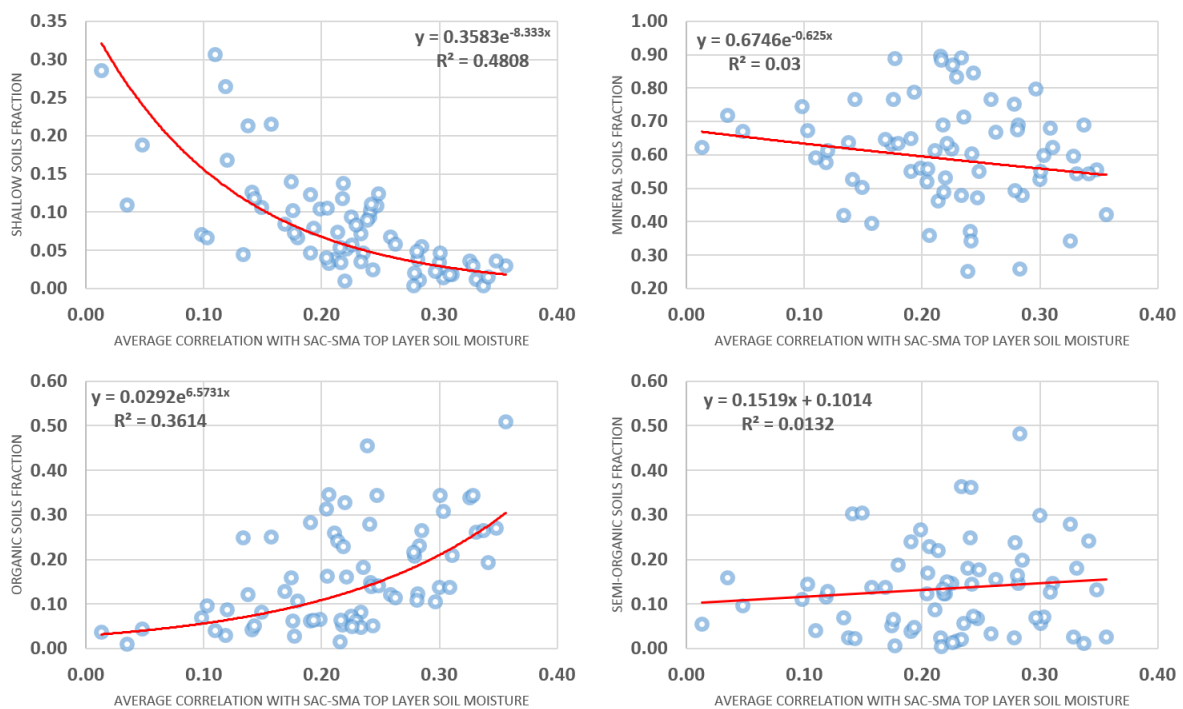


Figure 45: ESA CCI SM PASSIVE product correlation with SAC-SMA model top layer soil moisture dependency on pixel-wise major soil/vegetation type fraction size.



In Figure 45, we provide corresponding diagrams of major soil/vegetation type fraction sizes against PASSIVE soil moisture retrieval correlation with SAC-SMA model top layer soil moisture estimates. As with ACTIVE soil moisture retrieval analysis, a best fit trend line along with the equation describing the relationship and with the R-squared value is also provided. For PASSIVE soil moisture retrievals, multiple relationships exist between major soil type fraction size and correlation with SAC-SMA model top layer soil moisture. In contrast to the ACTIVE soil moisture retrieval relationship with shallow soil fraction size, PASSIVE soil moisture retrievals exhibit a negative exponential trend (with an R-squared value of 0.4808) in correlation. The relationship is given as:

$$y = 0.3583e^{-8.333x}$$

where,  $y$  is the correlation of PASSIVE soil moisture retrieval with SAC-SMA model top layer soil moisture and  $x$  is the size of shallow soils fraction within a pixel. The size of organic soil fraction size also exhibits a somewhat significant relationship with PASSIVE soil moisture retrieval correlation with SAC-SMA model top layer soil moisture. In contrast to shallow soil fraction size, this relationship can be expressed with a positive exponential trend (with an R-squared value of 0.3614). The relationship is given as:

$$y = 0.0292e^{6.5731x}$$

where,  $y$  is the correlation of PASSIVE soil moisture retrieval with SAC-SMA model top layer soil moisture and  $x$  is the size of organic soils fraction within a pixel. Dependencies also exist between the other (mineral soil and semi-organic soil) major soil/vegetation type fractions size and PASSIVE soil moisture retrieval correlation with SAC-SMA top layer soil moisture, but these relationships alone are rather weak (see Figure 45).

As part of the spatial association assessment, we also calculate the study domain wide average inter-pixel cross-correlation for each year as a measure of general soil moisture time series similarity between the pixels. The higher the domain wide average inter-pixel cross-correlation, and the higher the negative correlation between pixel-pair and distance vectors, the less variability there is between the pixels' soil moisture time series and the more of this variation can be explained solely by the distances between pixels. Conversely, the lower the domain wide average pixel-pair correlation, the more soil moisture time series variability there is between the pixels. Further, the lower the negative correlation between the pixel-pair and distance vectors, the more other factors in conjunction with distance determine inter-pixel cross-correlations. The yearly average inter-pixel soil moisture cross-correlation, as well as distance dependent correlation decay values, are provided in *Table 8*. The relationship between individual pixel-pair vector member correlations and corresponding distance vector members is illustrated in Figure 46. As a reference, we also compute the same spatial association metrics for FMI interpolated daily 10 km resolution precipitation observations, as well as SAC-SMA model top layer soil moisture estimates.





Table 8: Yearly, study domain wide average inter-pixel soil moisture cross-correlation and inter-pixel soil moisture cross-correlation dependency on (correlation with) distance between pixel-pairs for ESA CCI ACTIVE and PASSIVE soil moisture data and SAC-SMA top layer model soil moisture data, as well as spatial autocorrelation for FMI interpolated precipitation observations.

YEAR	Domain Wide Average Inter-Pixel Soil Moisture Cross-Correlation				Inter-Pixel Soil Moisture Cross-Correlation Dependency on (Correlation with) Distance			
	ACTIVE	PRECIP.	PASSIVE	SAC-SMA	ACTIVE	PRECIP.	PASSIVE	SAC-SMA
2003	0.82	0.77	0.60	0.77	-0.77	-0.84	-0.62	-0.49
2004	0.92	0.75	0.77	0.78	-0.89	-0.92	-0.59	-0.67
2005	0.79	0.78	0.71	0.82	-0.94	-0.82	-0.59	-0.42
2006	0.83	0.76	0.56	0.83	-0.91	-0.78	-0.67	-0.42
2007	0.90	0.76	0.75	0.80	-0.93	-0.79	-0.46	-0.61
2008	0.90	0.74	0.76	0.70	-0.92	-0.87	-0.69	-0.85
2009	0.88	0.79	0.64	0.82	-0.94	-0.88	-0.68	-0.52
2010	0.92	0.77	0.65	0.72	-0.91	-0.78	-0.74	-0.71
2011	0.84	0.79	0.58	0.74	-0.95	-0.86	-0.77	-0.77
2012	0.87	0.79	0.59	0.84	-0.92	-0.94	-0.41	-0.63
2013	0.91	0.75	0.47	0.79	-0.90	-0.82	-0.57	-0.54
2014	0.91	0.80	0.50	0.80	-0.90	-0.88	-0.63	-0.61
2015	0.86	0.85	0.55	0.84	-0.95	-0.92	-0.62	-0.65
Average	0.87	0.78	0.63	0.79	-0.91	-0.85	-0.62	-0.61

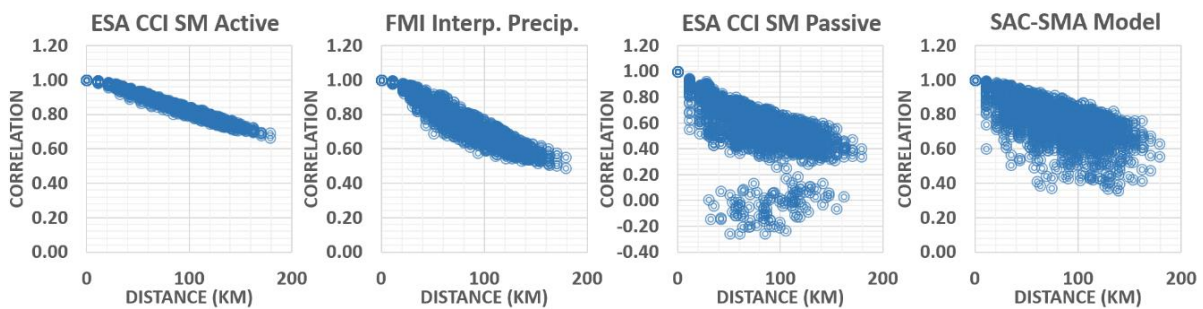


Figure 46: Distance-based decay of inter-pixel soil moisture cross-correlation for ESA CCI ACTIVE and PASSIVE soil moisture data and SAC-SMA top layer model soil moisture data, as well as spatial autocorrelation for FMI interpolated precipitation observations.

Both the ACTIVE soil moisture product and FMI interpolated daily 10 km resolution precipitation observations exhibit high yearly average inter-pixel cross-correlations and high negative yearly inter-pixel cross-correlation with distance. This appears to indicate that nearby pixels' soil moistures tend to correlate with each other irrespective of the physiographic differences between them. Low spatial variability for precipitation in northern latitudes, such as in the Sodankylä region, is expected since the majority of precipitation events are known to be caused by precipitation fronts rather than by convective storm cells. However, this



should not necessarily be the case for soil moisture, which is affected by not only meteorological conditions, but also by physiographic characteristics as well, which in the Sodankylä region exhibit considerable variation from ESA CCI SM pixel to pixel. This, and the very high dependency of these correlations to shallow soils fractions, as well as the known rapid response of these soil types to both precipitation and evaporation, raises the question that the relatively good performance of the ACTIVE product with SAC-SMA model top soil estimates may be good “for the wrong reasons”. We therefore argue that it is possible that ACTIVE soil moisture retrievals likely respond mainly to direct changes in precipitation and possibly to moisture on vegetation surfaces rather than to actual moisture in the top soil layer. Although the correlation between PASSIVE soil moisture retrievals and SAC-SMA model top layer soil moisture is rather low, they both exhibit a similar, low negative correlation between pixel-pairs and distance. This, and the fact that the PASSIVE product appears to be responding to differences in soil type distributions between pixels, points to the greater ability of the PASSIVE product to represent changes in soil moisture over the ACTIVE product in the Sodankylä region.

## 6 Conclusions

The overall conclusion from the various and diverse studies described in this report (involving comparisons against in-situ datasets, model simulations, and data assimilation analyses) is that the ECV soil moisture v04.2 product is generally suitable for representing the spatio-temporal evolution of the land surface (in particular, its temporal dynamics) at most locations in the World. However, as documented elsewhere for other soil moisture datasets, the ECV soil moisture product suffers shortcomings at northern high latitudes (northward of 60°N, though improving from earlier products), over regions with complex topography and regions with dense vegetation, all areas well known to be difficult to monitor from remote sensing platforms.

Within the ESA ECV soil moisture itself, there is evidence that the active ECV product performs better than the passive ECV product in comparison to independent soil moisture datasets. Nevertheless, the performance of the combined product (current and forerunner versions) suggests that the product is reaching maturity.

Technical issues were identified in the v05.0 product that have prevented its general release as the latest public version of the product.

Finally, we note the potential of data assimilation for adding value to the ECV soil moisture product, e.g., by providing soil moisture information at higher spatial resolution in the horizontal, and in the vertical (e.g., providing information on root zone soil moisture). This is especially relevant for regions where high quality precipitation data sets are lacking, here the ESA CCI SM product can provide valuable additional information of the state of the land surface. Various workshops and meetings within the ESA CCI for soil moisture have identified the importance of root zone soil moisture information for studies of the climate system, including the hydrological and carbon cycles.

## 7 Bibliography

### Reference documents:

[RD-01] Product Validation and Intercomparison Report Revision 2 (PVIR), June 2017

Albergel, C., Rüdiger, C., Carrer, D., Calvet, J.-C., Fritz, N., Naeimi, V., Bartalis, Z., and Hasenauer, S. (2009). An evaluation of ascat surface soil moisture products with in-situ observations in southwestern France. *Hydrology and Earth System Sciences*, 13, 115–124.

Albergel, C., Brocca, L., Wagner, W., de Rosnay, P., and Calvet, J.C. (2013). Selection of performance metrics for global soil moisture products: the case of ASCAT product. In *Remote Sensing of Energy Fluxes and Soil Moisture Content*; Petropoulos, G. P., Ed.; CRC Press: Boca Raton, FL, USA, 427-444.

Balsamo, G., et al. (2015), ERA-Interim/Land: a global land surface reanalysis data set, *Hydrol. Earth Syst. Sci.*, 19, 389-407.

Balsamo, G., et al. (2012), ERA-Interim/Land: A global land-surface reanalysis based on ERA-Interim meteorological forcing, Technical Report ECMWF, ERA Report Series(13), 349-362.

Brocca, L., Melone, F., Moramarco, T., and Morbidelli, R. (2010). Spatial-temporal variability of soil moisture and its estimation across scales. *Water Resources Research*, 46(2), doi: 10.1029/2009WR008016.

Burnash, R.J.C. (1995). The NWS river forecast system—catchment modeling, In: Singh, V.P. (Ed.), *Computer Models of Watershed Hydrology*. Water Resources Publications, Littleton, Colorado, pp. 311–366, 1995.

Decharme, B., Boone, A., Delire, C., Noilhan, J. (2011), Local evaluation of the Interaction between Soil Biosphere Atmosphere soil multilayer diffusion scheme using four pedotransfer functions, *Journal of Geophysical Research - Atmospheres*, 116, 10.1029/2011JD016002.

Dee, D. P., et al. (2011), The ERA-Interim reanalysis: configuration and performance of the data assimilation system, *Quarterly Journal of the Royal Meteorological Society*, 137(656), 553-597.

Diamond, H., and Coauthors, 2013: U.S. Climate Reference Network after one decade of operations: Status and assessment. *Bull. Amer. Meteor. Soc.*, 94, 485–498, <https://doi.org/10.1175/BAMS-D-12-00170.1>.

Dorigo, W.A., Wagner, W., Hohensinn, R., Hahn, S., Paulik, C., Xaver, A., Gruber, A., Drusch, M., Mecklenburg, S., van Oevelen, P., Robock, A., and Jackson, T. (2011). The international soil moisture network: a data hosting facility for global in situ soil moisture measurements. *Hydrol. Earth Syst. Sci.* 15, 1675–1698, <http://dx.doi.org/10.5194/hess-15-1675-2011>.

Dorigo, W. A., W. Wagner, R. Hohensinn, S. Hahn, C. Paulik, M. Drusch, S. Mecklenburg, P. Van Oevelen, A. Robock, and T. Jackson (2011), The International Soil Moisture Network: a data hosting facility for global in situ soil moisture measurements, *Hydrology and Earth System Sciences Discussions*, 8(1), 1609-1663.

Dorigo, W. A., et al. (2015), Evaluation of the ESA CCI soil moisture product using ground-based observations, *Remote Sensing of Environment*, 162, 380-395.

Dorigo, W. A., K. Scipal, R. M. Parinussa, Y. Y. Liu, W. Wagner, R. A. M. de Jeu, and V. Naeimi (2010), Error characterisation of global active and passive microwave soil moisture datasets, *Hydrology and Earth System Sciences*, 14(12), 2605-2616.

Dorigo, W., et al., ESA CCI Soil Moisture for improved Earth system understanding: State-of-the art and future directions, *Remote Sensing of Environment* (2017)

Draper, C., Reichle, R., de Jeu, R., Naeimi, V., Parinussa, R., and Wagner, W., (2013). Estimating root mean square errors in remotely sensed soil moisture over the continental scale domains. *Remote Sens. Environ.*, 137, 288-298.

Giordani

Gupta, H. V., Klilng, H., Yilmaz, K. K., and Martinez, G. F. (2009). Decomposition of the mean squared error and NSE performance criteria: Implications for improving hydrological modelling. *J. Hydrol.*, 377, 80-91.

Griesfeller, A., Lahoz, W.A., de Jeu, R.A.M., Dorigo, W., Haugen, L.E., Svendby, T.M., and Wagner, W. (2016). Evaluation of satellite soil moisture products over Norway using ground-based observations, *International Journal of Applied Earth Observation and Geoinformation*, 45, 155-164, ISSN 0303-2434, <http://dx.doi.org/10.1016/j.jag.2015.04.016>.

Gruber, A., Su, C. H., Zwieback, S., Crow, W., Dorigo, W., and Wagner, W. (2016). Recent advances in (soil moisture) triple collocation analysis. *Int. J. Appl. Earth Obs. Geoinf.*, 45, part B, 200-211.

Ikonen, J., Vehviläinen, J., Rautiainen, K., Smolander, T., Lemmetyinen, J., Bircher, S., Pulliainen, J. (2016), The Sodankylä in-situ soil moisture observation network: An example application to ESA CCI soil moisture product evaluation, *Geosci. Instrum. Method. Data Syst. Discuss.*, 5, 599-629, doi:10.5194/gid-5-599-2015.

Koren, V.I., Smith, M., Wang, D., and Zhang, Z. (2000). Use of Soil Property Data in the Derivation of Conceptual Rainfall-Runoff Model Parameters, *Proceedings of the 15th Conference on Hydrology*, AMS, Long Beach, CA, pp. 103–106, 2000.

Kuria, D. N., T. Koike, L. Hui, H. Tsutsui, and T. Graf (2007), Field-supported verification and improvement of a passive microwave surface emission model for rough, bare, and wet soil surfaces by incorporating shadowing effects, *Geoscience and Remote Sensing, IEEE Transactions on*, 45(5), 1207-1216.

Lahoz, W.A., and G.J.M. De Lannoy (2014). Closing the Gaps in our Knowledge of the Hydrological Cycle over Land: Conceptual Problems. *Surveys in Geophysics*, 35, 623-660, doi: 10.1007/s10712-013-9221-7.

Lahoz, W.A., Errera, Q., Swinbank, R. and Fonteyn, D. (2007). Data assimilation of stratospheric constituents: A review. *Atmos. Chem. Phys.*, 7, 5745-5773.

Le Moigne, P. (2012). SURFEX Scientific documentation. Available from Météo-France.



- Liu, Y.Y., Parinussa, R.M., Dorigo, W.A., de Jeu, R.A.M., Wagner, W., van Dijk, A., McCabe, F.M., and Evans, J.P. (2011). Developing an improved soil moisture dataset by blending passive and active microwave satellite-based retrievals. *Hydrology and Earth System Sciences*, 15, 425-436.
- Noilhan, J. and Lacarrere, P. (1995), GCM grid-scale evaporation from mesoscale modelling, *Journal of Climate*, 8(2), 206-223.
- Oudin, L., Hervieu, F., Michel, C., Perrin, C., Andreassian V., Anctil, F., and Loumagne, C. (2004). Which potential evapotranspiration input for a lumpedrainfall–runoff model? Part 2: Towards a simple and efficient potential evapotranspiration model for rainfall–runoff modelling. *Journal of Hydrology* 303, 290-306.
- Pathe, C., Wagner, W., Sabel, D., Doubkova, M., and Basara, J.B, (2009). Using ENVISAT ASAR global mode data for surface soil moisture retrieval over Oklahoma, USA. *IEEE Trans, Geoscience and Remote Sensing* 47, 468-480.
- Pratola, C., Barrett, B., Gruber, A., and Dwyer, E. (2015). Quality Assessment of the CCI ECV Soil Moisture product using ENVISAT ASAR Wide Swath data over Spain, Ireland and Finland. *Remote Sens.*, 7, 15388-15423.
- Reichle, R. H., De Lannoy, G.J., Liu, Q., Ardizzone, J.V., Colliander, A., Conaty, A., Crow, W., Jackson, T.J., Jones, L.A., Kimball, J.S. and Koster, R.D., (2017), Assessment of the SMAP Level-4 surface and root-zone soil moisture product using in situ measurements. *Journal of hydrometeorology*, 18 (10), 2621-2645.
- Sakov, P. and Oke, P.R. (2008). Implications of the form of the ensemble transformation in the ensemble square root filters. *Mon. Weather Rev.*, 136, 1042-1053.
- Wagner, W., Naeimi, V., Scipal, K., de Jeu, R., and Martinez-Fernandez, J. (2007). Soil moisture for operational meteorological satellites. *Hydrogeol. J.*, 15, 121-131.
- Willmott, C., and Matsuura, K. (2005). Advantages of the mean absolute error (MAE) over the root means square error (RMSE) in assessing average model performance. *Clim. Res.*, 30, 79-82.





## 8 Appendix

### Global relationships for the period 1997 to 2013

#### GPCP 1.2 precipitation and CCI SM – Absolute values:

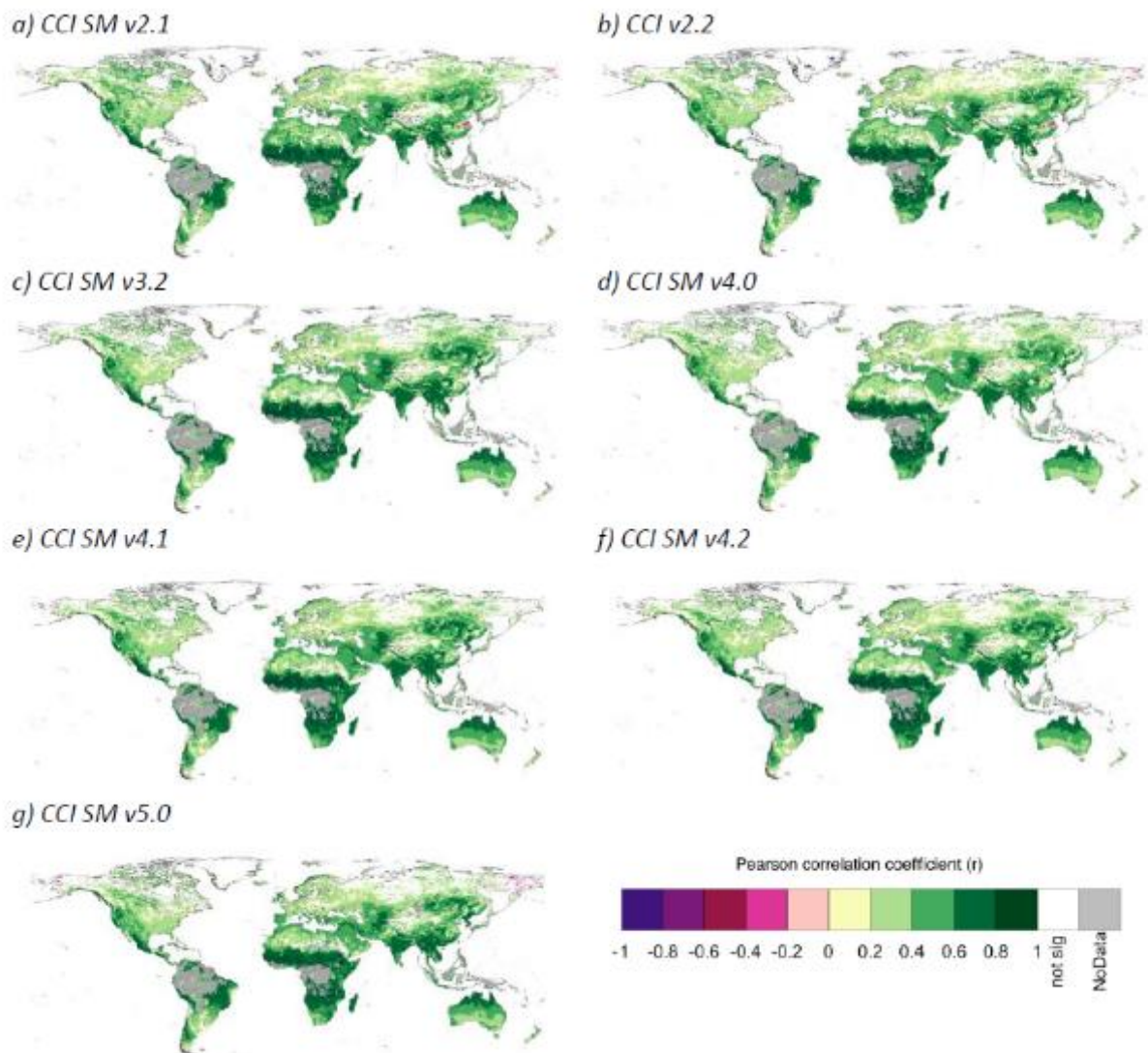


Figure 47: Pearson correlation coefficient  $R$  for GPCP v1.2 precipitation estimates and a) CCI SM v0.1, b) CCI v02.1, c) CCI v02.2, d) CCI v03.2, e) CCI v04.0, f) CCI v04.1, g) CCI v04.2 and h) CCI v05.0 for the period 1997 to 2010. Calculations are based on half-monthly absolute values.





**GPCP 1.2 precipitation and CCI SM – Anomaly values:**

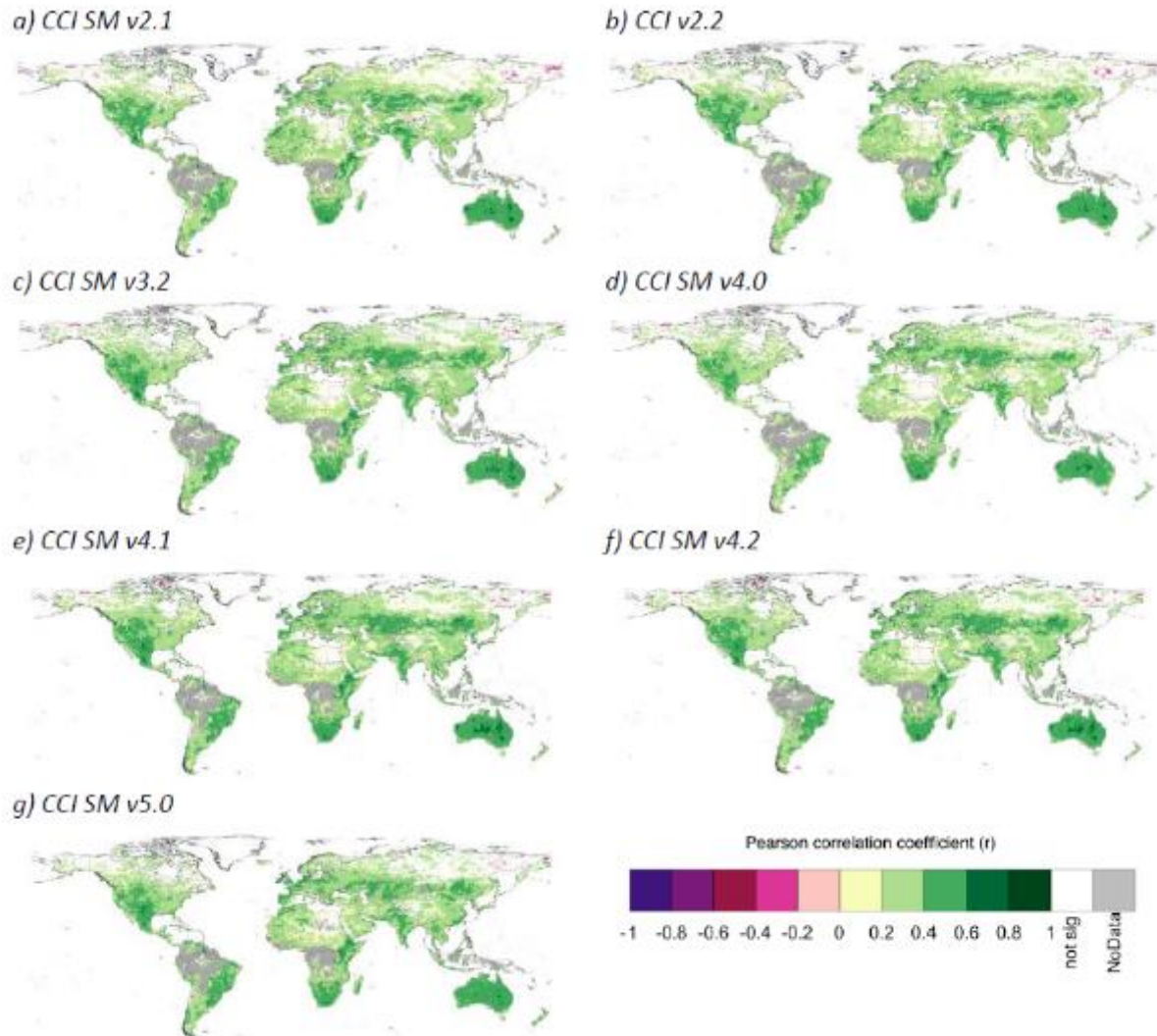


Figure 48: Pearson correlation coefficient  $R$  for GPCP v1.2 precipitation estimates and a) CCI SM v0.1, b) CCI v02.1, c) CCI v02.2, d) CCI v03.2, e) CCI v04.0, f) CCI v04.1, g) CCI v04.2 and h) CCI v05.0 for the period 1997 to 2010. Calculations are based on half-monthly anomaly values.



### ERA Land and CCI SM – Absolute values

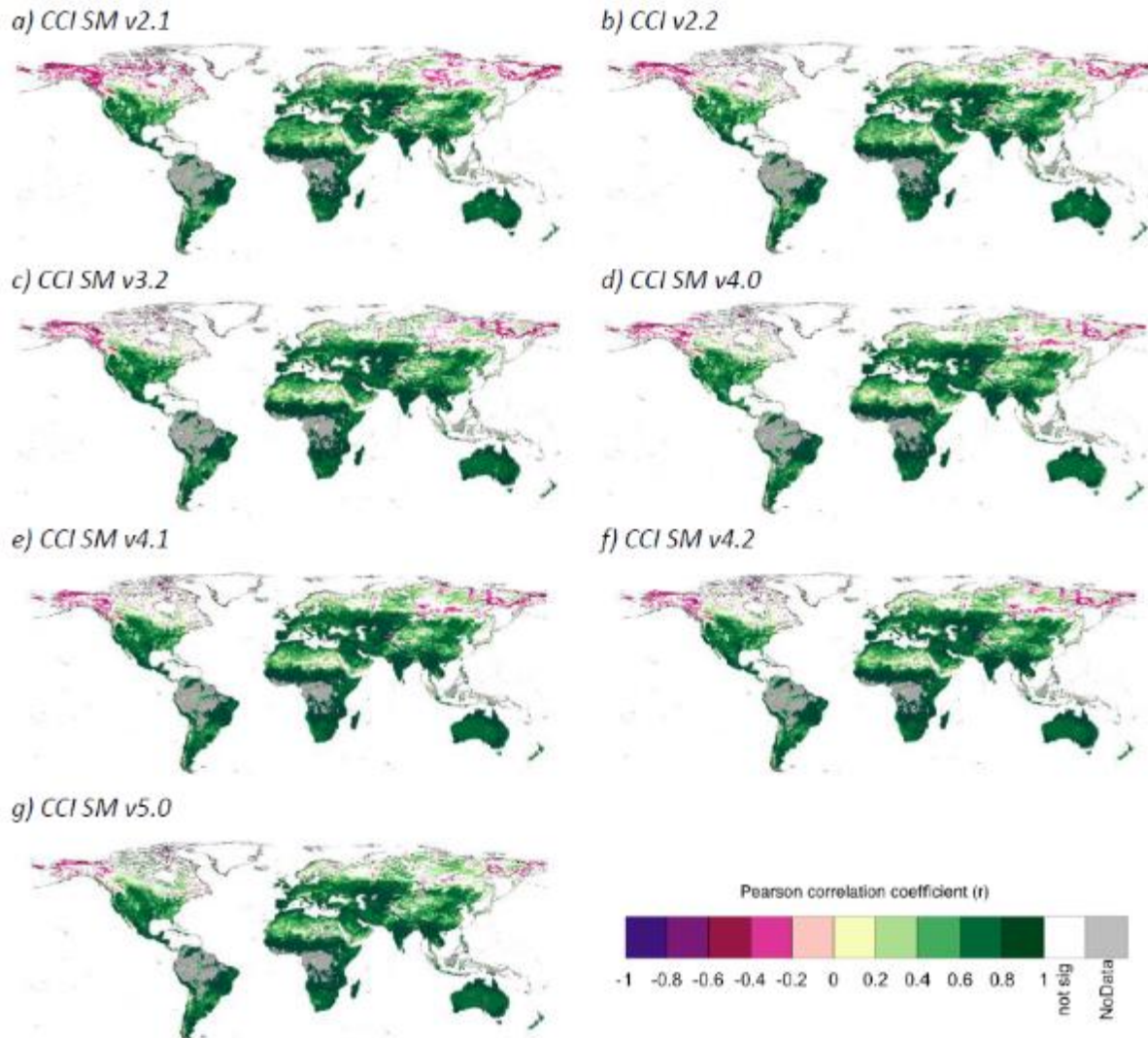


Figure 49: Pearson correlation coefficient  $R$  for ERA-Land soil moisture estimates a) CCI v02.1, b) CCI v02.2, c) CCI v03.2, d) CCI v04.0, e) CCI v04.1, f) CCI v04.2 and g) CCI v05.0 for the period 1997 to 2013. Calculations are based on half-monthly absolute values.



### ERA Land and CCI SM – Anomaly values

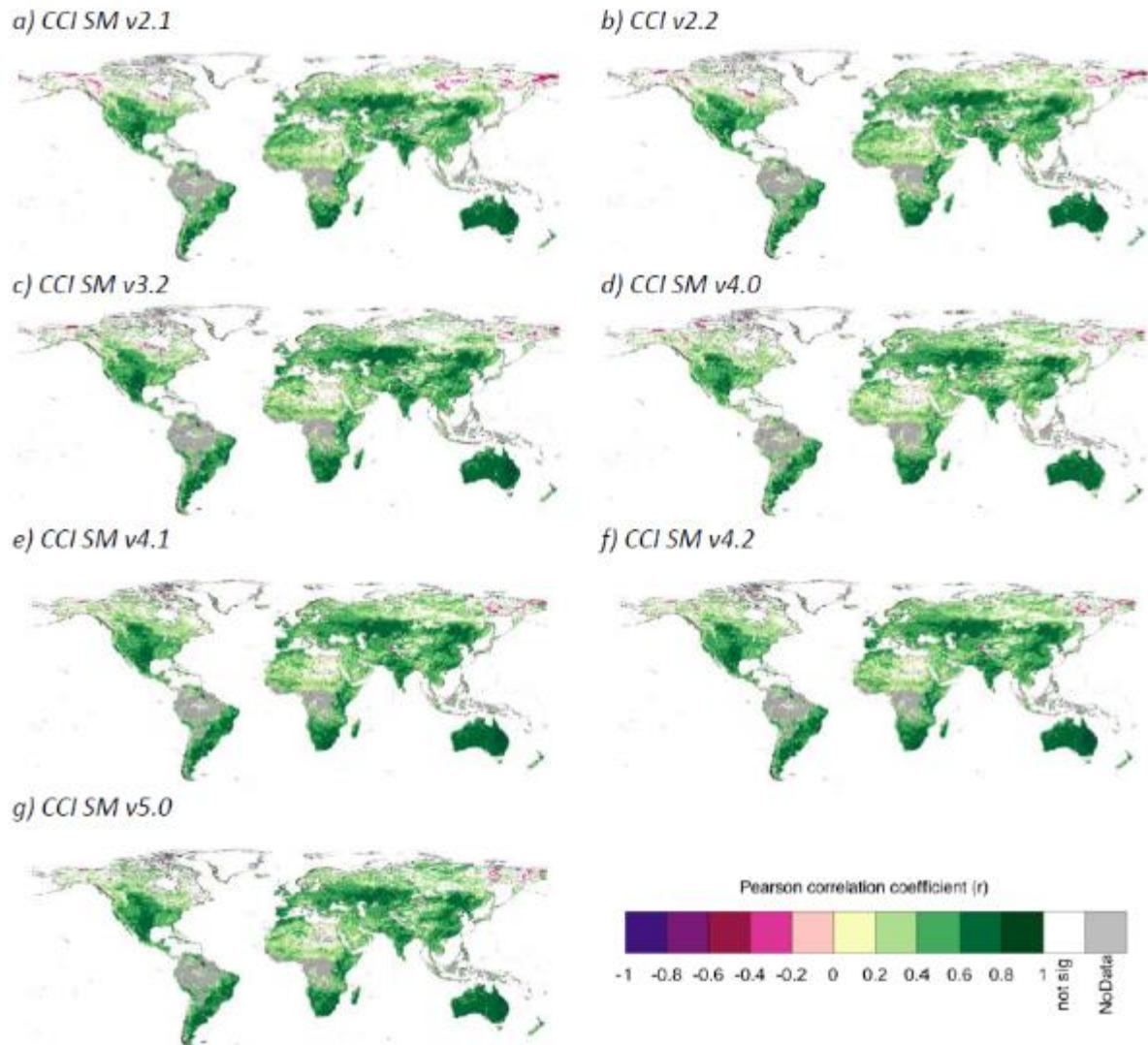


Figure 50: Pearson correlation coefficient  $R$  for ERA-Land soil moisture estimates and a) CCI v02.1, b) CCI v02.2, c) CCI v03.2, d) CCI v04.0, e) CCI v04.1, f) CCI v04.2 and g) CCI v05.0 for the period 1997 to 2013. Calculations are based on half-monthly anomaly values.





### GIMMS NDVI3g and CCI SM – Absolute values

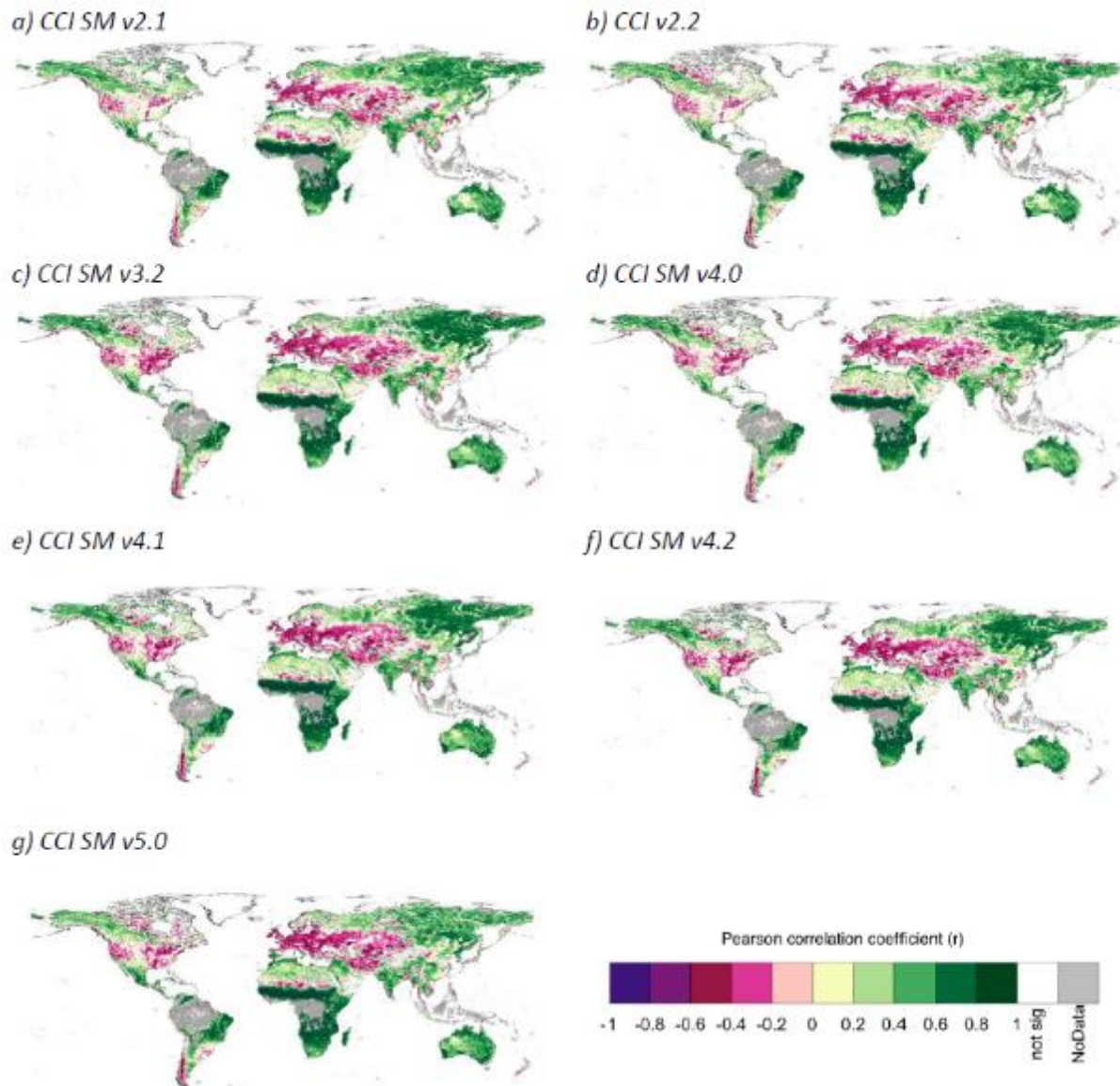


Figure 51: Pearson correlation coefficient  $R$  for GIMMS NDVI3g estimates and a) CCI v02.1, b) CCI v02.2, c) CCI v03.2, d) CCI v04.0, e) CCI v04.1, f) CCI v04.2 and g) CCI v05.0 for the period 1997 to 2013. Calculations are based on half-monthly absolute values and a shift of one half-month was applied.



## GIMMS NDVI3g and CCI SM – Anomaly values

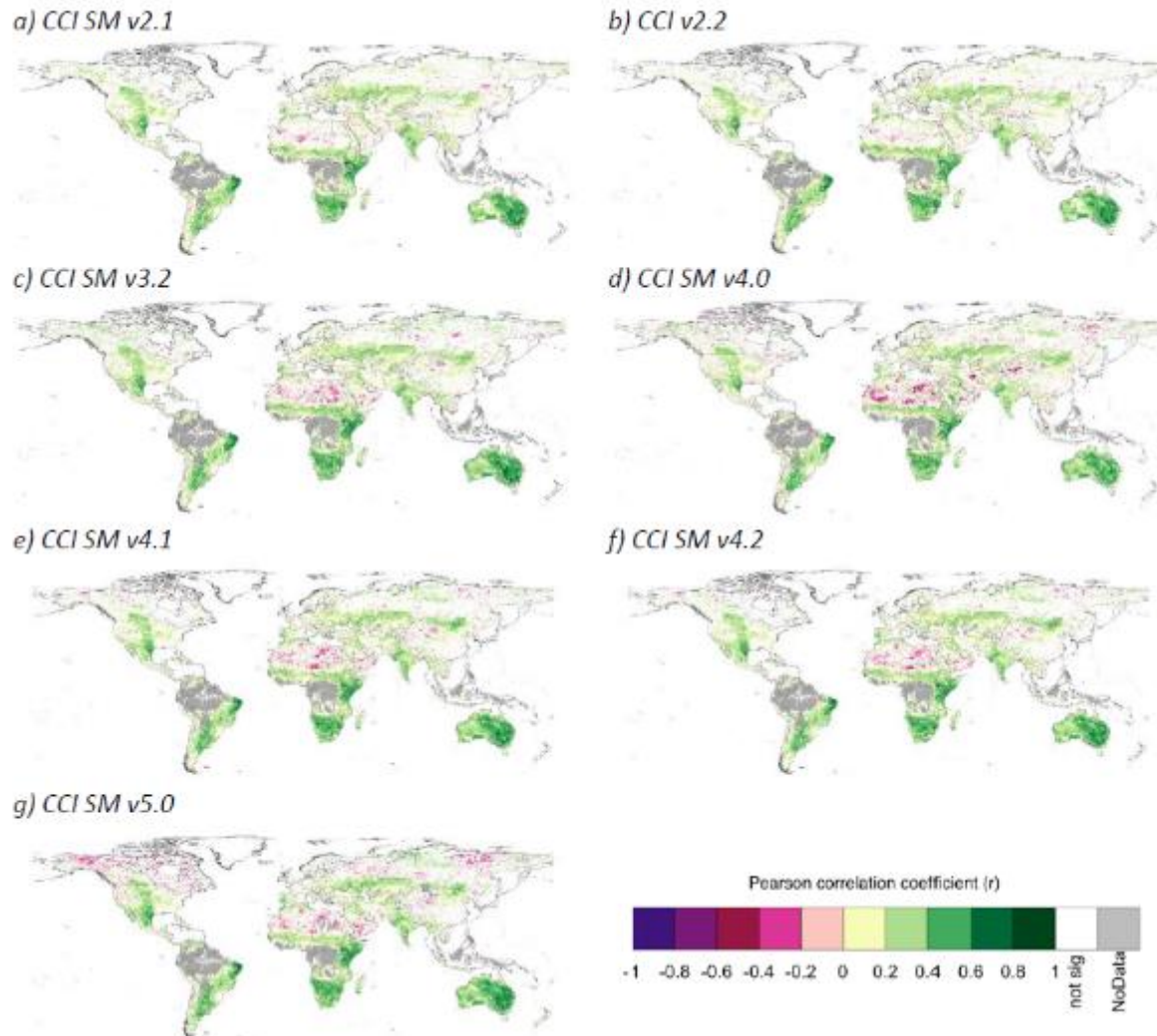


Figure 52: Pearson correlation coefficient  $R$  for GIMMS NDVI3g estimates and a) CCI v02.1, b) CCI v02.2, c) CCI v03.2, d) CCI v04.0, e) CCI v04.1, f) CCI v04.2 and g) CCI v05.0 for the period 1997 to 2013. Calculations are based on half-monthly anomaly values and a shift of one half-month was applied.



**Difference GPCP 1.2. precipitation and CCI SM – Absolute values**

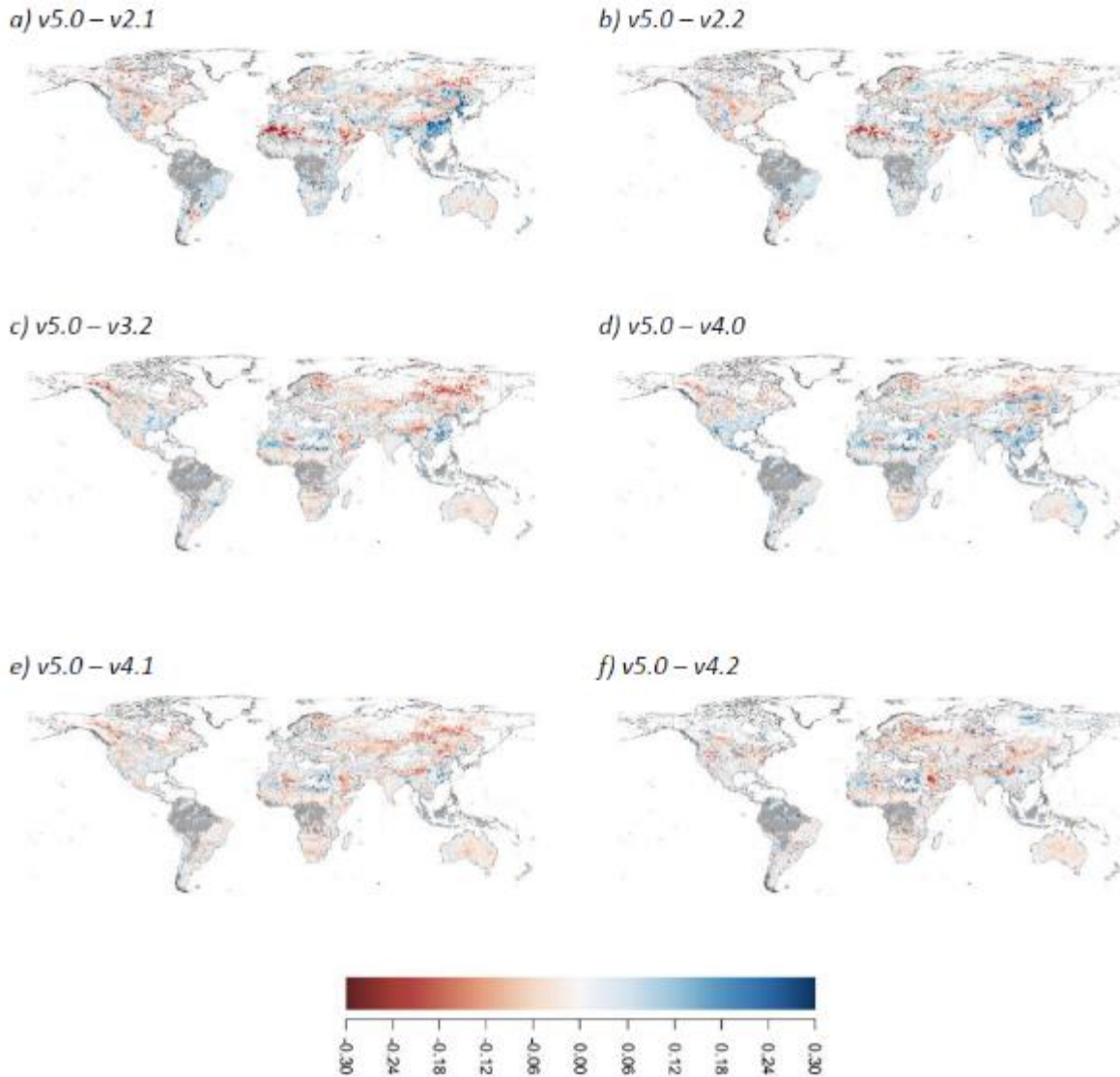


Figure 53: Difference between Pearson correlation coefficient  $R$  derived for GPCP v1.2 precipitation estimates and different versions of CCI SM for the period 1997 to 2013. Calculations are based on half-monthly absolute values.





### Difference GPCP 1.2. precipitation and CCI SM – Anomaly values

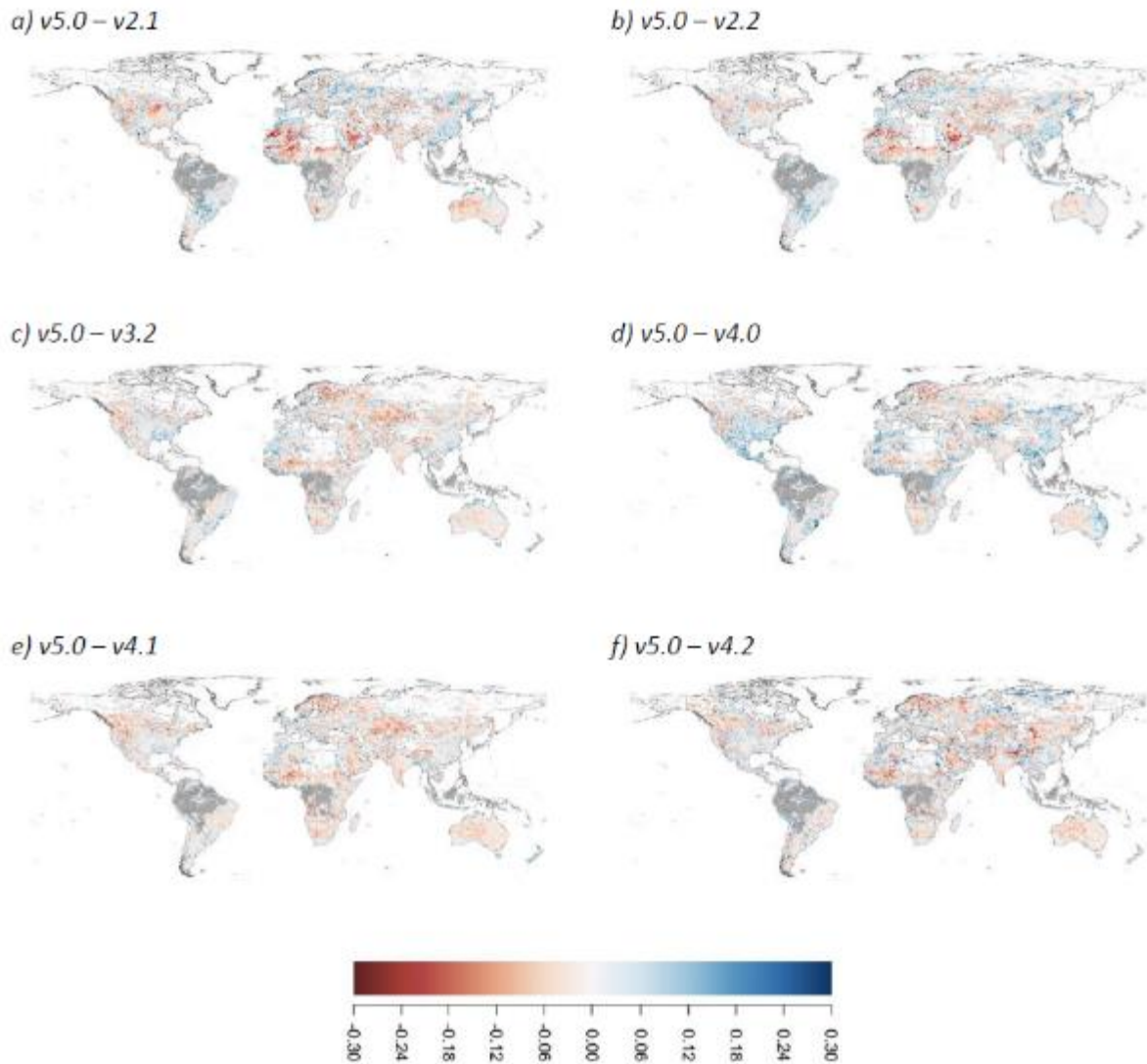


Figure 54: Difference between Pearson correlation coefficient  $R$  derived for GPCP v1.2 precipitation estimates and different versions of CCI SM for the period 1997 to 2013. Calculations are based on half-monthly anomaly values.



### Difference ERA Land and CCI SM – Absolute values

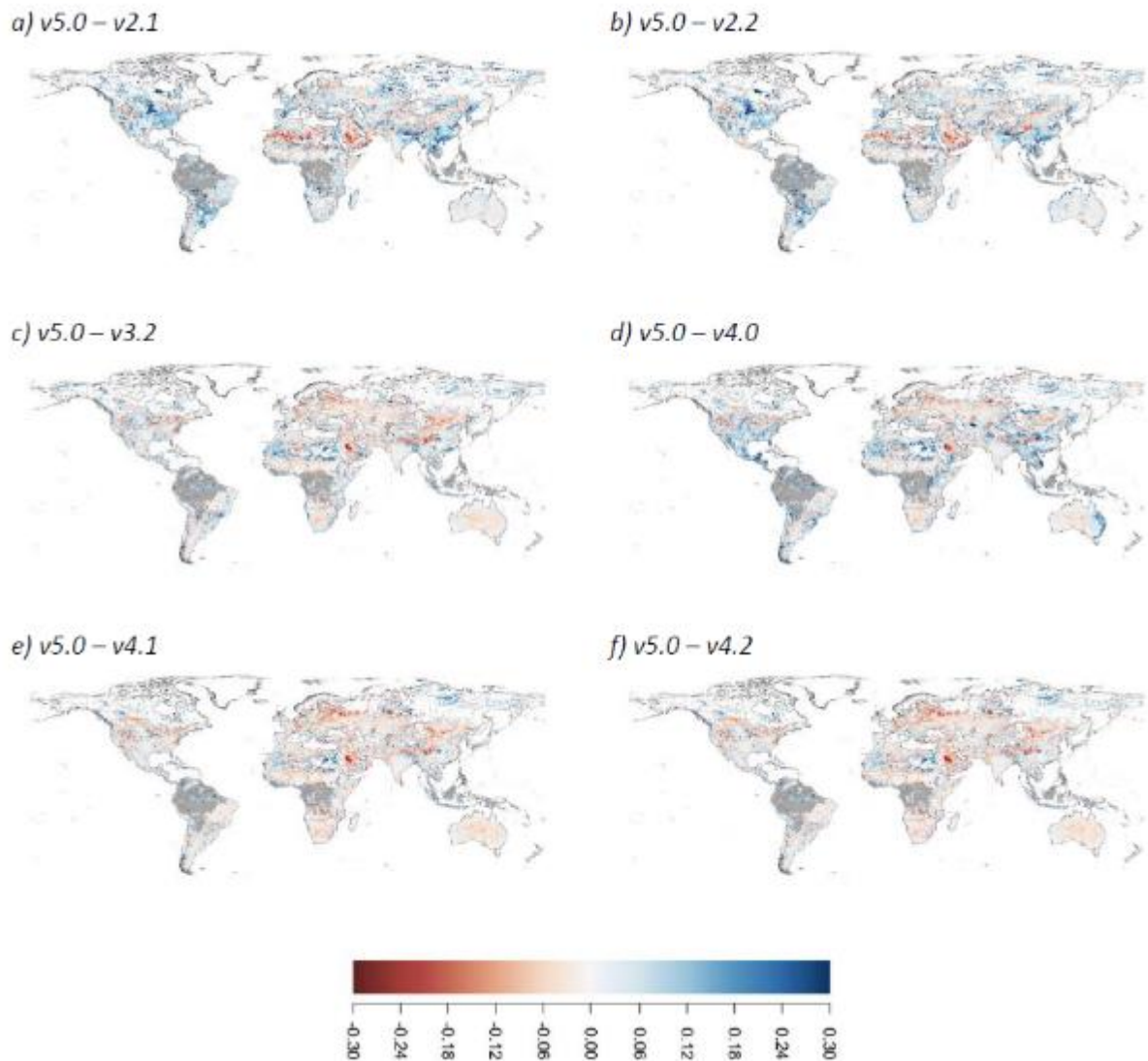


Figure 55: Difference between Pearson correlation coefficient  $R$  derived for ERA Land estimates and different versions of CCI SM for the period 1997 to 2013. Calculations are based on half-monthly absolute values.



### Difference ERA Land and CCI SM – Anomaly values

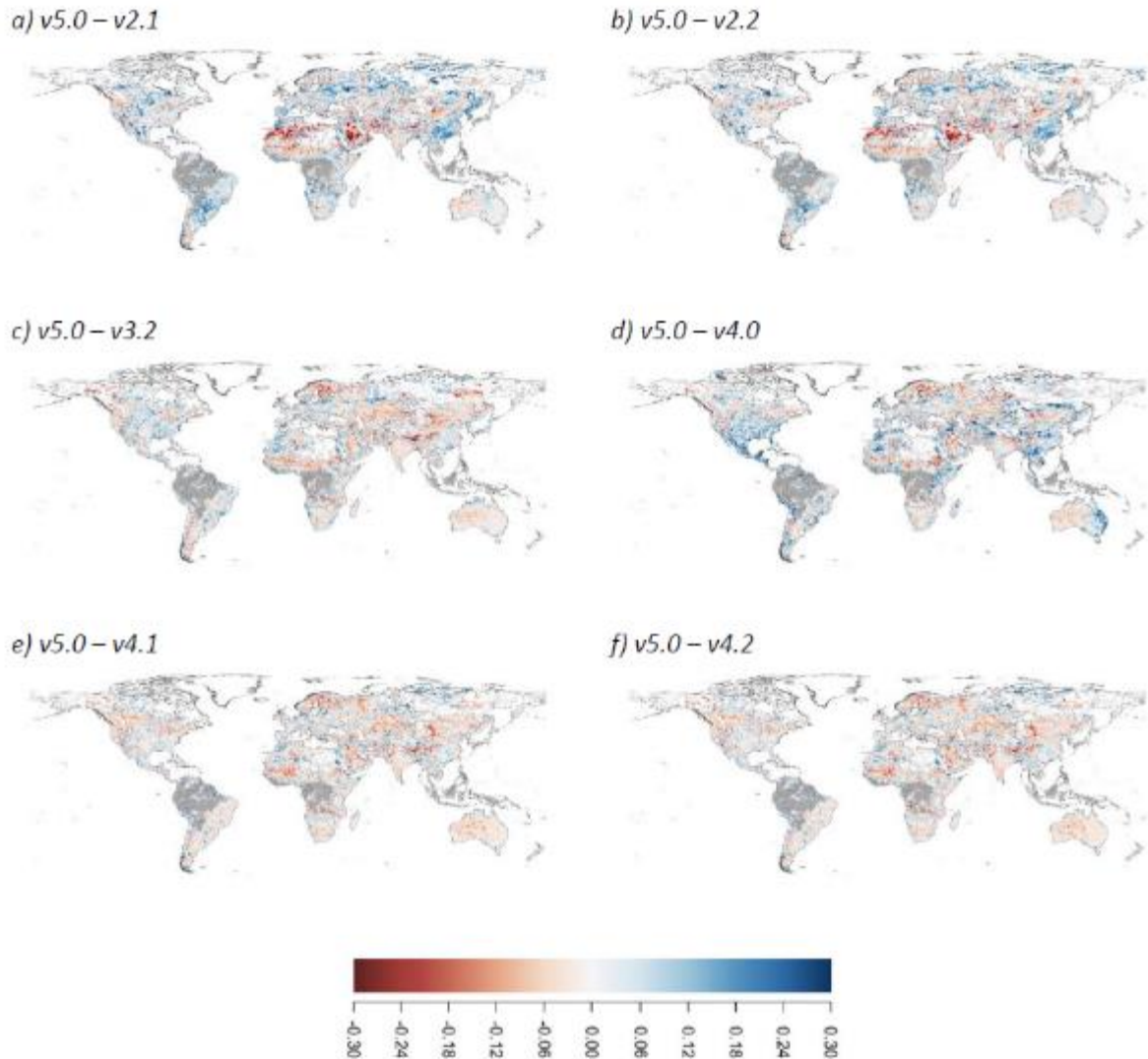


Figure 56: Difference between Pearson correlation coefficient  $R$  derived for ERA Land estimates and different versions of CCI SM for the period 1997 to 2013. Calculations are based on half-monthly anomaly values.



### Difference GIMMS NDVI3g and CCI SM – Absolute values

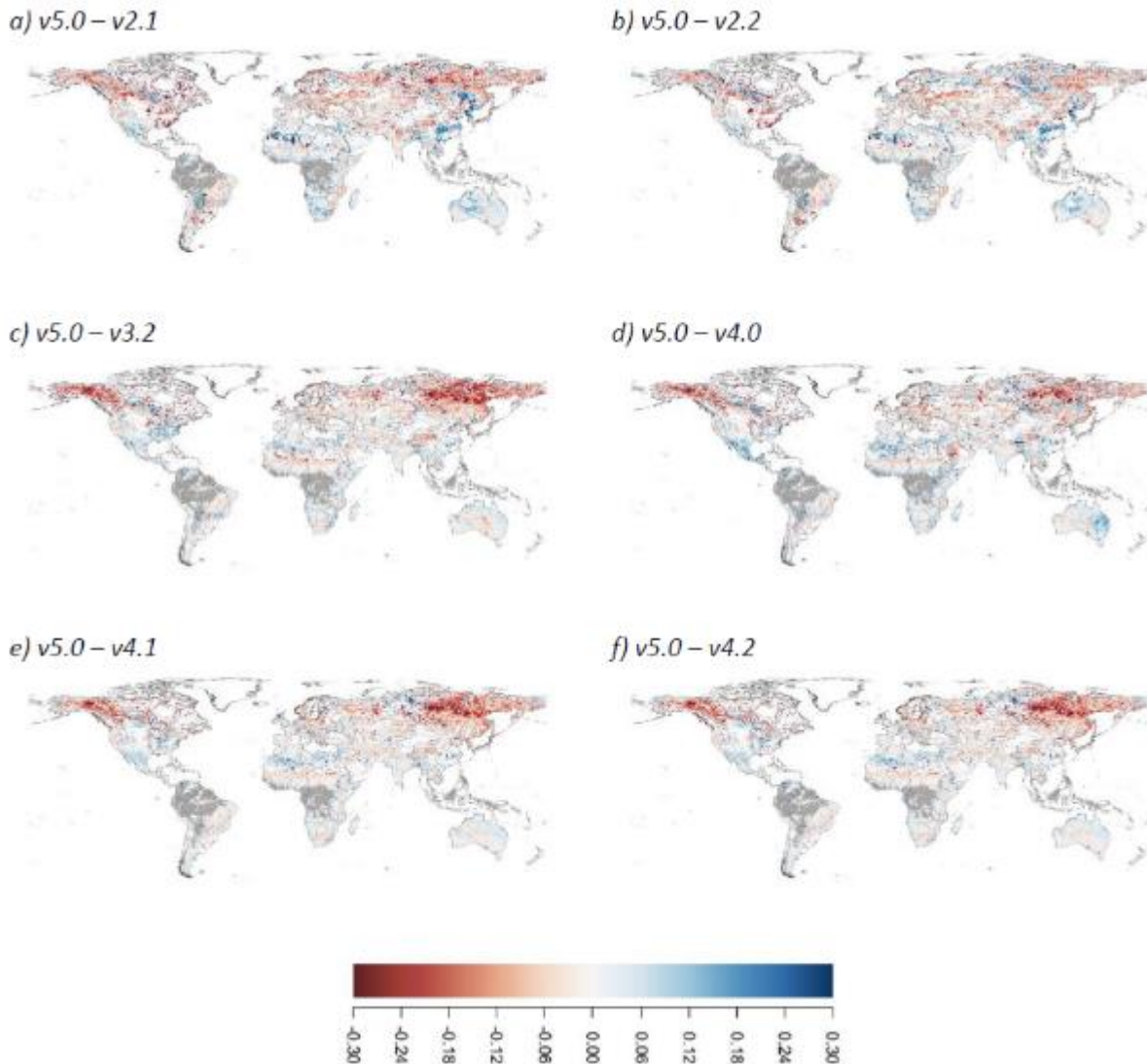


Figure 57: Difference between Pearson correlation coefficient  $R$  derived for GIMMS NDVI3g estimates and different versions of CCI SM for the period 1997 to 2013. Calculations are based on half-monthly absolute values and a shift of one half-month was applied for deriving  $R$ .



### Difference GIMMS NDVI3g and CCI SM – Anomaly values

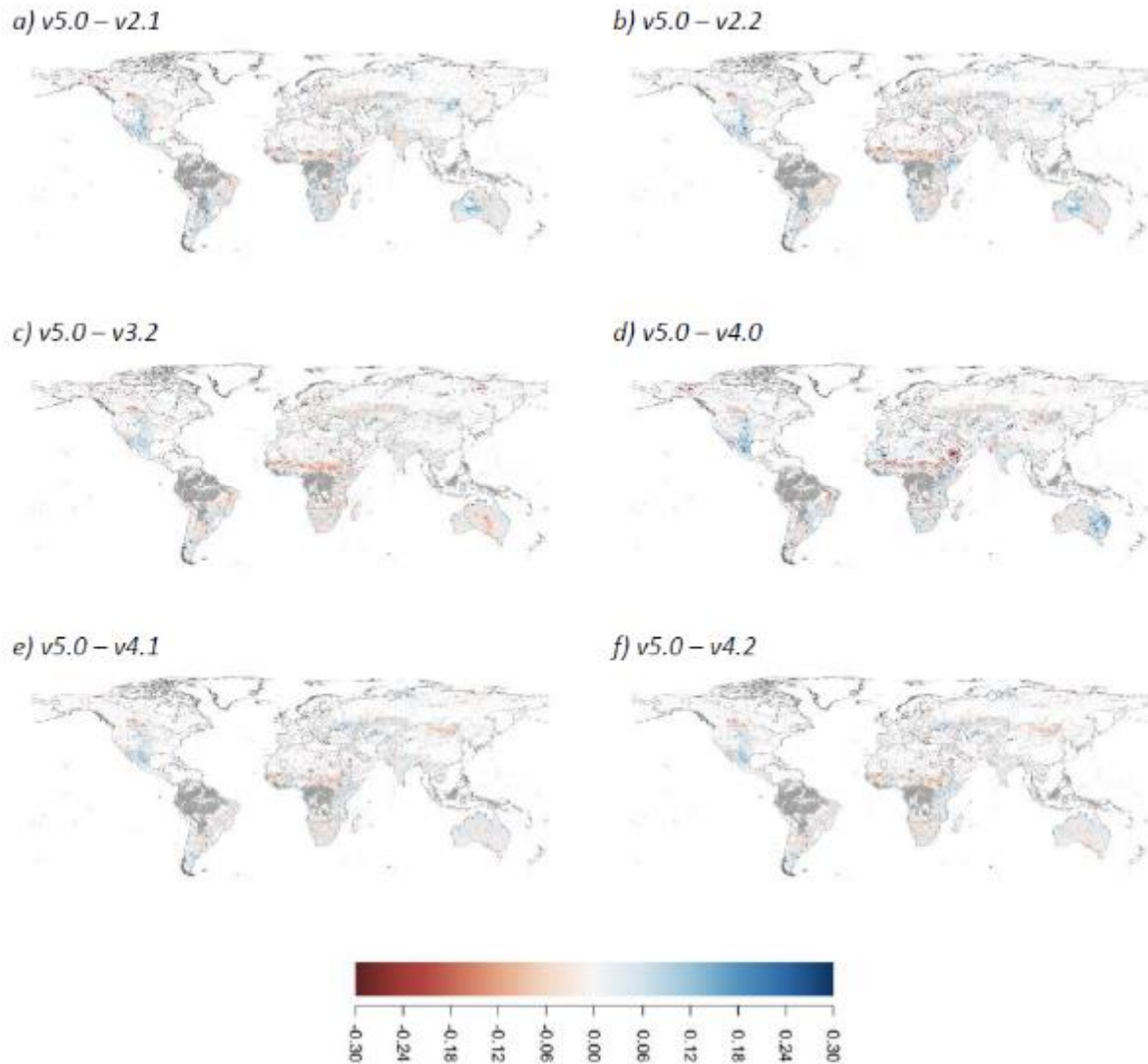


Figure 58: Difference between Pearson correlation coefficient  $R$  derived for GIMMS NDVI3g estimates and different versions of CCI SM for the period 1997 to 2013. Calculations are based on half-monthly anomaly values and a shift of one half-month was applied for deriving  $R$ .